1-1-2014

Activity-Regulated MicroRNAs: Modulators of Synaptic Growth at the Drosophila Neuromuscular Junction

Katherine Ruth Nesler
University of Denver

Activity-Regulated microRNAs: Modulators of Synaptic Growth at the *Drosophila* Neuromuscular Junction

---

A Dissertation

Presented to

The Faculty of Natural Sciences and Mathematics

University of Denver

In Partial Fulfillment

of the Requirements for the Degree

Doctor of Philosophy

---

by

Katherine R. Nesler

June 2014

Advisor: Dr. Scott A. Barbee

Author: Katherine R. Nesler
Title: Activity-Regulated microRNAs: Modulators of Synaptic Growth at the *Drosophila* Neuromuscular Junction
Advisor: Dr. Scott A. Barbee
Degree Date: June 2014

ABSTRACT

It is well established that long-term changes in synaptic structure and function are mediated by rapid activity-dependent gene transcription and new protein synthesis. A growing body of evidence supports the involvement of the microRNA (miRNA) pathway in these processes. We have used the *Drosophila* neuromuscular junction (NMJ) as a model synapse to characterize activity-regulated miRNAs and their important mRNA targets. Here, we have identified five neuronal miRNAs (miRs-1, -8, -289, -314, and -958) that are significantly downregulated in response to neuronal activity. Furthermore we have discovered that neuronal misexpression of three of these miRNAs (miR-8, -289, and -958) is capable of suppressing new synaptic growth in response to activity suggesting that these miRNAs control the translation of biologically relevant target mRNAs. Putative targets of the activity-regulated miRNAs-8 and -289 are significantly enriched in clusters mapping to functional processes including axon development, pathfinding, and axon growth.

We demonstrate that activity-regulated miR-8 regulates the 3'UTR of *wingless*, a presynaptic regulatory protein involved in the process of activity-dependent axon terminal growth. Additionally, we show that the 3'UTR of the protein tyrosine phosophatase *leukocyte antengen related* (*lar*), a protein required for axon guidance and synaptic growth, is regulated by activity-regulated miRNAs-8, -289, and -958 *in vitro*.

Both *wg* and *lar* were identified as relevant putative targets for co-regulation based through our functional cluster analysis.

One putative target of miR-289 is the Ca^{2+}/calmodulin-dependent protein kinase II (*CamKII*). While *CamKII* is not predicted as a target for co-regulation by multiple activity-regulated miRNAs we identified it as an especially pertinent target for analysis in our system for two reasons. First, *CamKII* has an extremely well characterized role in postsynaptic plasticity, but its presynaptic role is less well characterized and bears further analysis. Second, local translation of *CamKII* mRNA is regulated in part by the miRNA pathway in an activity-dependent manner in dendrites. We find that the *CamKII* 3'UTR is regulated by miR-289 *in-vitro* and this regulation is alleviated by mutating the 'seed region' of the miR-289 binding site within the *CamKII* 3'UTR. Furthermore, we demonstrate a requirement for local translation of *CamKII* in motoneurons in the process of activity-regulated axon terminal growth.

ACKNOWLEDGEMENTS

I would like to thank my advisor Dr. Scott Barbee for his guidance and support in my research. Additionally I would like to thank my thesis committee members; Dr. Todd Blankenship, Dr. Jack Kinnamon, and Dr. Tom Quinn, for their roles in guiding this project. For all of the work they do making it possible to be effective in my teaching and research endeavors I would like to thank Dr. Kritin Andrud and Angela Hebel. For assistance in learning new lab techniques I would like to thank Sarala Pradhan and Leslie Rozeboom. For assistance with experiments that contributed to this body of work I would like to thank Bob Sand, Nathan Boin, Anna Laun, and Dr. Breanna Symmes. Last but certainly not least, I would like to especially thank my family and friends for being incredibly supportive and helping me through the past five years, for that I am eternally greatful.

TABLE OF CONTENTS

LIST OF FIGURES

Chapter 1

Chapter 3

Chapter 4

Chapter 5

CHAPTER ONE: BACKGROUND AND SIGNIFICANCE

1.1 Cellular and molecular mechanisms underlying memory formation

The proper assembly and regulation of complex neural circuits is critical for the processes of learning, memory, and higher order thought. Once a neuronal circuit has been formed it cannot simply exist in a static state. Neurons must have the ability to establish long-lasting structural and functional changes in their synapses in response to different stimuli in order to meet the demands of formation and storage. Two classes of memory formation and storage include short-term (STM), lasting across the span of several minutes or hours and long-term memory (LTM), which can persist for a much longer time period from several weeks or potentially an entire lifetime; both require specific and distinct neuronal adaptations (McGaugh, 2000). Due to the dynamic nature of memory formation, neurons must adapt and respond to these stimuli by maintaining finely tuned control of gene expression both spatially and temporally (McNeill and Van Vactor, 2012). One major distinguishing factor between STM and LTM is that for LTM formation to occur, neurons must be capable of *de novo* protein synthesis. It is now widely accepted that in order for information to be stored in the brain, adjustments must be made to the size and strength of synapses (Gkogkas et al., 2010). Without the capability for neurons to perform local translation, storage of long term memories and long-lasting changes in synaptic size and strength would not be possible. Because of this

necessity for *de novo* protein synthesis, local translation in neurons is a central area of focus for researchers trying to uncover the molecular mechanisms underlying memory formation and synaptic plasticity.

1.2 Eukaryotic translation and translational regulation

The process of eukaryotic translation where mRNA is translated into protein is typically cap-dependent in neurons (Wang et al., 2010). Cap-dependent translation involves three major events: initiation, elongation, and termination. Under most conditions in eukaryotes the initiation step of translation is the rate-limiting step and thus is the main target for translational control. The initiation step is mediated by initiation factors (eIFs; see Figure 1 for a detailed depiction of the process) and can be broken down into three steps: formation of a 43S ribosomal preinitiation complex (PIC), binding of mRNA to the PIC, and the formation of an 80S ribosomal complex (Costa-Mattioli et al., 2009). The small 40S ribosomal subunit is loaded with the methionyl tRNA specialized for initiation (Met-tRNAi) and eIFs 1, 1A, 2, 3 and 5 forming the 43S PIC. The PIC binds the mRNA near the 5'-7-methylguanosine cap with the assistance of poly(A)-binding protein (PABP), and eIFs including eIF4F (Hinnebusch and Lorsch, 2012). Once bound, the PIC locates and decodes the AUG start codon following the 5' untranslated region (UTR) via a downstream scanning mechanism in which the start codon is recognized via complementarity with the anticodon of Met-tRNAi (Sonenberg and Hinnebusch, 2009; Hinnebusch and Lorsch, 2012). While bound to the surface of the 40S subunit, eIFs1, 2, and 3 disrupt interaction with the 60S subunit preventing elongation (Costa-Mattioli et al., 2009). GTPase-activating protein (GAP) eIF5 and the GTPase eIF5B facilitate hydrolysis of eIF2-bound GTP from the small subunit and

displace other factors allowing joining of the 60S ribosome subunit (Pestova et al., 2000; Costa-Mattioli et al., 2009).

Following initiation, translation proceeds with the elongation and termination steps. Elongation is mediated by eukaryotic elongation factors (eEF) that are recruited to the mRNA to synthesize the polypeptide chain including a GTPase necessary for tRNA entry onto the ribosome (eEF1A), a guanine nucletide exchange factor (GEF) required for eEF1A (eEF1B), and finally eEF2 which is responsible for ribosomal translocation along the mRNA once the peptide bond has been formed (Costa-Mattioli et al., 2009). Once the protein has been synthesized and the ribosome encounters a stop codon, termination factors facilitate release of the completed polypeptide chain from the mRNA/ribosome complex (Costa-Mattioli et al., 2009). For a detailed illustration of the process of eukaryotic translation please see Figure 1 (Jackson et al., 2010).

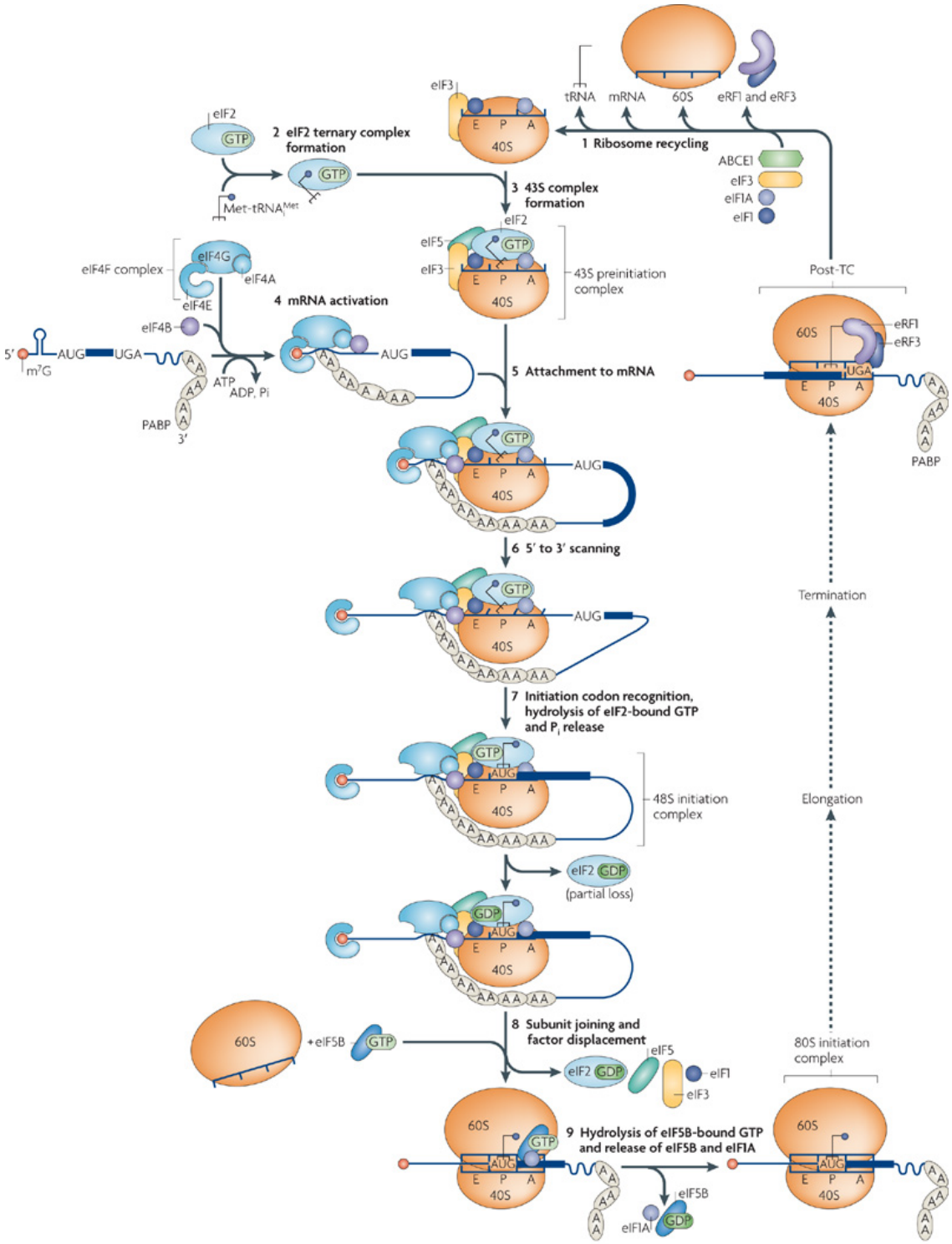

Figure 1. Model of the canonical pathway of eukaryotic translation initiation.
Reprinted by permission from Macmillan Publishers Ltd: [Nature Reviews Molecular Cell Biology] (Jackson et al., 2010), copyright (2010), license number 3393320774353.

The canonical pathway of eukaryotic translation initiation is divided into eight stages (2-9). These stages follow the recycling of post-termination complexes (post-TCs; 1) to yield separated 40S and 60S ribosomal subunits, and results in the formation of an 80S ribosomal initiation complex, in which Met-tRNA^{Met} is base paired with the initiation codon in the ribosomal P-site and which is competent to start the translation elongation stage. These stages are: eukaryotic initiation factor 2 (eIF2)-GTP-Met-tRNA^{Met} ternary complex formation (2); formation of a 43S preinitiation complex comprising a 40S subunit, eIF1, eIF1A, eIF3, eIF2-GTP-Met-tRNA^{Met}, and probably eIF 5 (3); mRNA activation, during which the mRNA cap-proximal region is unwound in an ATP-dependent manner by eIF4F with eIF4B (4); attachment of the 43S complexes (6); recognition of the initiation codon and 48S initiation complex formation, which switches the scanning complex to a 'closed' conformation and leads to displacement of eIF1 to allow eIF5-medaited hydrolysis of eIF2-bound GTP and P release (7); joining of 60S subunits to 48S complexes and concomitant displacement oe eIF2-GDP and other factors (eIF1, eIF3, eIF4B and eIF5) mediated by eIF5B (8); and GTP hydrolysis by eIF5B and release of eIF1A and GDP-bound eIF5B from assembled elongation-competent 80S ribosomes (9). Translation is a cyclical process, in which termination follows elongation and leads to recycling (1), which generates separated ribosomal subunits.

1.2.1 Local translation in neurons

In the classical view of synaptic transmission, axons were viewed as having a simpler role as information transmitters. Dendrites have long taken center stage being viewed as information receivers, which is one reason why postsynaptic local translation in dendrites has been more extensively studied than in axons (Holt and Schuman, 2013). The study of translation in axons is nonetheless critical to understanding the proper functioning of neurons and has been gaining an increasing amount of traction in recent years. We believe presynaptic translation in axons is an under-studied field of immense importance. For this reason our research and the body of work presented here focuses extensively on presynaptic mechanisms.

Proper maintenance of neuronal polarity and function requires differential distribution and translation of neuronal mRNAs. During neurogenesis, differential expression of mRNAs is required for formation of axons and dendrites in establishing neuronal polarity and for axon path-finding, a process during which axons respond to specific cues that ensure appropriate target finding (Sinnamon and Czaplinski, 2011; Jung et al., 2012). The requirement for spatially and temporally differential expression of neuronal mRNAs does not cease in mature neurons. On the contrary, neurons must constantly adapt and undergo fine-tuning in response to stimuli. The response of a neuron following stimulation must be rapid and spatially controlled. To meet the unique demands placed on neurons, a theory has arisen whereby neuronally expressed mRNAs can be transported in a repressed state form from the cell body to distal pre- or postsynaptic sites until their expression is triggered by the appropriate stimulus. Local storage in axon terminals or dendrites would allow for a more rapid translational response

than would be possible if mRNAs were stored in the cell body and only upon stimulation transported to the synapse where expression could occur.

Ribonucleoprotein (RNP) particles, or RNA granules, are a heterogeneous population of particles containing proteins and mRNA. They are found in many eukaryotic species including *C.elegans, Drosophila,* and mammals. Protein composition differs between species and within individual species depending on tissue type and function of the specific granule. Particles often contain translational repressor proteins to silence mRNA within the granule. These particles can be translocated via active microtubule-dependent transport, their final destination at the synapse, where mRNA expression can be triggered by an appropriate stimulus (Costa-Mattioli et al., 2008; Kinder and Kreienkamp, 2012).

1.2.1.1 Local translation in dendrites

Post–synaptic translation in neuronal dendrites has been the subject of extensive research efforts both in elucidating the molecular mechanisms involved and in identifying and characterizing mRNAs with specific dendritic localization. In dendrites polyribosome complexes have been observed in the cytoplasm positioned in close proximity beneath postsynaptic sites and at the base of spines, indicating the capacity for dendrites to conduct local translation (Steward and Levy, 1982; Steward and Schuman, 2001). Additionally, local protein synthesis has been observed in isolated dendrites using metabolic labeling, demonstrating the capability for local protein synthesis by ruling out rapid somatodendritic protein transport (Torre and Steward, 1992; Feig and Lipton, 1993). See Figure 2 for a detailed depiction of mRNA transport and regulated postsynaptic local translation in dendrites (Wang et al., 2010).

The occurrence of local translation in dendrites leaves open the question of how mRNAs are transported in a repressed state from the cell body to distal locations, avoiding aberrant expression. RNA granules are excellent candidates for this mechanism of transit. Dendritic processing bodies (P-bodies) are a class of RNA granules shown to contain proteins that have key functions in the micro-RNA (miRNA) pathway including GW182, fragile x mental retardation protein (FMRP), and the argonaute (Ago) proteins, which are members of the RNA induced silencing complex (RISC). Additionally, the translational repressor DEAD-box helicase Rck (Me31B/Dhh1p), the RNA binding proteins involved in RNA transport zipcode binding protein (ZBP1) and Staufen (Stau), the 5' to 3' exoribonuclease Xrn1, and other RNA-binding proteins and translational repressors depending on specific cellular conditions are also found in P-bodies (Cougot et al, 2008; Hillebrand et al., 2007). The presence of such components strongly suggests that these granules have the capacity to transport mRNA in a repressed state.

Studies using *in-situ* hybridization both *in-vivo* and *in-vitro* have visualized individual mRNAs in dendrites including those that encode microtubule-associated cytoskeletal protein MAP2 (Garner et al., 1988), the multi-domain proteins termed 'Shanks' that interact with postsynaptic membrane receptors as well as the cytoskeleton (Boeckers et al., 2002), Ca^{2+}/calmodulin-dependent protein kinase II (CamKII), brain-derived neurotrophic factor (BDNF), beta actin, activity-regulated cytoskeleton-associated protein (Arc), and many others (Martin and Zukin, 2006; Wang et al., 2010; Perycz et al., 2011). Rapid translation of the aforementioned mRNAs would allow synapses to dynamically respond to stimulation by physically remodeling or adapting to stimuli in a manner that is tightly controlled both temporally and spatially.

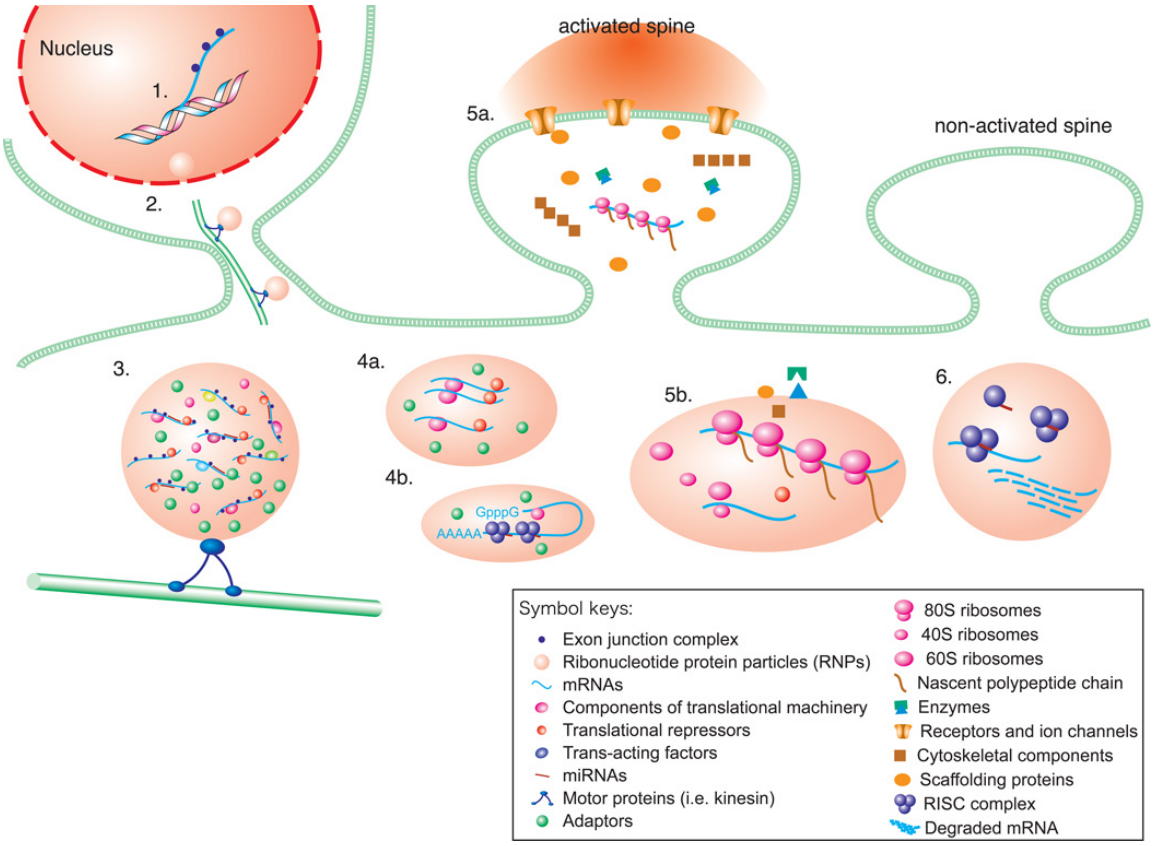

Figure 2. Model of mRNA transport and regulated local translation in dendrites.
Reprinted by permission from Macmillan Publishers Ltd: [Trends in Neurosciences] (Wang et al., 2010), copyright (2010), license number 3393321320359.
(1) Transcription of mRNAs and co-transcriptional recruitment of transacting factors such as the exon junction complex; (2) Assembly and export of RNPs; (3) The cytoplasmic RNP is packaged into a transport granule consisting of mRNAs; components of the translational machinery, translational repressors; trans-acting factors; miRNAs, kinesin and adaptors, which are transported along microtubules by molecular motors into dendrites; (4) Mechanisms by which dendritic mRNA are thought to be maintained in a translationally repressed state are a) repression by assembly of mRNAs together with transational repressors into structures known as RNPs; and b) repression by assembly of mRNAs together with miRNAs to form the RISC complex within structures kP-bodies; (5) a) Activation of neurotransmitter receptors and voltage-gated ion channels engages intracellular second messenger cascades such as the mTOR pathway, which promote translation by turning on the translational machinery and/or by removing translational repressors; b) Active translation at a stimulated synapse 80S ribosome, 40S ribosomes, 60S ribosomes, nascent polypeptide chain; newly synthesized proteins (enzymes, receptors and ion channels, cytoskeletal components, scaffolding proteins) are incorporated into the synapse; (6) Local degradation of mRNAs. miRNA-RISC-mediated localdegradation of mRNAs in P-bodies (RISC complex; mRNA prior to degradation; degraded mRNA; miRNA).

1.2.1.2 Local translation in axons

Electron microscopical studies have thus far failed to identify rough endoplasmic reticulum (RER) or Golgi apparatus in vertebrate axons, and ribosomes have rarely been observed in adult axons (Holt and Schuman, 2013; Jung et al., 2012). Although at first glance this presents a bit of a conundrum, there are several intriguing potential explanations for this ribosomal scarcity. This leaves open the possibility that there exist functional equivalents of RER and Golgi apparatus required for the secretion of locally synthesized proteins, at least in some axons (Jung et al., 2012). While it is true that polyribosmes are not observed as frequently in axon terminals as they are in dendrites, there are several plausible explanations for the rare instances of their observation. Ribosomes have been observed in close proximity to axonal plasma membranes, allowing for the direct association of ribosomal subunits with surface receptors (Sotelo-Silveira et al., 2008; Tcherkezian et al., 2010; Holt and Schuman, 2013). Furthermore, translation is required for proper growth cone turning in growing axons, and axons are capable of correct navigation after somal removal, strongly suggesting the requirement of local translation in axons (Harris et al., 1987; Merianda et al., 2009).

Studies on axonal transcriptomes revealed that in both growing and mature axons there exist a diverse and complex population of mRNAs, with particular enrichment in mRNAs encoding protein synthesis machinery, mitochondrial proteins, and cytoskeletal components (Jung et al., 2012; Holt and Schuman, 2013). As is observed in dendrites, a significant number of RNA binding proteins are localized to axons including but not limited to cytoplasmic polyadenylation element-binding protein (CPEB), FMRP, and ZBP1. These and other RPBs in axons regulate target mRNAs involved in processes

including axon growth, branching, and guidance (Hornberg and Holt, 2013). Studies indicate that mRNAs are targeted to axons based on cis-acting elements within their 3'UTRs, that these mRNAs are transported to distal axon compartments via kinesin-driven microtubule-based transit in RNA granules, and that these mRNAs remain translationally silent until their expression is triggered by specific cues (Jung et al., 2012). A detailed model of RNA-specific transport and translation in axons can be seen in Figure 3.

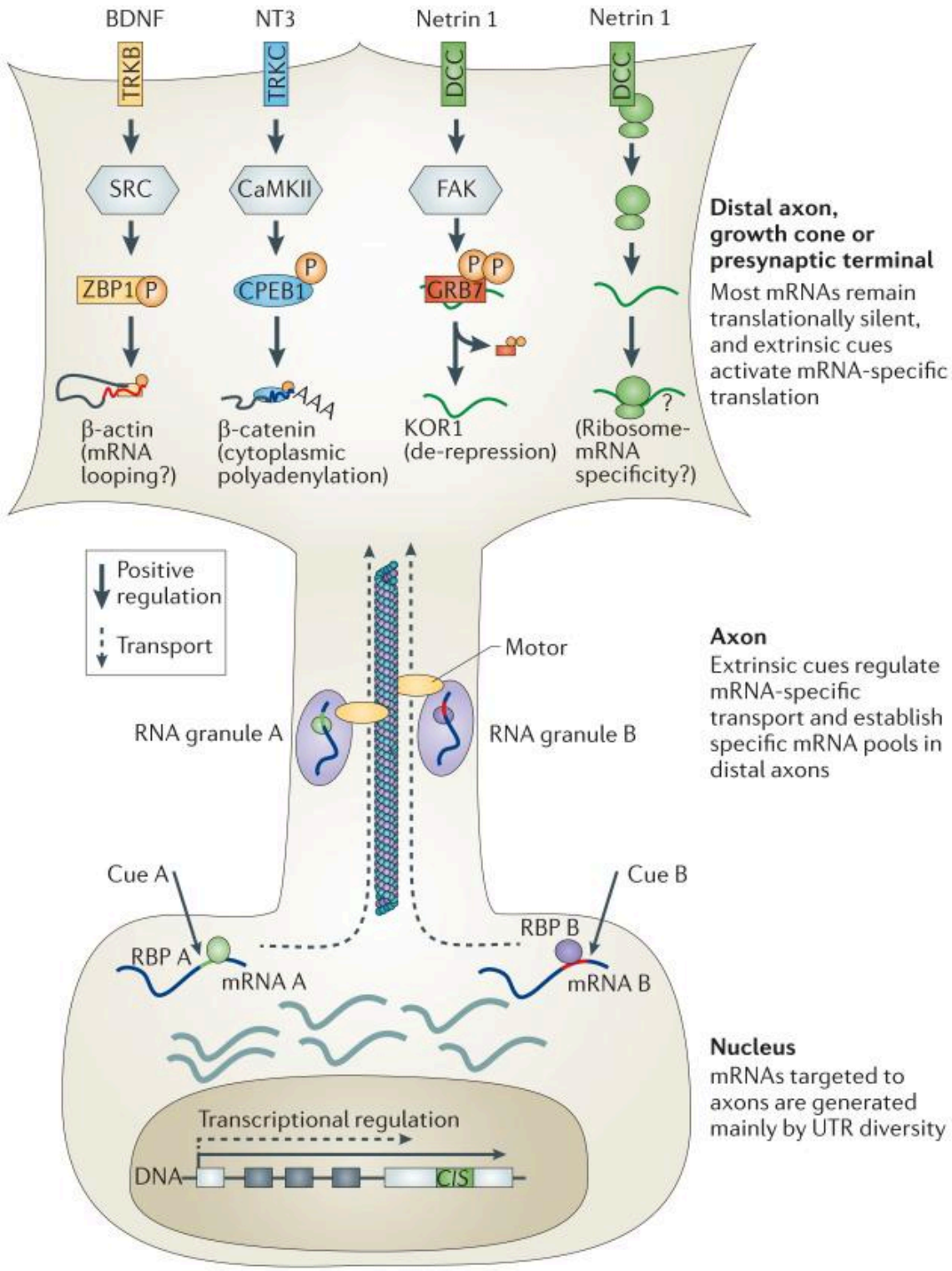

Figure 3. RNA-specific transport and translation.
Reprinted by permission from Macmillan Publishers Ltd: [Nature Reviews Neuroscience] (Jung et al., 2012), copyright (2012), license number 3393330769763.

Axonal targeting of mRNAs is directed by *cis*-acting elements that are mainly localized to the 3′-untranslated regions (UTRs) of mRNAs. Retention of these axon-targeting *cis*-acting elements is commonly regulated by the use of different transcriptional termination sites. Extrinsic cues influence axonal mRNA repertoires by promoting transport of specific mRNAs. Axonally targeted mRNAs are recruited to RNA granules (transport RNPs) by specific RBPs and are transported along microtubules probably by kinesin motors. mRNAs remain translationally silent during transport. Extracellular signals activate the translation of specific mRNAs mainly by regulating RBPs. For example, neurotrophins and guidance cues activate the kinases SRC, CamKII and focal adhesion kinase (FAK), which phosphorylate the RBPs, ZBP1, CPEB1, and growth factor receptor-bound protein 7 (GRB7), respectively. Cell surface receptors might regulate mRNA-specific translation by directly regulating ribosomes. For example, unstimulated netrin receptor DCC directly binds to ribosomes and inhibits translation, and ribosome composition influences mRNA selectivity. Different receptors may bind to ribosomes that are pre-tuned to specific mRNAs, and ligand stimulation might release such ribosomes and result in mRNA-specific translation. BDNF, brain-derived neurotrophic factor; KOR1, κ-type opioid receptor; NT3, neurotrophin 3; TRK, tyrosine kinase receptor.

1.2.2 microRNAs: Biogenesis and translational regulation

miRNAs are a class of small, noncoding RNAs and are excellent candidates for tightly regulated gene expression in pre- and postsynaptic neuronal compartments. miRNAs are generally 21-24 nucleotides in length, although there are certain atypical miRNAs that approach 30 nucleotides. They are *trans*-acting factors that posttranscriptionally regulate the expression of mRNA targets by binding to sequences usually within the 3'UTR by imperfect complementarity (Lucas and Raikhel, 2013). The only strict requirement for base pair matching between a miRNA and its mRNA target is within the "seed sequence" (located at positions 2-8 of the miRNA). miRNAs must exhibit perfect complementarity only within the seed to mediate negative post-transcriptional regulation of its target, giving each miRNA the potential to simultaneously regulate the expression of hundreds to thousands of mRNAs throughout a single organism (Lai, 2002).

Biogenesis of miRNAs traditionally begins in the nucleus, where they are transcribed by RNA polymerase II (Lee et al., 2004; Rodriguez et al., 2004). Following transcription, the miRNA transcript forms a hairpin loop structure termed a "pri-miRNA" complete with 5' cap and 3' poly-A signal (Lee et al., 2004). This structured hairpin is then received by a microprocessor complex approximately 500kDa consisting of the RNAse II enzyme Drosha, and Pasha (DGR8), a double stranded RNA (dsRNA) binding protein (Denli et al., 2004; Kim et al., 2009; Lucas and Raikhel, 2013). The microprocessor complex recognizes the region of the pri-miRNA where the flanking single-stranded RNA meets the double-stranded stem structure; upon proper association the processing center of Drosha is located 11bp into the stem structure where cleavage

occurs, resulting in the 70nt pre-miRNA (Han et al., 2006). After the Drosha/Pasha complex mediates cleavage of the pri-miRNA structure into the pre-miRNA it associates with double-stranded binding receptor Exportin 5 that mediates nuclear export and provides protection from nuclease digestion (Yi et al., 2003; Lund et al., 2004). Once in the cytoplasm, the pre-miRNA is cleaved by Dicer, another RNase II enzyme, resulting in the formation of a miRNA-miRNA* duplex. Traditionally, the star (*) or 'passenger' strand has been considered secondary to the mature 'guide' strand and it is assumed that it would be degraded (Khvorova et al., 2003), however, numerous recent studies demonstrate important regulatory roles for passenger strand miRNAs (Winter and Diederichs, 2013; Yang et al., 2013; Rubio et al, 2013; Yuan et al., 2013). Once a miRNA has been generated, in order for it to perform its role in translational repression, it must associate with the RNA-induced silencing complex, or RISC. RISC assembly involves two successive steps, the first of which is inserting the small RNA duplex into the Ago protein. Next, the two strands of the RNA duplex are separated and one dissociates, leaving one bound within the RISC for subsequent association with and repression of mRNA targets via binding with perfect complementarity in the seed sequence (Kawamata and Tomari 2010). A summary of miRNA biogensis is depicted in Figure 4 (Carroll and Schaefer, 2013).

The localization of Ago proteins to neuronal granules in *Drosophila* lends more credence to the notion that miRNAs may be important regulators of neuronal mRNA expression in this system. Studies indicate that miRNAs play an important role in axon development and in presynaptic plasticity in mature nerve terminals. Furthermore, studies have revealed a diverse population of miRNAs in axons and the presynaptic

terminal, but these miRNAs and their target genes are largely uncharacterized (Kaplan et al., 2013). Figure 5 is an illustrated model of how miRNAs may function in neurons to regulate gene expression in cellular compartments including the cell body, axon, and dendrites.

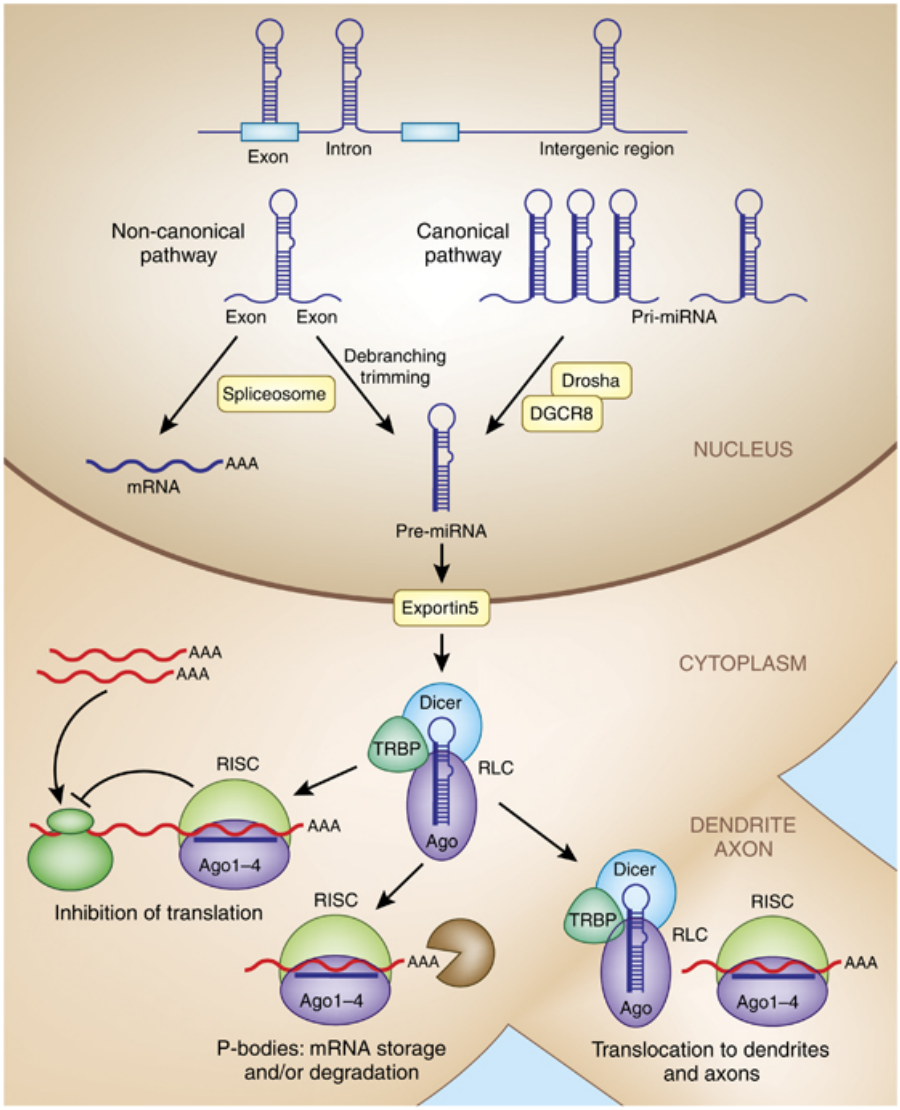

Figure 4. Schematic overview of canonical and noncanonical miRNA biosynthesis.
Reprinted by permission from Macmillan Publishers Ltd: [Neuropsychopharmacology] (Carroll and Schaefer, 2012), copyright (2012), license number 3393331032978.
The canonical miRNA pathway produces pri-miRNA transcripts from miRNA genes encoded in exonic, intronic, or intergenic regions, followed by Drosha/DGCR8 processing of the pri-miRNA transcripts into pre-miRNAs. Intronic pre-miRNA hairpins of the noncanonical mirtron pathway are formed by splicing, debranching, and trimming of short introns without Drosha processing. Pre-miRNAs generated by the canonical and noncanonical pathways are exported from the nucleus via Exportin 5, followed by subsequent Dicer cleavage within the RISC loading complex (RLC), unwinding of the miRNA/miRNA* duplex via Argonaute, and TRBP-dependent loading onto the RISC. Binding of target mRNAs to miRNAs in RISC is followed by inhibition of translation and/or mRNA degradation within p-bodies in the cytosol. The transport of RLC and RISC into the dendritic and axonal compartments occurs via a still unknown mechanism.

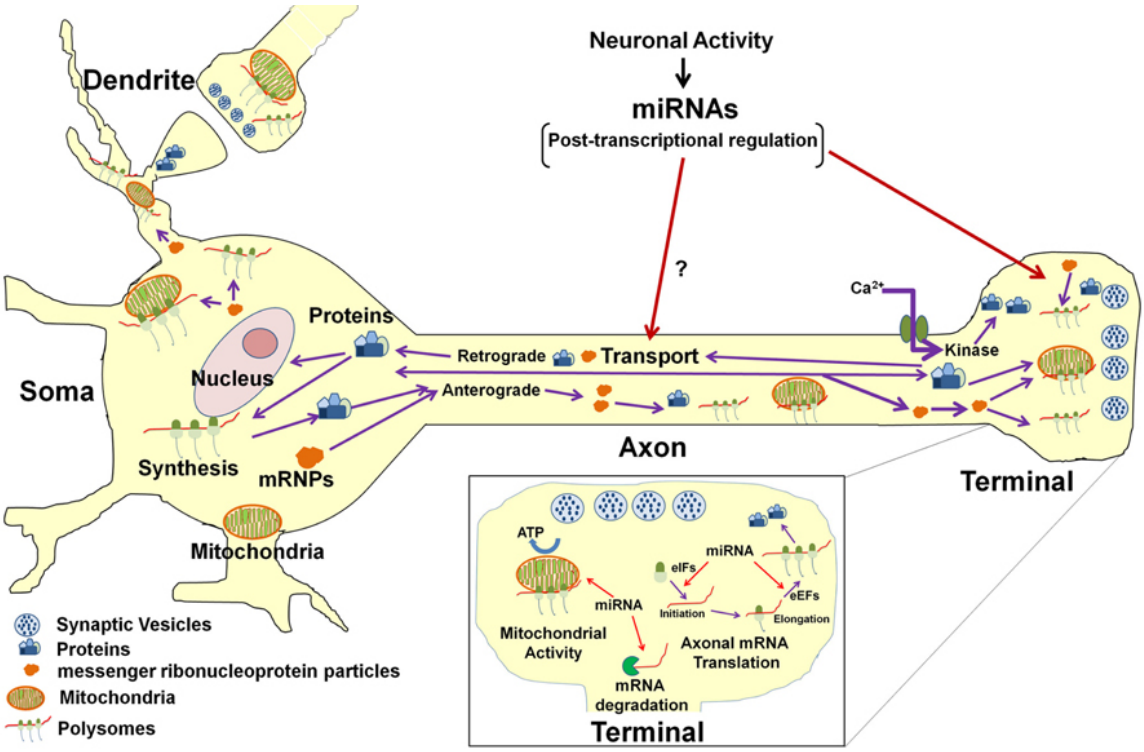

Figure 5. Model for miRNA-mediated regulation of neuronal function.
Figure reproduced as published in Kaplan et al., 2013.
In the neuron, protein synthesis occurs in multiple compartments that include the cell body, dendrite, axon, and presynaptic nerve terminal. A subset of mRNAs transcribed in the nucleus are packaged into stable messenger RNPs and are selectively and rapidly transported to the distal structural/functional domains of the neuron. The selective translation of these localized mRNAs plays key roles in neuronal development, axon growth and maintenance, and synaptic plasticity. Neuronal miRNAs function at multiple levels within the neuronal gene expression system to modulate neuronal activity and function. It has been shown that miRNAs regulate the local post-transcriptional gene expression of specific target mRNAs that encode factors affecting mitochondrial activity (see inset) as well as axonal growth and branching. In addition, miRNAs can also modulate translation of multiple mRNAs in the axon and nerve terminal by regulating local expression of eukaryotic translation factors (see inset). It is also conceivable that miRNAs might regulate the local synthesis and retrograde transport of transcription factors in response to growth factors or neural injury and hence influence gene transcription in the parental soma. Last, miRNA control of the local synthesis of cytoskeletal and/or motor proteins might facilitate the regulation of their own anterograde transport to their ultimate sites of function.

Postsynaptic studies have revealed the presence of key components of the miRNA pathway. For example, in mammalian neurons, dendritic P-body-like structures (dlPbodies) have been observed to stain positively for Ago2, GW182, and Dcp1a, and *in situ* hybridization revealed the presence of the miRNA let-7 which is highly expressed in the brain as well as miR-128, which is expressed specifically in neurons (Smirnova et al., 2005; Cougot et al., 2008). Further evidence for miRNA-mediated translational regulation in neurons includes the regulation of CamKII mRNA in dendrites. In *Drosophila,* neural activity triggers the translocation of CamKII mRNA to postsynaptic sites where rapid translation occurs. This rapid translation occurs following protesome-mediated degradation of the key RISC pathway component, Armitage (Ashraf et al., 2006). *Drosophila* CamKII is a predicted target of activity-regulated miRNA-289 and we postulate a mechanism in which a decrease of miR-289 (and other activity-regulated miRNAs) in response to neuronal activity results in increased translation of their mRNA targets, including CamKII. Last, miRNA control of the local synthesis of cytoskeletal and/or motor proteins might facilitate the regulation of their own anterograde transport to their ultimate sites of function.

Studies in *Drosophila* indicate that spaced synaptic depolarization induces new synaptic growth at the larval NMJ (Ataman et al., 2008). We postulate a mechanism whereby acute synaptic stimulation regulates differential expression of neuronally enriched miRNAs. These miRNAs in turn either repress or derepress mRNA targets depending on the miRNA is up- or down-regulated in response to activity. We believe this alteration in miRNA levels modulates the gene expression needed for new synaptic

growth in response to neuronal activity. One such miRNA/mRNA target pair that could play an especially

important role in modulating new synaptic growth in response to activity is miR-289 and its predicted target CamKII.

1.3 Calcium/calmodulin-dependent protein kinase II

CamKII is an important and extensively studied protein kinase implicated in both the establishment of long-term potentiation (LTP; Malinow et al., 1989; Silva et al., 1992) and more recently long-term depression (LTD; Mockett et al., 2011; Coultrap et al., 2014). While there are four isoforms of CamKII in mammals (α, β, δ, and γ), two of these isoforms (α and β) are primarily localized to the nervous system, one of which is restricted exclusively to neurons (CamKIIα; Kolodziej et al., 2000). Studies in the rat brain have shown that CamKIIα is highly enriched, 0.74% of total protein in whole brain and especially concentrated in the hippocampus where it comprises 1.4% of total protein (Erondu and Kennedy, 1985). Furthermore, CamKIIα has been demonstrated to be restricted to excitatory, glutamatergic synapses in the CA1 region of rat hippocampus, displaying localization both pre- and postsynaptically (Liu and Jones, 1997). When CamKII is activated it has the capacity to phosphorylate Ser and Thr residues in various proteins, including those implicated in neurotransmitter synthesis and release, transcriptional, translational, and cytoskeletal regulation; Ca^{2+} homeostasis; as well as receptor channel function, thereby modulating their function (Kolodziej et al., 2000) alluding to the notion that it has the capacity to activate key proteins involved in the control of synaptic structure and function.

1.3.1 Structure and function of calcium/calmodulin-dependent protein kinase II

CamKII has a highly complex and unique structure that enables it to phosphorylate targets by two distinct mechanisms. The first mechanism is common to most kinases involving the binding of a protein substrate within a catalytic domain where ATP is hydrolysed and phosphorylation occurs. The second phosphorylation mechanism of CamKII is the more unique feature of autophosphorylation (Lucchesi et al., 2011). Three-dimensional reconstruction of the mammalian alpha form of the kinase (found only in neurons) is composed of 12 subunits stacked into the conformation of two hexameric rings with functional domains clustered in foot-like processes (Kolodziej et al., 2000). This unique structure is postulated to be a favorable arrangement for its autophosphorylation of Thr-286, an amino acid located within the regulatory domain of CamKII adjacent to the calmodulin-binding domain, that when phosphorylated, leads to Ca^{2+}/calmodulin-independent kinase activity (Theil et al., 1988; Miller et al., 1988). When calmodulin is not present in the cell, an auto-inhibitory domain remains bound, blocking peptide and ATP binding to the kinase domains that would otherwise be active (Rosenberg et al., 2005). Within this regulatory segment is Thr-286, phosphorylation of which renders CamKII independent, the association of the auto-inhibitory domain holds Thr-286 away from catalytic sites which would otherwise be able to phosphorylate the residue, leading to activation of the kinase without the presence of Ca^{2+} or calmodulin (Rosenberg et al., 2005). The activation and function of CamKII depends on three key steps. First, Ca2+/CaM removes the autoinhibitory segment located C-terminal to the kinase domain (Rosenberg et al., 2005), following dissociation of the coiled autoinhibitory domain, Thr-286 is phosphorylated by another kinase domain within the

holoenzyme (Theil et al., 1988; Miller et al., 1988; Yang and Schulman, 1999; Rosenberg et al., 2005). Lastly, once Thr-286 is phosphorylated, CamKII is able to maintain activity in the absence of Ca2+/CaM by blocking the reassociation of the autoinhibitory domain (Yang and Schulman, 1999; Miller et al., 1988). This autophosphorylation between subunits of CamKII prevents reassociation that is able to persist because even if dephosphorylation occurs in some subunits, the activity of adjacent autophosphorylated subunits can rephosphorylate them, leading to continued activity. Evidence also suggests that it may be possible for the holoenzyme to survive protein turnover, because as individual subunits are degraded, newly synthesized replacements can be integrated and phosphorylated (Irvine et al., 2006).

While autophosphorylation of CamKII is considered to be an important and unique feature of the kinase it is interesting to note that studies have identified for mutant mice that lack the ability to autophosphorylate αCamKII due to an amino acid substitution at Thr-289 (T289A). While these mutants were unable to form LTM after a single trial of a passive avoidance task, they were able to form avoidance LTM following a massed training protocol, indicating that even though these mutants lack the ability to autophosphorylate, they are still able to store hippocampus- and amygdala-dependent LTM. Thus autophosphorylation of αCaMKII appears to be required for rapid learning tasks but not for memory retention (Irvine et al., 2006).

1.3.2 Postsynaptic functions of Calcium/calmodulin-dependent protein kinase II

While the focus of the body of work that will be presented here is presynaptic, CamKII has been extensively studied postsynaptically and some of these more notable functions bear mention. At the *Drosophila* neuromuscular junction (NMJ), the system in

which our analyses are conducted, CamKII has been shown to be required for the localization of glutamate receptors (GluRs). Introduction of a postsynaptic inhibitory peptide, Ala, results in increased density of GluRIIA, conversely postsynaptic expression of constitutively active CamKII (T287D) lead to reduced GluRIIA at synapses (Morimoto et al., 2010). Furthermore, CamKII is implicated in to be involved in retrograde signaling at the *Drosophila* NMJ during synaptogenesis where postsynaptic activation of CamKII resulted in increased nerve terminal area, number of active zones, and frequency of miniature excitatory synaptic currents (Kazama et al., 2007).

Subtypes of excitatory glutamate receptors, NMDA receptors, play important roles in synaptic plasticity in the CNS. This receptor comprises multiple subunits, the core subunit termed NR1 plus one or more regulatory subunits, including NR2B, which is localized to the postsynaptic density (PSD) of glutamatergic synapses (Kennedy, 1997). Studies indicate that the NR2B subunit is a target of CamKII phosphorylation. Curiously however, phosphorylation of NMDA receptors by CamKII does not appear to change channel function, suggesting this phosporylation could lead to association between NR2B and proteins in the cytosol that do not directly modulate channel function (Kennedy, 1997). A role for autophosphorylated CamKIIα is implicated in the establishment of LTD in the rat hippocampus where activation of mGluRs leads to an increased level of phosphorylated CamKII and enhanced eIF4E phosphorylation in a CamKII-dependent manner, suggesting that CamKII-dependent protein synthesis could depend on eIF4E phosphorylation. The exact mechanism by which CamKII contributes to protein synthesis is yet unclear (Mockett et al., 2011).

The mRNA transcript that encodes the α-subunit of CamKII localizes to dendrites of hippocampal neurons and is the most widely studied locally translated neuronal transcript. The synthesis of αCamKII at the synapse is required for consolidation of memories (Weill et al., 2012). In rat hippocampal neurons following light stimulation, αCamKII mRNA is polyadenylated and locally translated (Wu et al., 1998). Proper localization of αCamKII mRNA to dendrites in mice is dependent on the endogenous CamKII 3'UTR, without appropriate targeting of αCamKII mRNA in these animals late-phase long-term potentiation (LTP), spatial memory, and LTM are disrupted (Miller et al., 2002). Studies show that upon neural stimulation, αCamKII mRNA is polyadenylated and subsequently translated locally in dendrites (Weill et al., 2002).

Of all of the many postsynaptic studies on CamKII, perhaps the most relevant to this body of work was conducted in the *Drosophila* olfactory system, examining localization and expression of CamKII mRNA following a classical conditioning paradigm used to induce formation of LTM. In this study, upon neuronal activity, CamKII mRNA is localized to dendrites, where it is rapidly translated (Ashraf et al., 2006). This transport of CamKII mRNA is mediated by components of the RISC pathway and upon stimulation, the helicase Armitage is degraded in a proteosome-dependent manner, thereby releasing bound CamKII mRNA allowing for translation to occur (Ashraf et al., 2006). This activity-regulated expression of CamKII postsynaptically in neurons in mammalian systems and *Drosophila* raises the intriguing possibility that a similar mechanism may be occurring in presynaptic axon terminals. This is diagrammed in detail in Figure 6 (Weill et al., 2002).

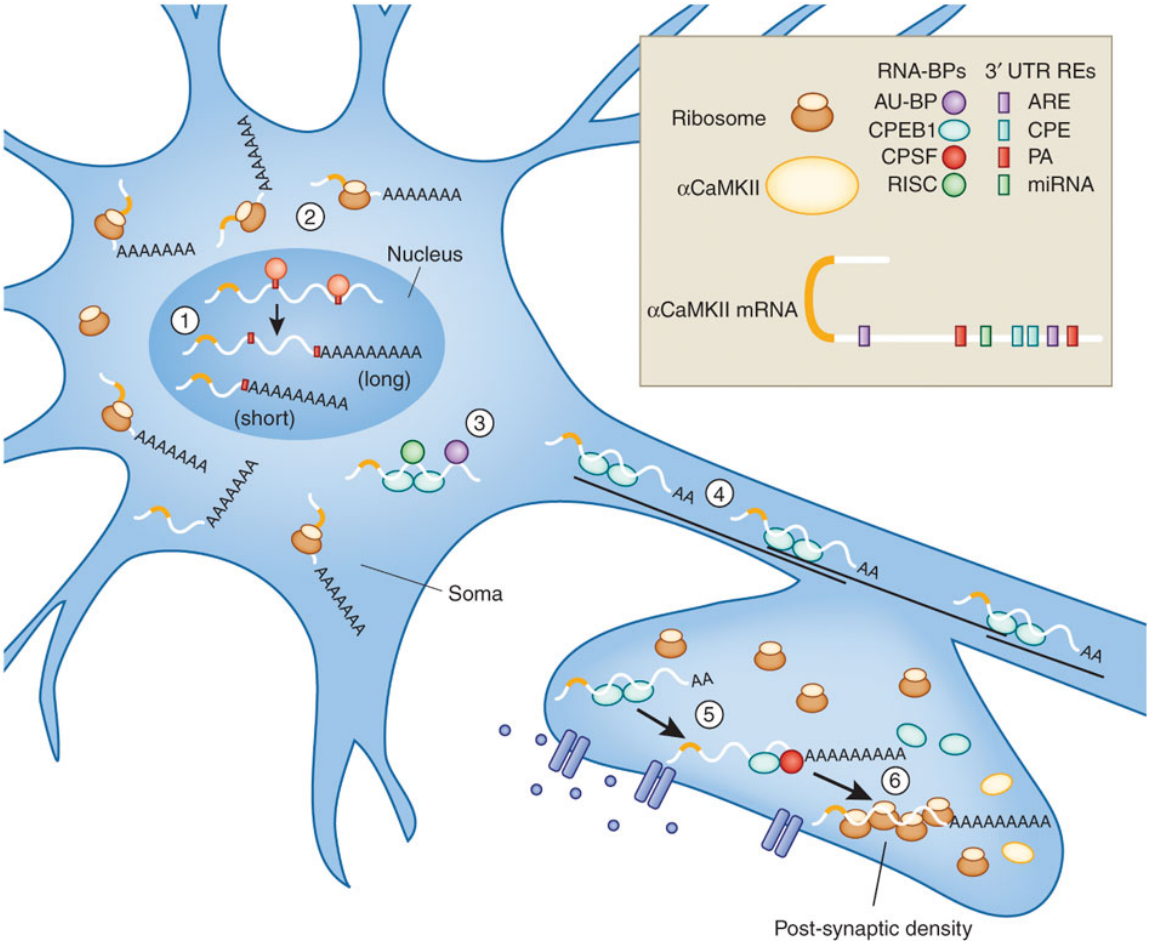

Figure 6. CamKII mRNA is recycled in neurons and local translation is triggered in the postsynaptic density by neuronal stimulation.

Reprinted by permission from Macmillan Publishers Ltd: [Nature Structural and Molecular Biology] (Weill et al., 2012), copyright (2012), license number 3393331307561.

APA of αCaMKII mRNA generates two transcripts with 3′ UTRs of different lengths (1). Both transcripts are polyadenylated in the nucleus, but the composition of the *cis*-elements in their 3′ UTR modifies their cytoplasmic fates. The short isoform is translated mainly in the soma (2), whereas miRNA binding sites, AREs and CPE mediate deadenylation, repression (3) and transport (4) of the long transcript to dendrites. Upon neuronal stimulation in the post-synaptic densities (PSD), CamKII mRNA is locally translated in dendrites (5-6).

1.3.3 Presynaptic functions of Calcium/calmodulin-dependnet protein kinase II

Using electron microscopy CamKII has been observed in nerve terminals and light microscopy has detected immunoreactivity of CamKII in axons, albeit at lower levels than in dendritic spines in both cases (Ouimet et al., 1984). Furthermore, activated phosphorylated CamKII has been shown to associate with synaptosomes in isolated nerve terminals, a Ca^{2+}-dependent neurosecretory system (Gorelick et al., 1988). The functional evidence for presynaptic CamKII came from the study of the squid giant synapse, where upon injection of CamKII into the presynaptic terminal, results in increased synaptic transmission as measured by the postsynaptic potential (Llinas et al., 1985). This result lead to the hypothesis that upon Ca^{2+} influx into the presynaptic nerve terminal, CamKII is activated and then phosphorylates synapsin I, leading to its dissociation from synaptic vesicles, which are then freed from a constraint of release (Llinas et al., 1985 and 1991).

Evidence for presynaptic function of CamKII exists in mammalian systems, where injection of autophosphorylated CamKII into isolated nerve terminals (synaptosomes) increases the release of glutamate and noradrenaline. Additionally, upon peptide inhibition of CamKII in the same system, glutamate release is inhibited, supporting the notion that activated presynaptic CamKII may remove a constraint on neurotransmitter release (Nichols et al., 1990). Another instance of CamKII playing a role in presynaptic neurotransmitter release comes from a study in which protein kinase inhibitors were applied extracellularly to examine the effects on synaptic transmission in the CA1 region of rat hippocampus. This study revealed that inhibition of CamKII

results in decreased phosphorylation of synapsin I at the CamKII specific site (serine 566 and serine 603) and lead to decreased excitatory synaptic responses, lending more credence to the idea that presynaptic CamKII activity is required for sustained synaptic transmission at this mammalian synapse (Waxham et al., 1993; Wang, 2009). CamKII has also been shown to bind to the C-terminal domain of Cav2.1 channels in presynaptic terminals and plays an important role regulating the phosphorylation of proteins including synapsin 1, and in short term synaptic plasticity (Magupalli et al., 2013).

In presynaptic motor neuron terminals in *Drosophila* CamKII is activated by Ca^{2+} released from the presynaptic ER. This release and activation is required for post-tetanic potentiation of neuropeptide secretion, this presynaptic signaling pathway results in increased dense-core vesicle (DCV) mobility and is required for synaptic plasticity (Shakiryanova et al., 2007). At the *Drosophila* NMJ, the *ether a go-go* (*eag*) potassium channel is shown to be a substrate of CamKII where it is phosphorylated at Thr-787. Inhibition of CamKII in this context leads to hyperexcitability at the larval NMJ and memory formation defects in the adult (Wang et al., 2002).

Numerous other potential targets for CamKII phosphorylation are located in the presynaptic nerve terminal including the BK channel, Cav2.1 voltage sensitive Ca^{2+} channels (P/Q type), the Ca2+ releasing channels named ryanodine receptors (RyR), and SNARES (Wang, 2009). While exact physiological significance of some of these interactions is unclear, it does seem likely that CamKII modulates neurotransmitter release presynaptically through several possible molecular mechanisms (Wang, 2009). Collectively, these studies of presynaptic targets of CamKII phosphorylation indicate that

CamKII is indeed active in both pre- and postsynaptic terminals and may be an excellent candidate for modulation of synaptic changes in response to neuronal activity.

1.4 Summary

All together, we present a central hypothesis that neuronal activity downregulates and/or destabilizes a specific subset of miRNAs present in the *Drosophila* larval CNS and/or the miRISC. Following these events, a translational up-regulation of mRNA targets involved in axon terminal growth resulting in an activity-dependent increase in presynaptic growth at the larval NMJ. To this end, we set out to identify and characterize activity-regulated miRNAs as well as pertinent mRNA targets whose local translation is required for new synaptic growth following neural activity.

CHAPTER TWO: MATERIALS AND METHODS

2.1 Fly stocks

Fly stocks were all raised on standard Bloomington media with the exception of Channel Rhodopsin 2 (ChR2) expressing fly lines. In order to facilitate ChR2 activity *in vivo*, lines expressing ChR2 were raised on standard Bloomington media supplemented with 100 mM all-trans retinal as described previously (Nagel et al., 2002; Schroll et al., 2006). All fly stocks were raised at 25°C in diurnal incubators. *Canton S, w^{1118}, C380-Gal4, UAS-ChR2, UAS-$wg^{HMS00794}$, UAS-$lar^{HMS00822}$, camkii* RNAi lines, fly strains were all obtained from the Bloomington *Drosophila* stock center. The *miR-8Δ1* and *miR-8Δ2* deletion flies were a gift from S. Cohen (Karres et al., 2007). *UAS-miR-8 SP #10* (miR-8 sponge) flies were a gift from D. Van Vactor (Loya et al., 2009).

2.2 Activity assays

ChR2 stimulation was executed using an apparatus made in the lab by former graduate student Bob Sand based on general descriptions described previously (Ataman et al., 2008; Schroll et al., 2006). Briefly, nonwandering third instar larvae were collected, washed twice with haemolymph-like dissection buffer (HL-3; Stewart et al., 1994), and placed into the stimulation chamber. The larvae were run through five spaced 5-minute stimulation steps with each step composed of a series of cycles (2 seconds on, 3 seconds off) where emission of 470 nm light from two blue LEDs (Luexon V; Luexon

Star) was controlled by a pulse stimulator (A-M Systems) essentially as previously described (Ataman et al., 2008). Following each 5-minute stimulation step the larvae were allowed to rest for a period of 15 minutes. Upon completion of the final 5-minute stimulation, the larvae completed a final resting step 134 minutes in length. Control larvae were subjected to identical conditions but not subjected to the stimulation cycles. Following stimulation paradigms, larval preparations were either processed for NMJ analysis or the CNS was explanted for RNA isolation. CNS preparations included the two optic lobes and the ventral ganglia, with all attached discs removed. The high K^+ stimulation paradigm was performed essentially as previously described (Ataman et al., 2008; Freeman et al., 2011; Nesler et al., 2013). Wandering third instar larvae were collected and semi-dissected in HL-3, leaving the CNS intact. To perform the semi-dissections, larvae were pinned at the anterior and posterior ends being careful not to stretch the larvae. A cut was then made between the trachea of the larvae and the guts gently teased out so that the CNS is readily exposed to the HL-3. Before proceeding with the paradigm, all larvae were checked to ensure the CNS remained intact following the semi-dissection. Next, the larvae were subjected to a stimulation paradigm where they were treated with high K^+ HL-3 (90mM KCl) adjusted for osmolarity before sterile filtering and adjusted to a pH of 7.3 before each use (Roche et al., 2002; Nesler et al., 2013). The larvae were stimulated in a pattern of 2, 2, 2, 4, and 6 minute pulses (5x high K+ stimulation) where each pulse step was a stimulation period where the larvae were immersed in 90mM K+ HL-3. For 3x high K^+ stimulations, larvae were stimulated in a pattern of 2, 2, and 2 minute pulses. Each stimulation step was separated by a 15-minute rest period in 5mM K+ (normal) HL-3, concluding with a 74 minute rest period following

the last stimulation. Control larvae were subjected to identical conditions except the high K^+ HL-3 was replaced with normal HL-3 during each pulse step. Upon completion of the stimulation paradigm, arvae were either processed for NMJ analysis or the CNS was explanted for RNA or protein isolation. CNS preparations included the two optic lobes and the ventral ganglia, with all attached discs removed.

2.3 Microarray analysis

Microarray analysis was conducted as described in Nesler et al., 2013. For miRNA array analysis, two genotypes (w^{1118} and *UAS-ChR2 x C380-Gal4*) were used. ChR2-expressing larvae were taken through either the light- or mock-stimulation paradigm. At the end of each paradigm, 30–50 larval CNS (ventral ganglia+optic lobes) samples were manually dissected, eye imaginal discs and residual body wall removed, and collected in lysis buffer on ice. Total RNA was extracted using the miRCURY RNA Isolation kit (Exiqon) yielding ~125 ng of total RNA per CNS. RNA was eluted with 40 µl of RNAse free water (Ambion), flash frozen using liquid nitrogen, and stored at −80°C. miRNA microarray profiling was carried out at Exiqon using standard protocols. Briefly, each RNA sample was labeled with Hy3 and a common reference standard with Hy5 using the miRCURY LNA Array power labeling kit (Exiqon). The common reference sample consisted of equal amounts of RNA from w^{1118}, ChR2 light, and ChR2 mock-stimulated CNS samples. The Hy3-labeled samples and the Hy5-labeled reference RNA sample were mixed pair-wise and hybridized to the miRCURY LNA array version 11.0 Other Species (Exiqon), which contains capture probes targeting all *Drosophila* miRNAs registered in miRBASE version 14.0. Exiqon analyzed all miRNA array data. Briefly, image analysis was carried out using the ImaGene 8.0 software (BioDiscovery, Inc.). The

quantified signals were background corrected (Normexp with offset value 10) and normalized using the global Lowess (locally weighted scatterplot smoothing) regression algorithm (Ritchie et al., 2007). Relative expression levels were calculated as the $\log_2$ normalized signal intensity between the Hy3 and Hy5. Exiqon determined the presence or absence of specific miRNAs in each sample Changes in expression levels (fold changes) were calculated between the w^{1118}, ChR2 light-, and ChR2 mock-stimulated groups (Nesler et al., 2013).

2.4 RT-qPCR analysis

RT-qPCR analysis was conducted as described in Nesler et al., 2013. Three biological replicates of one genotype (*Canton S*) and two treatment groups (high K^+ or mock stimulation were used). At the end of each paradigm, 40 larval CNS (ventral ganglia+optic lobes) were dissected from the stimulated larvae. CNSs were carefully dissected by hand, removing the eye imaginal discs and any residual body wall tissue. Once CNS had been isolated, they were stored in lysis buffer on ice until RNA extraction. Total RNA was extracted using the miRNeasy RNA Isolation kit (Qiagen) resulting in a yield of ~150 ng RNA per CNS. 40 μl of RNAse free water (Ambion) was used to elute the RNA, a small aliquot was removed for quality control and the rest was then flash frozen, and stored at -80°C. RNA quality control was performed using an Experion automated electrophoresis system (BioRad). Samples with a RNA quality indicator (RQI) score <7 were discarded and re-extracted. Simultaneously, using the miScript reverse transcription kit (Qiagen), ~6 μg of total RNA per replicate was converted to cDNA. Using the miScript SYBR Green PCR Kit (Qiagen), three technical replicates of each biological replicate were amplified. Following melt curve analysis it

was determined that 14 of these primers amplified non-specific PCR product and were excluded from subsequent analysis. Three primer assays failed to amplify product in all biological replicates and were likewise excluded. The U1 snRNA (verified by BestKeeper software v1.0; Pfaffl et al., 2004) was used to normalize the results of the analysis. All assays were performed using an iCycler thermocycler equipped with the iQ5 real-time PCR detection system hood and controlled by the iQ5 optical system software v1.2 (Bio-Rad). Results from three technical replicates were averaged to generate C_t values for each biological replicate. Then, analysis of differential fold change based on C_t results was performed using the Livak ($\Delta\Delta C_t$) method (Livak and Schmittgen, 2001). Changes in relative miRNA expression between treatment groups were calculated yielding a fold change between the high K^+ stimulated and pseudostimulated control groups.

2.5 Construction of transgenic lines

To generate pri-miRNA expression transgenes, PCR primers were designed to amplify a sequence ~200 nt upstream and downstream of each miRNA hairpin from genomic DNA extracted from third instar *Drosophila larvae* (Silver et al., 2007). Using the Gateway cloning system (Invitrogen) the pri-miRNA PCR products were cloned into pENTR and then into the 3'UTR of mCherry in pUASM. This allowed us to drive the expression of our miRNA constructs tagged with mCherry in a tissue-specific manner using the UAS-Gal4 driver system.

2.6 Immunohistochemistry

To study NMJ morphology, third instar larve were dissected and body wall preparations were prepared to reveal the musculature for subsequent confocal analysis. For all activity assay experiments, dissections were carried out in the normal 5mM K^+ HL-3 used during the final rest period. For all other dissections, a calcium-free HL-3 solution was used as previously described (Stewart et al., 1994; Pradhan et al., 2012). Larval preparations were then fixed for a period of 20 minutes in 3.5% paraformaldehyde. Fixation was followed by a series of three 10-minute washes in 1x phosphate buffered saline (PBS) followed by one 10-minute wash in 1xPBS plus Triton X detergent to permeabilize the membrane. Next, the larval preps were incubated in a blocking solution to prevent non-specific antibody binding. Dilutions of primary antibody were made using the blocking solution and preps were incubated overnight at 4°C. Primary antibodies used were mouse anti-Dlg (Developmental Studies Hybridoma Bank), goat anti-HRP Dylight 594 or 649 (Jackson Labs), mouse anti-CamKII (CosmoBio), rabbit polyclonal anti-CamKII (a gift from S. Kunes), and rabbit anti-DVGLUT (Daniels et al., 2008). Following overnight incubation, larval preps were washed six times for 10 minutes apiece in 1xPBS+Triton X and then incubated for 1 hour in secondary antibody. Secondary antibodies used were Alexa 488-conjugated anti-mouse IgG (Molecular Probes) and Alexa 488-conjugated anti-rabbit secondary antibody (Molecular Probes). Secondary antibody was washed off in a series of two 10-minute washes in 1xPBS+Triton followed by a final 10-minute wash in 1xPBS. Preps were then mounted on slides using VECTASHIELD Mounting Media with Dapi (Vector Labs) and stored at -20°C until imaging.

2.7 NMJ morphological analysis

Larvae were imaged at abdominal segment 3, muscle 6/7 on an Olympus FluoView FV1000 scanning confocal microscope. All images were obtained using either a 60X (N.A. 1.35) or 100X (N.A. 1.4) objective and generated from stacks collected at intervals of 0.8 μM or a single 0.8 μM section where indicated. Stacked images were combined using FV1000 imaging software.

Analysis of boutons and ghost boutons was done essentially as described previously (Rohrbough et al., 2000; Ataman et al., 2008). Briefly, for standard NMJ analysis 1B (big) and 1S (small) boutons were counted using the Cell Counting plugin for ImageJ v1.45 (NIH). Boutons for standard analysis were counted only if they stained positively for presynaptic HRP and postsynaptic DLG. For ghost bouton analysis we implemented a 4-pixel size cutoff to eliminate ambiguity in what size constitutes a bouton. Structures were counted if they met this 4-pixel size criterion and stained positively for presynaptic HRP but were devoid of postsynaptic DLG staining. This analysis was done using Adobe Photoshop so that pre- and postsynaptic color channels could be readily toggled to evaluate the structures.

To analyze CamKII intensity relative to HRP or DVGLUT two different methods were used to define regions of interest (ROIs), both using ImageJ software. The initial steps in both processes were identical. First, the image color channels were split into the red, green, and blue channels (Image>Color>Split Channels) and all images were uniformly zoomed to 150% for analysis. Next, the ROI manager (Analyze>Tools>ROI Manager) was opened to compile a list of ROIs as defined by either boutons demarked by HRP or DVGLUT positive puncta from which measurements were taken. ImageJ was set to take relevant measurements (Analyze>Set Measurements…). For these purposes “mean gray

value" was used as our measurement of intensity for each ROI. For HRP images specifically, ROIs were selected by using the "freehand selections tool" carefully tracing around each individual bouton and adding them to the ROI list ("command+T" using a Mac computer). For DVGLUT puncta, ROIs were selected using a thresholding approach. First, the image in the DVGLUT channel (red) was thresholded by opening the threshold menu (Image>Adjust>Threshold) and selecting "Auto" followed by "Apply". Next, using the "Wand (tracing) tool" the DVGLUT puncta were selected and added to the ROI manager for measurement ("command+T"). Next, the image was closed and re-opened, next the colors were split again, keeping all of the data points in the ROI manager. This was done so that the red channel was no longer thresholded due to the fact that thresholding the image eliminates the variability in intensity in the puncta by turning them completely white. Measurements were taken for both the CamKII (green) and DVGLUT (red) channels for "mean gray value".

For both data sets measurements for each NMJ were recorded in an Excel spreadsheet. Following quantification for the entire data set, a mean value for green intensity (CamKII) and red intensity (HRP or DVGLUT, depending on the experiment) was calculated for each NMJ. This was done so that the data was not biased in favor of those NMJs containing a greater number of ROIs. Next, a ratio was calculated for green/red for each NMJ and recorded. Data was then exported to Prism for statistical analysis. For all fluorescence comparison experiments larvae were labeled and stained in the same dish and imaged under identical conditions.

Unless otherwise indicated, these represent paired NMJs from both hemisegments of ≥10 larvae. All images were randomized and scored blindly. No obvious differences in muscle size between genotypes or treatment groups were observed.

2.8 miRNA target analysis

Putative mRNA targets of miRNAs were identified using the miRecords online target prediction resource (http://mirecords.biolead.org; Xiao et al, 2009). For our purposes we restricted lists to targets that were predicted by three or more databases with the rationale that more predicted interactions would more likely indicate a true miRNA/mRNA interaction. To determine overlap between predicted targets of miRs-8, -289, and -958, lists of targets predicted in three or more databases were compiled and these lists were then cross-referenced using Microsoft Excel. Initial analysis using functional cluster analysis, we uploaded each list of putative target genes into the DAVID bioinformatics resource (http://david.abcc.ncifcrf.gov; Database for Annotation, Visualization and Integrated Discovery; Huang et al., 2009a; Huang et al., 2009b). We used the "Gene ID Conversion Tool" to convert all gene names to their Flybase gene ID number for these analyses. Default parameters were used (medium stringency) to determine enrichment scores within functional clusters. Benjamini-Hochberg corrected p-values were calculated by the DAVID software. For our purposes, non-neuronal-related clusters were excluded from subsequent analysis.

2.9 Cell culture, transfections, and luciferase assays

Plasmids for luciferase reporter assay experiments are identical to those described previously (Rehwinkel et al., 2006) with the exception that the firefly luciferase (Fluc) 3'UTR reporter and miRNA overexpression plasmids have been converted into Gateway destination vectors (Invitrogen) for ease of cloning. All mRNA target reporter vectors contained endogenous 3'UTRs and poly(A) signals. Cell culture experiments were performed using *Drosophila* Schneider 2 (S2) cells (S2-DRSC Line 181 from the *Drosophila*

Genomics Research Center) cultured in Schneider's media. Transfections were performed in three biological replicates in 6-well plates and transfected using Effectene (Qiagen). The transfection mixtures were composed of 0.1 μg of the Fluc 3'UTR mRNA reporter plasmid, 0.4 μg of the *Renilla* luciferase (Rluc) transfection control plasmid, and 0.5 μg of either a miRNA expression vector or an empty vector control identical to the miRNA expression vector except that it is devoid of a cloned pri-miRNA sequence. Cells were incubated at room temperature for three days prior to experimental analysis. Following the three day incubation period the cells were thoroughly scraped from the plates and pipetted up and down several times to ensure a uniform mixture of cells in each technical replicate. Luciferase activity for each biological replicate was measured in three technical replicates using a Synergy HT microplate reader (Biotech) in 96-well white opaque plates (Costar) using a dual-luciferase reporter assay system (Promega).

2.10 Western blotting

Western blots were conducted on protein extractions from *Drosophila* larval CNS at the 3rd instar stage from stimulated or unstimulated larvae as indicated. To extract protein, an equal number of larval CNS (15 was optimal) were extracted from larvae immediately the stimulation paradigm and placed into 150μL of NuPage sample loading buffer kept on ice. Following extraction, CNS were homogenized using a hand-held mortar and pestle with disposable tip. Throughout homogenization the solution was scraped off of the pestle using a pipette tip and the mixture was spun down to minimize sample loss resulting from foaming. Following homogenization, samples were spun at a speed >16,000g in a 4C cooled centrifuge. Following centrifugation using a p200 pipette (being careful not to touch the tip to the bottom of the tube and drawing solution up very slowly as to not dislodge the pellet

which cannot be seen in NuPage buffer) supernatant was drawn off in increments of 25μL. Subsequently DTT was added based on the final volume of NuPage/protein solution. Following the addition of dithiothreitol (DTT), samples were boiled for 5 minutes at 95C on a heat block then placed immediately on ice before loading into a protein gel.

Protein samples were loaded in volumes of 2.5μL per lane for this analysis. Gels were run at 150 volts until adequate separation had been achieved. Prior to gel transfer, the SDS gel and nitrocellulose membrane were both equilibrated in transfer buffer on a slow shaker for 15 minutes. Gel transfers to nitrocellulose membranes for Western blotting were run either overnight in a 4C cold room at 22V or for 55 minutes at 100V on a stir plate with the addition of an ice pack. Following gel transfer, membrane was labeled with antibody. This process began with a one hour blocking step in 5% dry milk solution followed by either an incubation in primary antibody in a sealed pouch on a fast shaker either: a) overnight at 4C or b) for two hours at room temperature. Primary antibodies used were mouse anti-CamKII (1:4000) and rabbit anti-β actin (1:1000) made in 5% dry milk solutions. Following primary antibody labeling, membranes were washed twice quickly in wash solution followed by three 10-minute washes at room temperature on the shaker. Following washes, secondary antibody was applied. Secondary antibody labeling was also done in a sealed pouch at the concentration of 1:3000 in all cases (anti-rabbit HRP and anti-mouse HRP were both used). After one hour, membranes were washed under the same conditions as they were following primary antibody. All blots were developed on film.

2.11 Statistical analysis

All statistical analysis including graphing was performed using Prism v6.0 (GraphPad software) and statistical significance was deemed to be at $p<0.05$. The specific tests used in

each experiment are indicated in the figure legend for each figure. Where indicated, data have been normalized to controls and are presented as mean ±SEM. In the NMJ experiments, the numbers on each column indicate the number of individual NMJs quantified for that group. For activity assay experiments, statistical outliers and their paired NMJ from the same larvae were removed using the ROUT method (robust regression and outlier removal; Q=1%; Motulsky et al., 2006). For fluorescence quantification comparison experiments, mean intensity values were taken for the boutons of each NMJ in both the red and green channels. A ratio was then calculated between the green (presynaptic) and red (postsynaptic) channel to give a green:red ratio for each NMJ rather than per bouton as to not bias the results in favor of NMJs that contained a greater number of boutons.

CHAPTER THREE: THE microRNA PATHWAY AND ACTIVITY-DEPENDENT SYNAPTIC GROWTH

3.1 Spaced depolarization induces rapid new synaptic growth at the *Drosophila* NMJ

Of central importance to our studies is the identification of differentially regulated miRNAs following synaptic stimulation. To achieve this goal we took advantage of two established spaced training paradigms that have been shown to induce new synaptic growth at the *Drosophila* larval NMJ in the form of "ghost boutons". Ghost boutons are presynaptic structures that represent new axon terminal growth at the *Drosophila* NMJ. These structures are observed at low frequency during development but upon stimulation, significant increases in their formation can be induced. Ataman et al. demonstrated that these structures are completely devoid of postsynaptic structures but do contain synaptic vesicles indicative of a yet undifferentiated bouton state and confirmed in live imaging studies that ghost boutons formed during development give rise to fully mature boutons (Ataman et al., 2006 and 2008). More recently, other studies have demonstrated that during development at the *Drosophila* NMJ there is a significant amount of remodeling that occurs, including the production of presynaptic membrane debris accompanied by appearance and shedding of undifferentiated ghost boutons (Fuentes-Mendel et al., 2009). This process of synapse elimination may be analogous to processes at the mammalian

NMJ involving axonal retraction of multiple nerve innervations on a single muscle cell (Chung and Barres, 2009).

The two paradigms we used to assay new synaptic axon terminal growth involved fundamentally different mechanisms of stimulation. The first paradigm stimulates semi-dissected larvae with a high (90 mM) K^+ solution leading to robust new synaptic growth in the form of "ghost boutons" (Ataman et al., 2008). The second paradigm we used took advantage of an optogenetic approach to stimulate synaptic activity in intact larvae specifically in motor neurons (Ataman et al., 2008; Nagel et al., 2002; Schroll et al., 2006). This second approach was designed to address any potentially non-physiological effects that could be induced by global depolarization induced by exposure to high K^+ solutions. While this second approach is arguably more physiological, it resulted in a much less robust ghost bouton induction.

In our first experiments using *Canton S* larvae and the high K^+ stimulation paradigm we see a baseline of ~1 ghost bouton per NMJ in pseudostimulated control larvae (Figure 1A-B). Following the five time spaced-depolarizaiton paradigm with the 90 mM K^+ solution we see a robust increase in new synaptic growth with a range of 4-6 ghost boutons per NMJ, a roughly 6-fold increase (Figure 1A-B; $p<0.0001$). Our second set of experiments took advantage of the inducible transgenic light-activated ion channel, Channelrhodopsin-2 (ChR2). Taking advantage of the UAS-Gal4 tissue-specific driver system in *Drosophila*, we specifically drove expression of ChR2 in motor neurons using the motor neuron-specific driver C380 (C380-Gal4>UAS-ChR2). The number of ghost boutons in unstimulated control larvae of this treatment group is consistent with that of the previous group, yielding ~1 ghost bouton per NMJ (Figure 1B). While this second

approach is more physiological it is substantially less robust. Stimulated larvae displayed only ~2 ghost boutons per NMJ following the light stimulation paradigm, a fold increase of around 2.5 (Figure 1B; $p<0.01$). This increase is not as dramatic as in the high K^+ stimulation paradigm, however it is still statistically significant and furthermore is consistent with published results (Ataman et al., 2008).

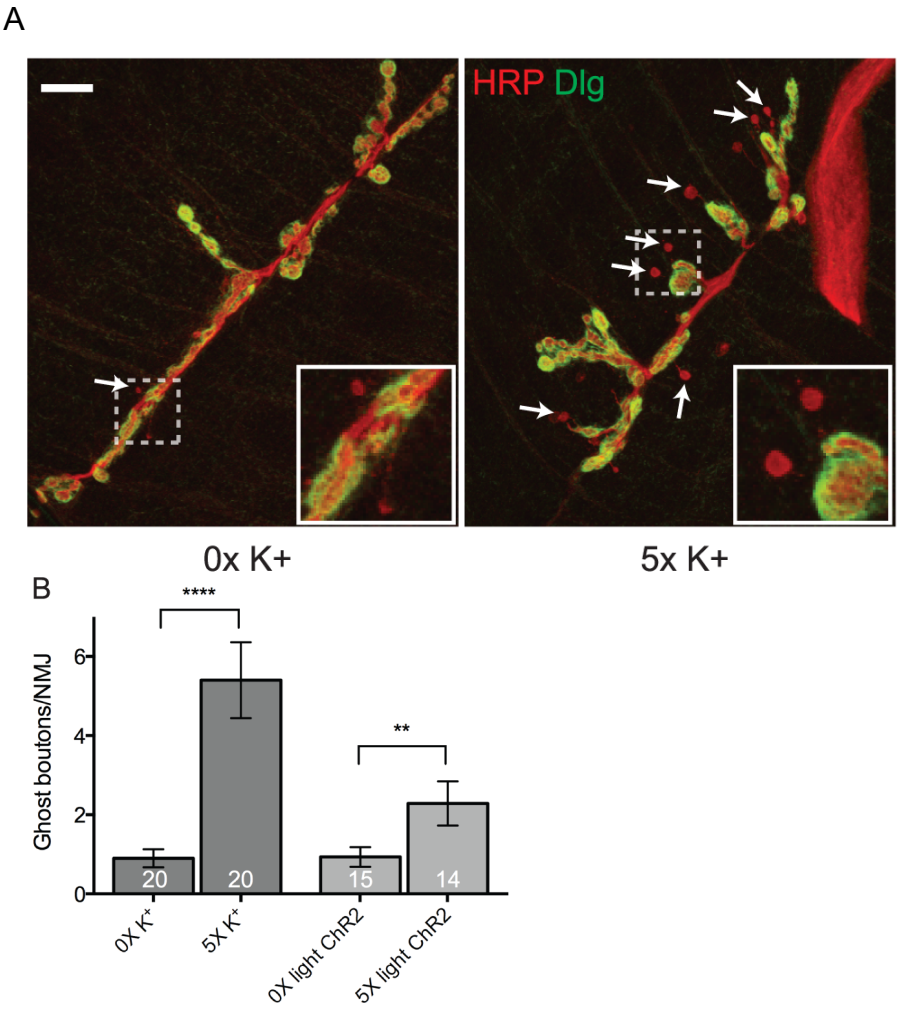

Figure 7. Acute spaced stimulation induces the formation of undifferentiated ghost boutons.

This figure is reproduced as published in Nesler et al., 2013. Former masters student Bob Sand performed the experiments presented here. Images were re-quantified using standardized criteria for ghost bouton quantification as outlined in the materials and methods section by Katherine Nesler.

(A) A representative *Canton S* third-instar NMJ at muscle 6/7 in abdominal segment 3 that was double stained with antibodies against presynaptic membrane marker, horseradish peroxidase (HRP; red) and postsynaptic discs large (DLG; green) after being subjected to 0x (control 5 mM) or 5x (90 mM) spaced depolarization. Arrows point at ghost boutons (HRP+ DLG-). Each inset corresponds to the indicated region (dashed box) and is blown up to help visualize ghost boutons. Scale bar indicates 20 μM. (B) Quantification of the number of ghost boutons per NMJ in *Canton S* (high K^+ stimulated) or animals expressing the transgenic light-gated ion channel, ChR2, in motor neurons (C380-Gal4>UAS-ChR2). There are 1-2 unpaired NMJs included in each larval treatment group. Error bars indicate the mean ± SEM. STATISTICS: Student's t-test. ** $p<0.01$ and **** $p<0.0001$.

3.2 Identification of microRNAs present in the *Drosophila* larval CNS

After determining that we were able to make both activity stimulation paradigms work in our hands we sought to determine which miRNAs were present in the larval CNS, and second which were differentially expressed in response to neuronal activity. To achieve this goal we used a miRNA microarray based analysis approach. This microarray chip covered 35% of the currently identified 426 mature *Drosophila melanogaster* miRNAs included in the latest iteration of miRbase (20.0; Griffiths-Jones et al., 2006 and 2008; Kozomara and Griffiths-Jones, 2011 and 2014). To begin, we used the ChR2 light-induced stimulation paradigm to induce new synaptic growth and differential miRNA expression (Figure 7B). Following stimulation, RNA was isolated from isolated CNS from control (w^{1118}) and unstimulated (0x mock) or stimulated (5x light) ChR2-expressing larvae (C380>UAS-ChR2). We identified 79 miRNAs expressed in the larval CNS, although surprisingly we did not observe a 2-fold change in expression (our arbitrary cutoff for biological significance) following the stimulation paradigm in any of these miRNAs (Figure 8A-B). We believe that while this ChR2 approach is arguably a more physiological stimulation paradigm, it did not generate a robust increase in new synaptic growth as assayed by ghost bouton formation. It may not be strong enough to induce significant changes in miRNA expression detectable over basal miRNA levels isolated from the CNS of unstimulated control animals.

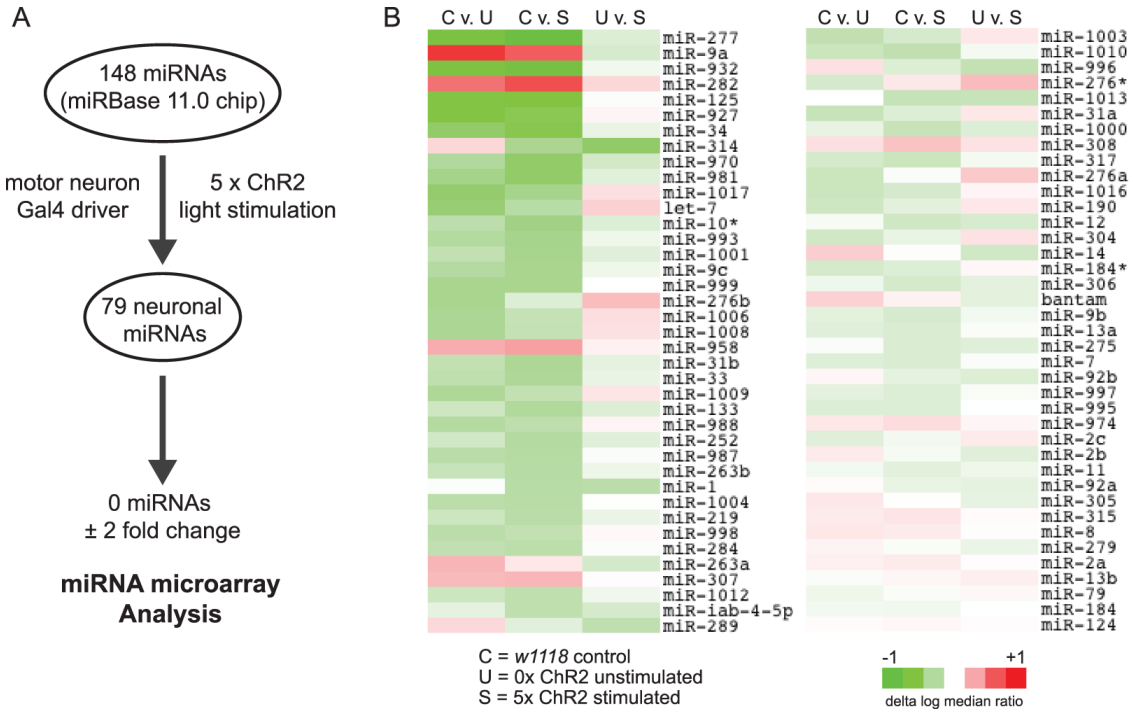

Figure 8. miRNA expression profile of the *Drosophila* larval CNS.
This figure is reproduced as published in Nesler et al., 2013. Former masters student Bob Sand performed the experiments presented here.
(A) Flowchart depicting miRNA microarray analysis. The expression of 79 mature miRNAs was detected in the *Drosophila* larval CNS. (B) Heat map showing fold-change of miRNAs in the CNS of W^{1118} (control or "C"), ChR2 mock-stimulated (unstimulated or "U"), and ChR2 light stimulated (stimulated or "S"). No neuronal miRNA exhibited greater than a 2-fold change in expression levels following ChR2 light stimulation. The largest differences observed were between the W^{1118} and C380-Gal4>*UAS-ChR2* genotypes.

While we did not see a significant change between stimulated and unstimulated ChR2 larvae (Figure 8B; "U vs. S" column), notably we did see between a 1.5- and 1.9-fold change in relative expression levels of eight miRNAs between our genetic background control (W^{1118}) and both ChR2 treatment groups (Figure 8B; "C vs. U" and "C vs. S") indicating a genotypic difference between these two lines. While this difference in miRNA expression between control and ChR2 larvae is not attributable to any activity-related process, it is possible that these eight miRNAs play at least a partial role in control of synaptic growth during larval development. This is based on our unpublished observations that the NMJs in W^{1118} larvae tend to be complex with a greater total number of boutons than more wild type genotypes we work with, such as *Canton S*.

3.3 Identification of activity-regulated microRNAs

Following the microarray analysis using the optogenitcs approach, we were unable to identify any miRNAs that were significantly up- or downregulated following neuronal activity. Nevertheless, we still strongly believed that miRNAs could play a critical role in the modulation of activity-dependent neuronal growth, so we modified our approach in two important ways. First, we switched to the more robust high K^+ stimulation paradigm for subsequent analyses allowing for global depolarization and stimulation of the entire larval CNS rather than in a subset of neurons as in the ChR2 paradigm (Figure 8A-B). Second, we developed an RT-qPCR assay to identify mature miRNA levels following high K^+ stimulation. Following primer quality control we proceeded to screen 62 of the 79 neuronal miRNAs we had identified using microarray analysis using our newly designed RT-qPCR approach (Figure 8B).

We conducted the high K^+ stimulation paradigm using third instar larvae of the *Canton S* wild-type genotype and isolated RNA from dissected CNS from pseudostimulated (0x mock) or stimulated (5x high K^+) treatment groups (Figure 9A). MiRNA expression profiles were analyzed and compared to determine if any miRNAs exhibited a 2-fold biologically significant and/or a statistically significant change in mature miRNA levels between the stimulated and pseudostimulated control groups. We found five miRNAs met our criteria for significance and appeared to be activity-regulated (miRs-1, -8, -289, -314, and -958; Figure 9B-C; $p<0.05$). Notably, all five of these activity-regulated miRNAs were rapidly downregulated following high K^+ spaced depolarization, no miRNAs were upregulated by a significant margin (Figure 9B).

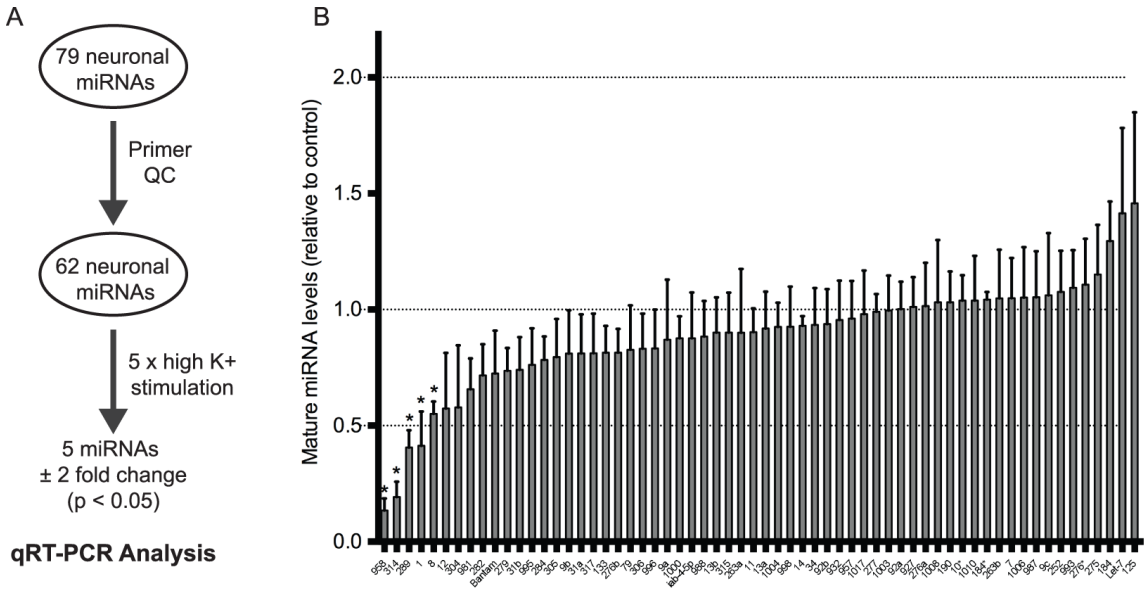

C

	fold change	P value
miR-958	7.5	0.02
miR-314	5.2	0.02
miR-289	2.5	0.01
miR-1	2.4	0.05
miR-8	1.8	0.04
miR-12	1.7	0.18
miR-304	1.7	0.17

Figure 9. miRs-1, -8, -289, -314, and -958 are rapidly downregulated by activity.
This figure is reproduced as published in Nesler et al., 2013. Former masters student Bob Sand performed the experiments presented here.
(A) Flowchart showing RT-qPCR analysis. 62 of 79 mature neuronal miRNAs were screened by RT-qPCR (see methods). (B) Five miRNAs were determined to exhibit either a 2-fold or statistically significant downregulation in expression levels following spaced high K^+ depolarization. Error bars indicate the mean ± SEM. STATISTICS: One-way ANOVA with a Tukey's post-hoc test (n = 3 replicates). * $p<0.05$. (C) Table showing fold downregulation and p-values for each activity-regulated miRNA. While not statistically significant, miRs-12 and -304 show a 1.7-fold activity-dependent downregulation. miRs-12 and -304 are both located in the miR-12/304/283 cluster.

We determined that two miRNAs that belong to the miR-12/304/283 cluster follow immediately after the five activity-regulated miRNAs but do not meet the criteria for significance (Figure 9C; miRs-12 and -304). While miR-283 is also a member of this cluster it was not detected in our screen of mature miRNAs present in the larval CNS (Figure 8B) and was thus excluded from these analyses. This is not surprising because published evidence demonstrates that while these three miRNAs are clustered together, miR-283 does not display an expression profile that correlates with that of miRs-12 and -304 (Ryazansky et al., 2011). While miRs-12 and -304 did not meet our criteria for significance, they bear mention because observing two miRNAs possibly under common transcriptional control being affected identically in this paradigm strengthens our other observations. Furthermore, we observed a significant correlation (Figure 10; $R=0.37$; $p<0.001$) between the optogenetic ChR2 microarray approach and the results of the high K^+ RT-qPCR approach (Figures 8 and 9, respectively) even though the results of the high K^+ stimulation are far more robust.

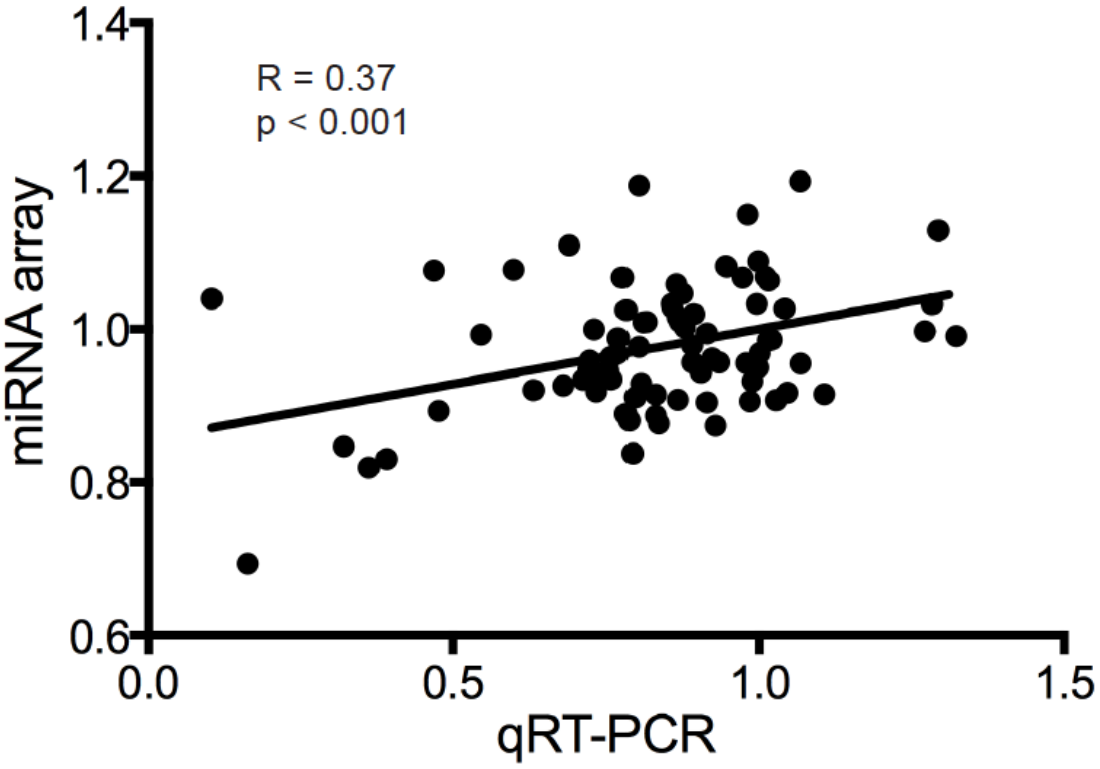

Figure 10. Correlation between ChR2 light and high K^+ stimulation paradigms.
This figure is reproduced as published in Nesler et al., 2013.
Regression analysis between calculated fold expression levels of all miRNAs analyzed in both the ChR2 microarray and high K^+ RT-qPCR experiments. The fitted regression line is shown. There is a highly statistically significant correlation in expression levels across all miRNAs analyzed ($p<0.001$).

3.4 Validation and characterization of activity-regulated microRNAs.

The observation that five mature miRNAs are rapidly downregulated in response to neuronal activity suggests that these miRNAs are involved in activity-dependent synaptic growth. However these data are merely correlative and conclusions cannot be drawn from them alone. Based on these observations we postulated that some (or all) of the activity-regulated miRNAs likely control the expression of neuronal mRNAs whose expression is required for activity-dependent synaptic growth (Figure 11A). To test this hypothesis we turned to the UAS-Gal4 driver system to examine the effects of misexpression of transgenic primary miRNA (pri-miRNA) constructs designed to overexpress miRs-1, -8, -289, -314, and -958 individually in a tissue-specific manner, in this case larval motor neurons. We believed that if these miRNAs were overexpressed in a manner that did not allow for transcriptional downregulation following synaptic activity we would observe a reduction in new synaptic growth following stimulation.

Transgenic and genetic background control (w^{1118}) larvae were crossed to motor neuron specific driver C380-Gal4 and pseudostimulated or stimulated via the high K^+ depolarization paradigm. Pseudostimulated genetic background control larvae (C380-Gal4>w^{1118}) displayed ~2 ghost boutons per NMJ and 4-6 following high K^+ depolarization, a roughly 3-fold increase (Figure 11B; $p<0.0001$).

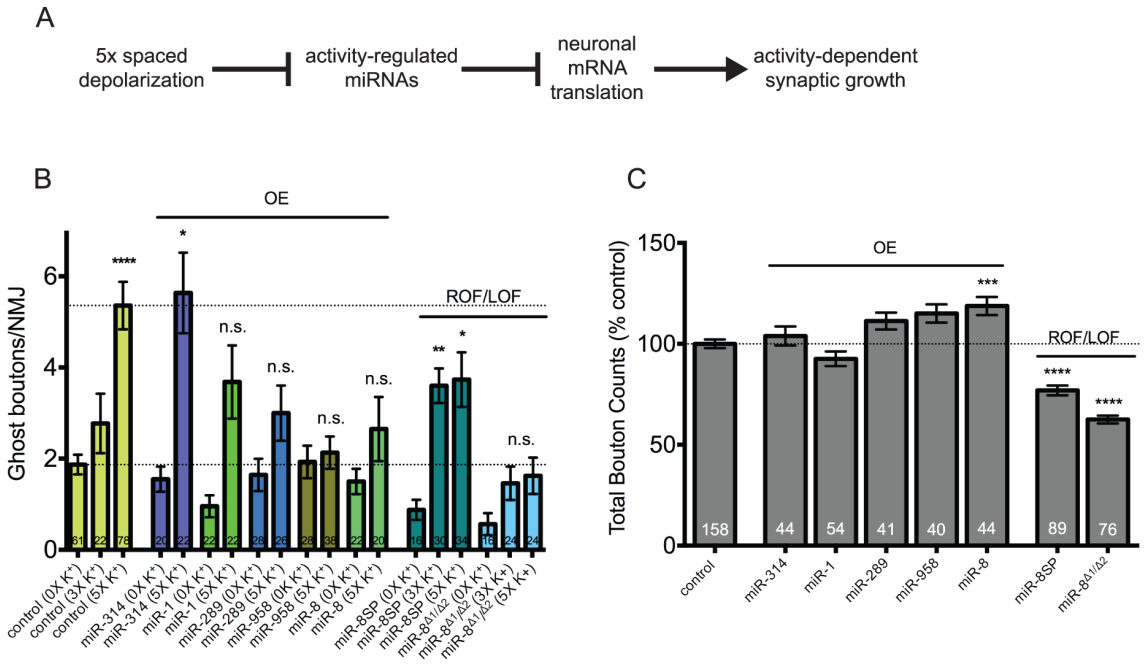

Figure 11. miRs -8, -289, and -958 are required for activity-dependent ghost bouton formation at the larval NMJ.

This figure is reproduced as published in Nesler et al., 2013.

(A) Model for miRNA-mediated control of activity-dependent synaptic growth at the NMJ. In unstimulated motor neurons, key activity-regulated miRNAs negatively regulate the expression of target mRNAs involved in activity-dependent synaptic growth. In contrast, our data suggests that acute spaced stimulation results in the rapid downregulation of mature miRNA levels resulting in the increased translation of target mRNAs and subsequent rapid activity-dependent synaptic growth. (B) Transgenic pri-miRNAs for miRs-1, -8, -289, -314, or -958 were misexpressed in larval motor neurons using the *C380-Gal4* driver (e.g. genotype *C380-Gal4/+; UAS-pri-miR/+*). Also examined were miR-8 knockdown (*C380-Gal4/+; UAS-miR-8SP/+*) or loss-of-function ($mir\text{-}8^{\Delta1/\Delta2}$) lines. Ghost boutons per NMJ were quantified under conditions of mock (0x), intermediate (3x) or high (5x) K^+ stimulation. Compared to matched unstimulated controls, misexpression of miRs-8, -289, and -958 did not result in a significant increase in ghost boutons following 5x high K^+ stimulation. In contrast, miR-8 knockdown (*UAS-miR-8SP*) and deletion ($mir\text{-}8^{\Delta1/\Delta2}$) larvae showed an enhanced ability to respond to intermediate stimulation. (C) Quantification of the combined number of synaptic boutons (stimulated and unstimulated) at the same NMJs assayed in (B). No significant difference in total bouton number was observed between unstimulated and stimulated NMJ within any miRNA genotype (data not shown). Note that only miR-8 has a significant effect on total bouton numbers when compared to controls (*C380-Gal4/+*). This suggests that miR-8 has a function in both ghost bouton maturation and development. (B-C) OE = overexpression; ROF = reduction-in-function; LOF = loss-of-function. Numbers located at the bottom of each column indicate the number of NMJs analyzed. Except in *C380-Gal4/+* there are 2 paired NMJs per treatment group. Error bars indicate the mean ± SEM. (B-C) STATISTICS: Kruskal-Wallis multiple comparison analysis with a Dunn's post-hoc test. n.s. = not significant * $p<0.05$ ** $p<0.01$ *** $p<0.001$ **** $p<0.0001$.

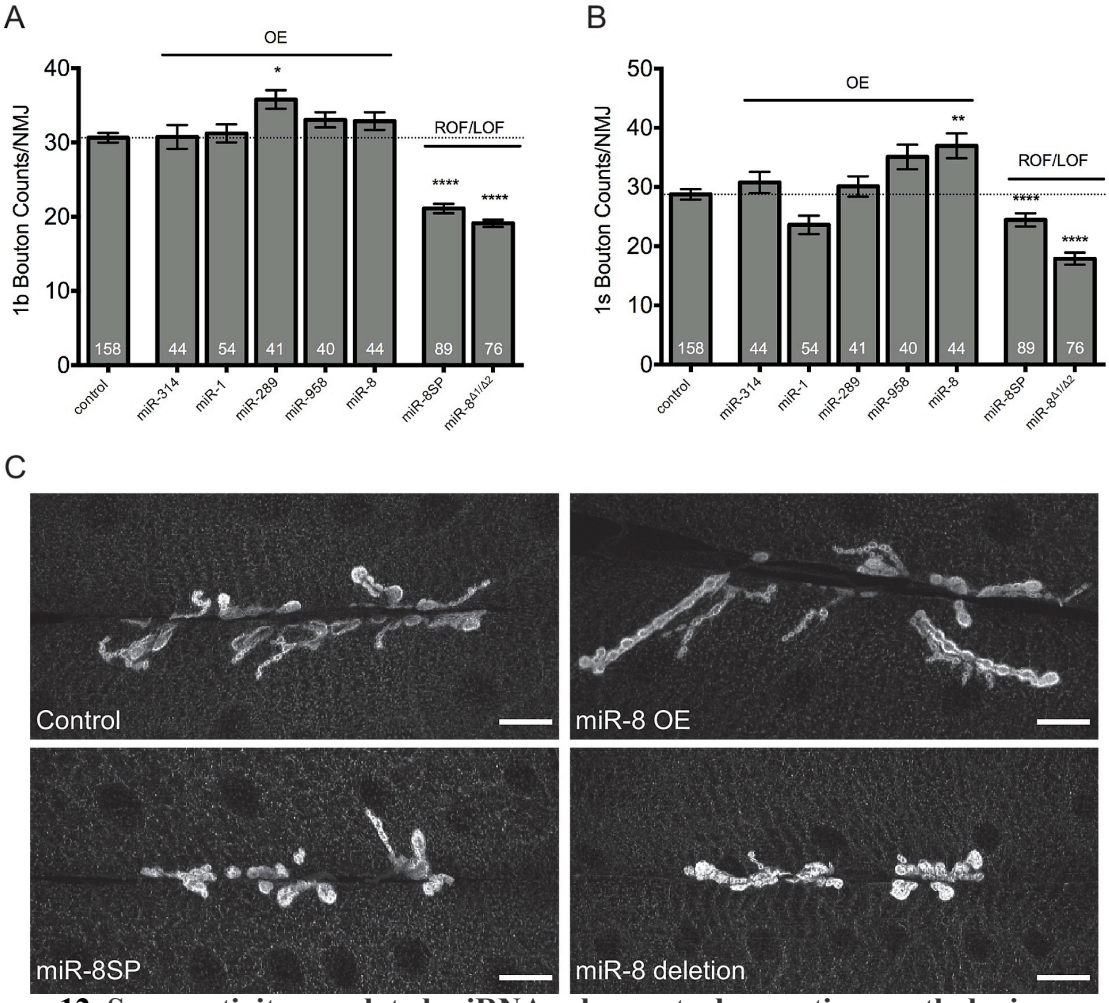

Figure 12. Some activity-regulated miRNAs also control synaptic growth during larval development.

This figure is reproduced as published in Nesler et al., 2013.

(A-B) At the same NMJs analyzed in figure 10C, type 1b (big) and 1s (small) boutons were quantified. Each type of bouton is derived from a distinct motor neuron. Type 1b boutons are highly plastic but can be easily distinguished by their larger size and higher levels of the postsynaptic density marker, Dlg. (A) miR-289 overexpression caused a significant increase in type 1b boutons compared to controls (17% increase; $p<0.05$). (A-B) miR-8 overexpression caused a significant increase in type 1s boutons compared to controls (29% increase; $p<0.01$). In contrast, miR-8 knockdown (*UAS-miR-8SP*) and deletion (*mir-8*$^{\Delta 1/\Delta 2}$) larvae showed a significant decrease in both type 1b (31% and 38% decrease respectively; $p<0.0001$) and type 1s boutons (15% and 38% decrease respectively; $p<0.0001$). As seen with total boutons, high K^+ stimulation has no effect on 1b or 1s bouton numbers compared to unstimulated controls (data not shown). The latter would have been indicative of spaced training affecting ghost bouton maturation or development. OE = overexpression; ROF = reduction-in-function; LOF = loss-of-function. Error bars indicate the mean ± SEM. (A-B) STATISTICS: Kruskal-Wallis multiple comparison analysis with a Dunn's post-hoc test. * $p<0.05$ ** $p<0.01$ ****

$p<0.0001$. (C) Representative third-instar NMJs from the indicated genotypes at larval muscle 6/7 in abdominal segment 3 that were stained with antibodies against the postsynaptic marker discs large (DLG). Note that the NMJs in both presynaptic miR-8 knockdown (*UAS-miR-8SP*) and deletion ($mir\text{-}8^{\Delta 1}/^{\Delta 2}$) larvae are phenotypically very similar and are significantly smaller than controls. In contrast, miR-8 overexpression NMJs exhibit some synaptic hyperplasia. Scale bars = 20 μM.

Presynaptic misexpression (C380-Gal4>UAS-miRNA construct) revealed that three out of the five activity-regulated miRNAs suppressed ghost bouton formation as we predicted in our model (Figure 11A). We observed no significant increase in activity-dependent synaptic growth upon misexpression of miRs-8, -289, and -958 following high K^+ stimulation as compared to pseudostimulated controls (Figure 11B). Conversely, activity-regulated miRs-1 and -314 do not play a role in ghost bouton formation, albeit for apparently different reasons. In the case of miR-314 misexpression we observe no negative effect on ghost bouton formation whatsoever. We observed a reduction in ghost bouton formation following stimulation in miR-1 misexpressing larvae as compared to genetic background controls (Figure 11B, ~3 ghost boutons per NMJ) but we do not believe that miR-1 plays a significant role in this process. We also observed the baseline in pseudostimulated miR-1 controls was likewise reduced (Figure 11B; ~1 ghost bouton per NMJ) yielding an approximately 3-fold increase in ghost bouton formation following stimulation, a result that parallels that of genetic background controls.

Next, we wished to confirm our misexpression results using mutant and transgenic reduction-in-function lines. Mutant lines available for miR-1 are embryonic or early larval lethal and therefore could not be used in this specific method of analysis (Kwon et al., 2005; Sokol et al., 2005). Available mutant miR-8 lines are viable until the pupal stage and are shown to exhibit a strong NMJ phenotype in third instar larvae (Karres et al., 2007; Loya et al., 2009). Reduction of function (ROF) lines were also available for miR-8 in the form of "sponge" constructs which express a strong binding

site for the target miRNA in a repetitive pattern (in this case a 10x repeat) and can be placed under the control of UAS elements allowing for transgenic expression (*UAS-miR8SP*; Loya et al., 2009). We predicted that if miR-8 is required for activity-dependent synaptic growth, loss of function or reduction of function lines would result in one, or perhaps both, of the following phenotypes. First, we thought we might see a significant increase in the total number of ghost boutons at each NMJ following 5x high K^+ stimulation. The second possibility was that we might observe a faster response to stimulation and instead of seeing a statistically significant increase in ghost bouton number following the normally requisite 5x stimulation we could perhaps see a significant increase in activity-dependent growth following only 3x high K^+ stimulation. We observed the later of those two phenotypes. Upon 3 cycles of stimulation in larvae expressing the miR-8 sponge (C380-Gal4>*UAS-miR-8-SP*) we observed a statistically significant increase in ghost bouton formation over unstimulated controls, a result not seen in genetic background control larvae (Figure 11B; $p<0.01$) indicating an enhanced ability to respond to synaptic stimulation when you reduce the presynaptic levels of miR-8. In miR-8 mutants we observed a similar trend in response to 3 cycles of stimulation but this result was not statistically significant (Figure 11B; miR-8Δ1/miR-8Δ2). When overexpressed presynaptically, miR-8 has a strong positive effect on total bouton number during NMJ development (Figure 11C). Furthermore, reduction or loss of miR-8 function presynaptically, postsynaptically, or globally leads to a marked reduction in bouton number during NMJ development leaving open the possibility that global disruption of miR-8 may likewise have a negative effect on activity-dependent synaptic growth (Figure 11C and Figure 12, Loya et al., 2009).

The possibility remains that these five miRNAs have a general negative effect on synaptic growth at the larval NMJ and not specifically on activity-dependent processes. To determine if the negative effect we saw was specific to activity-regulated processes we assayed synapse size as measured by total bouton number. By counting the combined total number of boutons at the same NMJs assayed for ghost bouton formation (Figure 11B-C) we observed no significant effect on total bouton number in any of the miRNA overexpression lines as compared to controls with the exception of miR-8 (Figure 11C; 19% increase; $p<0.0001$; Figure 12). Given the negative effect miR-8 had on activity-dependent synaptic growth (Figure 11B), a positive effect on growth during NMJ development was unexpected. Conversely, miR-8 mutants displayed a significant decrease in total bouton number as compared to controls (Figure 11C; Figure 12; *miR8Δ1/miR-8Δ2*; 38% decrease; $p<0.0001$; Loya et al., 2009). Furthermore, when we drove the expression of the miR-8 sponge in larval motor neurons we observed a similar negative effect on NMJ size (Figure 11C; Figure 12; C380-Gal4>UAS-*miR-8SP*; 31% decrease; $p<0.0001$). These data indicate that the activity-regulated miRNAs-8, 289 and/or -958 play a role in activity-dependent synaptic growth at the *Drosophila* NMJ. Intriguingly, it appears that the mechanisms controlling activity-dependent synaptic growth can be uncoupled from the mechanisms that underlie NMJ development (Figure 11B-C). Additionally, while miRs-1 and -314 are significantly downregulated in response to global depolarization, it does not appear that they have an activity-dependent function at this specific synapse, though the possibility remains that they may play important roles at other synapses.

3.5 Functional annotation cluster analysis of mRNA targets

To further investigate our hypothesis that activity-regulated miRNAs repress translation, we used an *in silico* based approach in order to characterize and evaluate potential targets of miRs-8, -289, and -958. Using the website miRecords which takes a combinatorial approach cross-referencing 11 miRNA/mRNA interaction prediction algorithms we identified a list of putative targets for each of the three activity-regulated miRNAs. These databases each have their own criteria for target predictions including probability of miRNA/mRNA binding based on thermodynamics (RNAhybrid, Rehmsmeier et al., 2004), while others use sequence homology between species to predict valid interactions (PicTar, Grün et al., 2005; TargetScan, Friedman et al., 2009; Grimson et al., 2007; Lewis et al., 2005). miRecords allowed us to combine predictions from all 11 databases and infer if an interaction is predicted in a greater number of databases, it is more likely to be a biologically relevant interaction. Bearing this in mind, we set the cutoff for database prediction hits to three for our initial analysis. Using this approach, we identified 490 putative targets for miR-8, 2494 for miR-289, and 304 for miR-958 (Figure 12A). We then predicted that mRNA targets predicted to be regulated by more than one (or even all three) activity-regulated miRNAs more likely encode for proteins that are involved in new synaptic growth following activity. By cross-referencing the lists of mRNA targets for each activity-regulated miRNA we identified 282 mRNAs are predicted to be regulated by miRs-8 and -289; 43 by miRs-8 and -958; and 154 by miRs-289 and -958. Interestingly, we found that 33 mRNAs are predicted as being co-regulated by all three activity-regulated miRNAs.

Next, we examined the functional classification of these target mRNAs in order to identify those belonging to annotation clusters pertinent to activity-regulated neuronal growth including neuron development, morphogenesis, and/or differentiation. To perform these analyses we used the DAVID bioinformatics resource system designed to systematically identify biological meaning and themes from large lists of genes, such as the one we were dealing with (Huang, 2009). The DAVID system compares genes from an input list (in our case predicted targets of activity-regulated miRNAs) and determines the degree to which these genes are enriched in certain qualitative categories compared to the population background (in our case the *Drosophila* genome). Subsequently, we used DAVID functional annotation clustering analysis, which measures relationships between annotation terms for all genes in a query list and associates them into functional clusters defined as 'heterogeneous yet highly similar' functional annotation groups. This kind of analysis allows a broad look at the kinds of biological processes target genes are involved in (Huang, 2009). Enrichment scores generated by this kind of analysis indicate the relative abundance of genes in a query list mapping to a specific functional cluster compared to the prevalence of genes mapping to the same cluster in the genome as a whole. This cluster analysis revealed that predicted targets of miRs-8 and -289 (individually) were enriched in those annotation clusters (Figure 13B-C; enrichment scores=6.1 and 15.9 respectively). Additionally, the 282 predicted co-regulated targets of miRs-8 and -289 display a significant number of mRNAs that map to the aforementioned annotation clusters (Figure 13A and D; 32 mRNA targets, 11%; enrichment score=2.8). On the other hand, the 33 mRNA targets predicted for co-regulation by miRs-8, -289, and -958, did not show significant enrichment in neuronal clusters.

These data lead to two particularly important conclusions. First, while we have restricted our primary analysis to the mRNA targets with relevant neuronal functions, the putative mRNA targets of all three activity-regulated miRNAs belong to a diverse pool of functional clusters involved in the control of a multitude of cellular processes during development and beyond (Figure 13; data not shown). Second, due to the significant enrichment of mRNA targets enriched in neuronal processes, miRs-8 and -289 emerged as exceptional candidates for the coordination of fine tuned mRNA expression required for processes such as axon pathfinding, development, and growth as well as other neuronal processes.

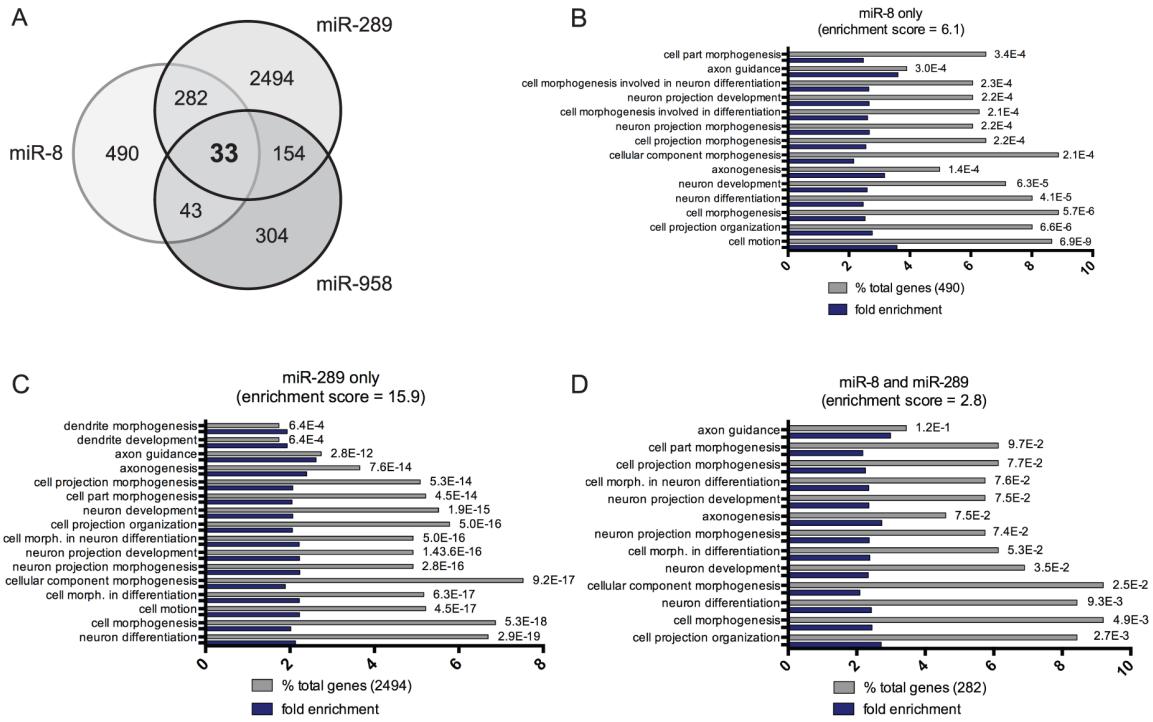

Figure 13. Predicted targets of miRs-8 and -289 are found in neuron-related enriched functional annotation clusters.

This figure is reproduced as published in Nesler et al., 2013.

(A) Venn diagram showing predicted mRNA targets for activity-regulated miRNAs. Notably, 33 mRNAs have putative binding sites for miRs-8, -289, and -958. 282 mRNAs have putative binding sites for miRs-8 and -289. (B-C) Functional annotation cluster analysis for predicted targets of miRs-8, -289 and both miRs-8 and -289. Only clusters enriched with targets significantly enriched in clusters involved in the control of neuronal processes are shown here. Note that the 304 predicted targets for miR-958 were not enriched in these clusters. Enrichment scores for each cluster are indicated (Huang et al., 2009a; Huang et al., 2009b). Genes within each category are indicated as a percentage of total genes (gray bar) and fold enrichment (blue bar) over expected number of genes in that category in the *Drosophila* genome. Statistical significance (Benjamini corrected p-values) for each category is indicated to right of gray columns.

3.6 Target validation and characterization of *lar* and *wg* mRNAs.

Our next area of focus was to identify biologically relevant target mRNAs of these activity-regulated miRNAs that encode for proteins involved in miRNA-mediated activity-dependent synaptic growth. We began by identifying mRNAs that were either predicted as co-regulated by miRs-8 and -289 that map to a neuron-related cluster (Table 1) as well as all genes potentially co-regulated by all three activity-regulated miRNAs (Table 2). Of particular interest were any genes with an annotated function in the control of axon development, guidance, and/or growth. We found that of the 282 mRNAs predicted as being regulated by both miRs-8 and -289, 32 of them map to a neuron-related functional cluster (Figure 12D; Table 1; 11%). Of these 32, 10 (31%) have an annotated function in the previously mentioned neuron-related categories (Table 1).

Two proteins targeted for co-regulation by miRs-8 and -289 include members of the BMP pathway, Wingless (Wg) and Wishful Thinking (Wit). Wg is a signaling molecule secreted in association with vesicles from presynaptic terminals at the *Drosophila* NMJ where it can bind to both pre- and postsynaptic Frizzled-2 (Fz2) receptors (Miech et al., 2008; Koles and Budnik, 2012). Loss of *wg* function leads to an alteration in number and structure of boutons at the *Drosophila* NMJ and notably can completely inhibit activity-dependent increases in new synaptic growth following a high K^+ spaced training paradigm (Miech et al., 2008; Ataman et al., 2008). Wit is a gene that encodes a BMP type II receptor that positively regulates synaptic growth at the *Drosophila* NMJ through a retrograde signaling mechanism binding to the BMP homolog Glass bottom boat (Gbb; McCabe et al., 2003). Wit mutant larvae display NMJs of greatly reduced size in comparison to the muscles they innervate, have reduced evoked

excitatory junctional potentials, display decreased levels of the synaptic cell adhesion molecule Fasciclin II (Fas II), and exhibit detached membranes at active zones (Aberle et al., 2002). Recently, experiments using a high-temperature assay to induce growth at the *Drosophila* NMJ have indicated a requirement for Wit signaling in activity-dependent synaptic growth (Berke et al., 2013). Other biologically relevant target mRNAs predicted to be co-regulated by miRs-8 and -289 include six conserved components of axon guidance pathways. Roundabout (Robo) receptors are repelled by chemorepelent Slit and this interaction plays a major role in axon guidance in the nervous system (Blockus and Chedotal, 2014). The *Drosophila* receptor protein tyrosine phosphatase (RPTP) Leukocyte-antigen-related-like (Lar) is a receptor-like transmembrane protein with an expression pattern nearly exclusively restricted to developing neurons has been shown to control the targeting ability of certain motor axons in the developing nervous system and is a putative target of all three activity-regulated miRNAs (Krueger et al., 1996; Sun et al., 2000). Studies have shown that Ableson (Abl) is a tyrosine kinase that works as an antagonist of Lar during early axon pathfinding (Wills et al., 1999). While Abl is not in this group of putative targets, Abl Interacting Protein (Abi) is a putative target of miRNAs-8 and -289. Abi works in conjunction with enabled (ena) to antagonize Abl function during *Drosophila* synaptogenesis (Lin et al., 2009). Protein tyrosine phosphatase 99A (PTP99A) is another PTP expressed in *Drosophila* found in nearly all axons in the developing embryo and is responsible for branching of segmental nerves (Lalima et al., 2012). The last putative target belonging to the group of conserved components of axon guidance pathways is Plexin A (PlexA), a *Drosophila* Semaphorin receptor for class 1 semaphorins including Semaphorin-1A (Sema-1A) required for

proper axon guidance in optic lobes during the development of the visual system, sensory neuron targeting, and controls motor and CNS axon guidance (Winberg et al., 1998; Zlatic et al., 2009; Yu et al., 2010). Moreover, studies have demonstrated a role for presynaptic transmembrane Sema-1A in synapse formation in addition to playing a role in pathfinding (Godenschwege et al., 2002). Evidence suggests that Semaphorin signaling is regulated by miRNAs in various other systems including during neural circuit formation and axon guidance leading us to believe that could well be the case in our system (Baudent et al., 2013). Longitudinals lacking (Lola) is a requisite transcription factor involved in midline crossing of CNS axons in *Drosophila* through interactions with Slit and Robo (Crowner et al., 2002). Finally, Bazooka (Baz) belongs to an evolutionarily conserved complex that regulates microtubule dynamics and in the glutamatergic synapses of *Drosophila* functioning to control the growth of new synaptic boutons (Ruiz-Canada et al., 2004; Nesler et al., 2013; Tables 1 and 2).

Three (9%) of the 33 putative mRNA targets of all three activity-regulated miRNAs have been implicated or experimentally shown to be involved in controlling axon or dendrite development (Table 2). As discussed above, *Drosophila* proteins Lar and Lola are involved in axon growth and/or guidance during development (Krueger et al., 1996; Sun et al., 2000; Crowner et al., 2002). The third mRNA in this class is the uncharacterized CG10077, fly ortholog of DEAD-box RNA helicase DDX5, an RNA helicase present in RNPs in mouse neurons (Kanai et al., 2004). The list of 33 putative targets of miRs-8, -289, and -958 contains 11 (33%) as of yet uncharacterized mRNAs. These mRNAs are named solely by a CG gene symbol and represent a group of novel

targets to be explored in activity-dependent synaptic growth at the larval NMJ (Nesler et al., 2013; Table 2).

Gene	Gene Name	Molecular Function
[1]ABI	Abelson Interacting Protein	protein binding
AP	apterous	DNA binding
B-H2	BarH2	transcription factor
[2]BAZ	bazooka	phosphatidylinositol binding
CBL	Dmel_CG7037	protein binding
CK	crinkled	actin-dependent ATPase activity
CRB	crumbs	protein kinase C binding
CSW	corkscrew	protein tyrosine phosphatase activity
DG	Dystroglycan	protein binding
DS	dachsous	cell adhesion molecule binding
FRY	furry	protein binding
GOGO	golden goal	receptor activity
HTH	homothorax	transcription factor activity
JUMU	jumeau	DNA binding
KAP3	Kinesin associated protein 3	protein binding
[3]LAR	Leukocyte-antigen-related-like	protein tyrosine phosphatase
[4]LOLA	longitudinals lacking	transcription factor
MID	midline	transcription factor
MLE	maleless	chromatin binding
PATJ	Patj homolog	protein kinase c binding
[5]PLEXA	plexin A	14-3-3 protein binding; semaphorin receptor
[6]PTP99A	Protein tyrosine phosphatase 99A	protein tyrosine phosphatase
PVF1	PDGF- and VEGF-related factor 1	heparin binding; receptor binding
[7]ROBO	roundabout	heparin binding; protein binding
RST	roughest	PDZ domain binding
[8]SEMA-1A	Semaphorin-1A	protein binding
SINA	seven in absentia	protein binding
SNA	snail	transcriptional repressor activity
VN	vein	heparin binding; receptor binding
[9]WG	wingless	frizzled-2 binding
[10]WIT	wishful thinking	TGFβ receptor
YKI	yorkie	protein binding; transcriptional coactivator activity

[1]Presynaptic Ableson Interacting Protein (Abi) acts to antagonize the Abl tyrosine kinase (Abl) in the control of synaptogenesis and neurite extension at the larval NMJ [52].
[2]A bazooka (Baz)/Par-6/aPKC complex controls new synaptic bouton growth at the NMJ [60].
[3]The leukocyte-antigen-related like (Lar) controls synapse morphogenesis at the larval NMJ [16].
[4]The longitudinals lacking (Lola) protein is required for embryonic axon growth and guidance [58].
[5]Plexin A (PlexA) is a conserved neuronal semaphorin receptor that controls axon guidance [53].
[6]The receptor tyrosine phosphatase (PTP99A) is required for embryonic motor axon guidance [46].
[7]Roundabout (Robo) controls axon crossing of the embryonic CNS midline [45].
[8]Semaphorin-1A (Sema-1A) is a ligand for PlexA and required for embryonic motor axon guidance [54].
[9]Secreted wingless (Wg) protein is required for activity-dependent synapse growth at the NMJ [12].
[10]The BMP type II receptor, wishful thinking (Wit), is required for axon terminal growth and synapse function at the larval NMJ [43,44].
doi:10.1371/journal.pone.0068385.t001

Table 1. Putative mRNA targets for co-regulation by miRs-8 and -289 that also map to a neuron-related functional annotation cluster (GO term enrichment).
This table is reproduced as published in Nesler et al., 2013.

Gene	Gene Name	Molecular Function
B4	Dmel_CG9239	unknown
CALPA	Calpain-A	calcium-dependent cysteine-type endopeptidase
[1]CG10077	Dmel_CG10077	RNA helicase activity
CG10731	Dmel_CG10731	hydrogen-exporting ATPase
CG1273	Dmel_CG1273	unknown
CG2519	Dmel_CG2519	unknown
CG31530	Dmel_CG31530	organic cation transmembrane transporter
CG32017	Dmel_CG32017	unknown
CG32365	Dmel_CG32365	unknown
CG32683	Dmel_CG32683	unknown
CG33981	Dmel_CG33981	unknown
CG4467	Dmel_CG4467	aminopeptidase
CG8475	Dmel_CCG8475	phosphorylase kinase regulator
CLK	Clock	transcription factor
CSW	corkscrew	protein tyrosine phosphatase
GUG	Grunge	histone deacetylase
H	Hairy	transcription corepressor activity
HTH	homothorax	transcription factor activity
[2]LAR	Leukocyte-antigen-related-like	protein tyrosine phosphatase
[2]LOLA	longitudinals lacking	transcription factor
LOOPIN-1	Loopin-1	aminopeptidase
PATJ	Patj homolog	protein kinase C binding
PLC21C	Phospholipase C at 21C	phosphatidylinositol phospholipase C
RBP9	RNA-binding protein 9	mRNA binding
RHOGEF3	Dmel_CG42378	Rho guanyl-nucleotide exchange factor
STAR1	allatostatin C receptor 1	allatostatin receptor
TOLLO	Tollo	transmembrane signaling receptor
UNC-4	Homeobox protein unc-4	transcription factor
UNK	unkempt	zinc ion binding; DNA binding
VACHT	Vesicular acetylcholine transporter	acetylcholine transmembrane transporter
VMAT	Vesicular monoamine transporter	synaptic vesicle amine transmembrane transporter
WRY	Weary	Notch binding
ZN72D	Zinc-finger protein at 72D	mRNA binding

[1]CG10077 is the *Drosophila* ortholog of the mammalian DEAD box RNA helicase, DDX5, which has been identified as a component of kinesin-containing neuronal RNPs in mice [61].
[2]Lar and Lola do have known functions in axonogenesis and are described in both the text and in Table 1.
doi:10.1371/journal.pone.0068385.t002

Table 2. Putative mRNA targets for co-regulation by miRs-8, -289, and -958 (miRBase).
This table is reproduced as published in Nesler et al., 2013.

3.7 Experimental validation of putative target mRNAs *lar* and *wg*.

Identification of putative miRNA targets using our *in silico*-based approach merely predicts a likely interaction between an activity-regulated miRNA and a potential mRNA target. In order to verify this interaction, direct experimental validation is required. To begin, we selected the two predicted targets *lar* and *wg*. We selected *lar* for two primary reasons: a) it is a putative target for co-regulation by all three activity-regulated miRNAs (Table 2); and b) it is required for axon guidance and/or growth during development (Krueger et al., 1995; Sun et al., 2000). Second, we selected *wg* because previous studies have shown a direct requirement for *wg* in activity-dependent new synaptic growth at this synapse (Ataman et al., 2008; Table 2). Within the 3'UTR of *lar* there is one predicted binding site for each miR-8, -289, and -958 as well as for a fourth activity-regulated miRNA, miR-1 (Figure 14A-C). The *wg* 3'UTR contains three predicted binding sites for miR-289 and two for miR-8 (Nesler et al., 2013). To test if *lar* and *wg* are bonafide targets of activity-regulated miRNAs we began by utilizing an *in-vitro* luciferase-based assay in which we cloned the 3'UTRs of *lar* and *wg* into firefly luciferase (FLuc) reporter vectors (Rehwinkel et al., 2006). When we co-transfected the *lar* 3'UTR reporter with each of the activity-regulated miRNAs we observed a significant repression in relative luciferase expression in each case (Figure 14A; miR-8=24%; miR-289=39%; miR-958=32%; $p<0.0001$ in all cases; Nesler et al., 2013). Conversely, when we co-transfected the *lar* 3'UTR reporter with a miRNA not predicted to bind within the *lar* 3'UTR (miR-9a) no repression was observed (Figure 14A). When the wg 3'UTR reporter was co-transfected with each of the activity-regulated miRNAs we observed repression only in the case of miR-8 (Figure 14B; miR-8=24%; $p<0.0001$; Nesler et al.,

2013). Observing no effect when miR-289 was co-transfected with the *wg* reporter was unexpected because there exist three predicted binding sites including two with perfect seed region basepairing. As with the *lar* 3'UTR experiment we observed no repression when we co-transfected our negative control miRNA (miR-9a) with the *wg* 3'UTR reporter (Figure 14B). Together, these data indicate that *lar* and *wg* are potential targets for activity-regulated miRNAs-8, -289, and -958 and that these miRNAs could be contributing to activity-dependent synaptic growth at least in part by regulating Lar and/or Wg expression in *Drosophila* motor neurons (Nesler et al., 2013).

We next hypothesized that if Lar and/or Wg are required for activity-dependent synaptic growth and if we knocked down *lar* and/or *wg* by RNAi, we would be able to recapitulate the results seen following misexpression of miR-8, -289 and -958 (Figure 11). Consistent with previous studies, following disruption of Wg expression we observed complete suppression of ghost bouton formation following spaced high K^+ depolarization (Figure 7C; *C380-Gal4>UAS-wg*^{HMS00794}; Ataman et al., 2008). Likewise, when we disrupted Lar expression by RNAi we observed complete prevention of activity-dependent ghost bouton formation following high K+ stimulation (Figure 7C; *C380-Gal4>UAS-lar*^{HMS00822}). Unexpectedly, following knockdown of either *lar* or *wg* we did not observe a significant effect on NMJ size during development (Figure 14D; Figure 15). Taken together these data provide further support for our hypothesis that the mechanisms behind activity-dependant synaptic growth and regulation of NMJ formation during development can be uncoupled from one another. Our data suggest that the regulation of synaptic growth during development is less susceptible to the modulation of

lar, *wg*, and miRNA levels than is the regulation of new synaptic growth following spaced depolarization (Nesler et al., 2013).

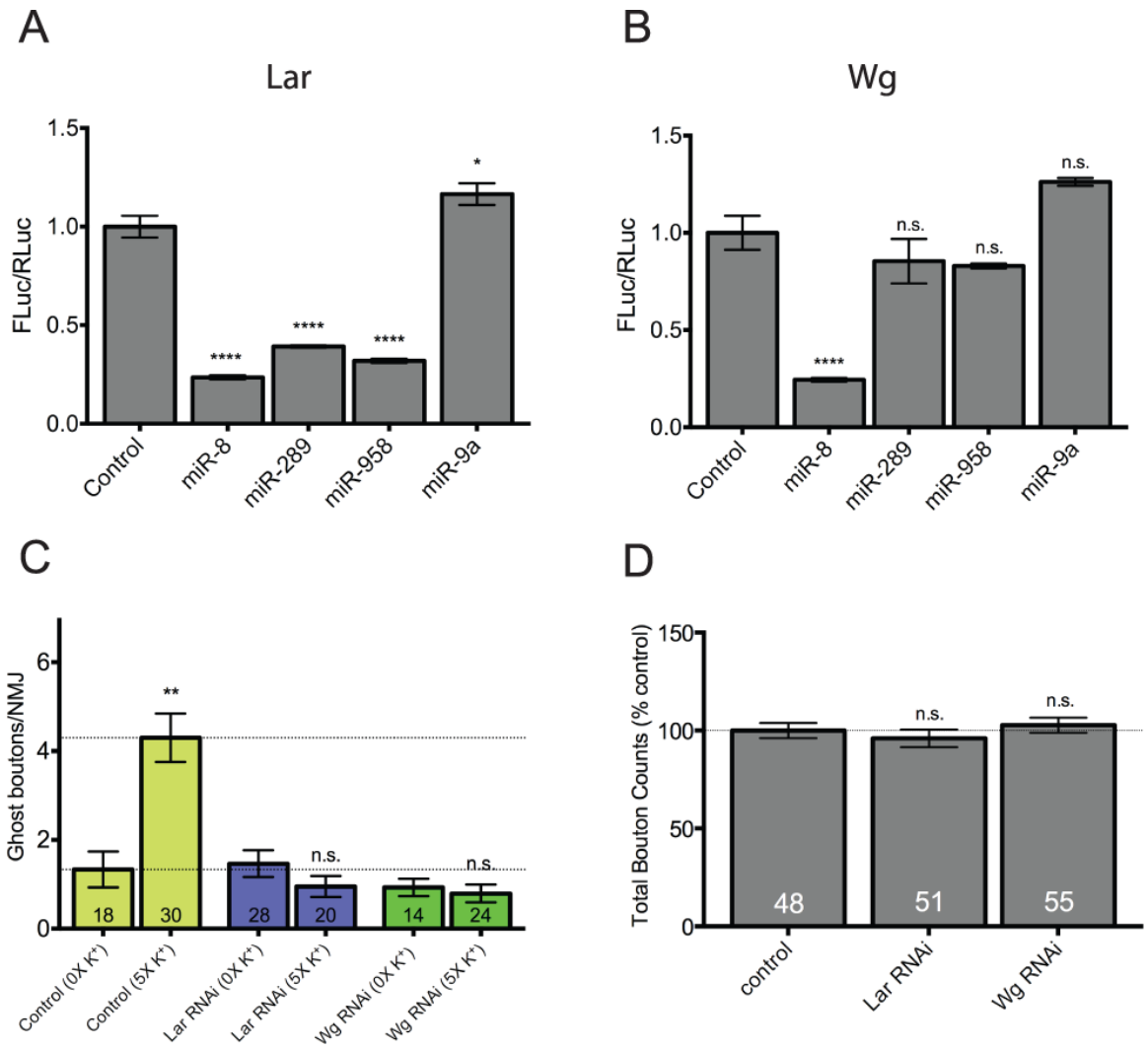

Figure 14. *Drosophila lar* and *wg* are authentic targets for translational repression by activity-regulated miRNAs.

This figure is reproduced as published in Nesler et al., 2013. S2 cell experiments presented here were conducted by PhD student Breanna Symmes.

(A and B) Reporter plasmids constitutively expressing firefly luciferase (FLuc) flanked by the 3′UTRs of *lar* and *wg* were cotransfected into S2 cells with plasmids expressing the indicated miRNA primary transcripts as indicated. *Renilla* luciferase (RLuc) was included as a transfection control. FLuc activity was normalized to RLuc activity in three independent experiments. Normalized FLuc activities in the absence of miRNA-expressing vectors (emply vector controls) were set to 1. (A) The *Drosophila lar* 3′UTR has one binding site each for miRs-1, -8, -289, and -958. miR-1 was not tested because it did not negatively regulate activity-dependent synaptic growth. miRs-8, -289, and -958 all significantly repress *lar* FLuc reporter activity. In contrast, a miRNA with no predicted binding site (miR-9a) has no effect on FLuc activity. (B) The *wg* 3′UTR has three predicted binding sites for miR-289 and two for miR-8. Interestingly, only miR-8 is capable of repressing *wg* FLuc reporter activity. miR-289, -958 nor -9a (not predicted to

bind) had an effect of FLuc activity. In both (A) and (B) error bars indicate the mean ± SEM (n = 3). (C) Transgenic hairpin RNAi constructs targeting *lar* and *wg* were misexpressed in larval motor neurons using the *C380-Gal4* driver (e.g. genotype *C380-Gal4/+; UAS-RNA^{hairpin}/+*). Note that both hairpin constructs completely prevented activity-dependent ghost bouton formation. (D) Quantification of the total number of synaptic boutons at the same NMJs assayed in above (C). Neither hairpin construct had a significant effect on total bouton numbers compared to controls (*C380-Gal4/+*) suggesting that activity-dependent processes may be more sensitive to disruption of genes involved in synaptic growth pathways. STATISTICS: (A-B; D) One-way ANOVA with a Dunnett's post-hoc test. (C) Kruskal-Wallis multiple comparison analysis with a Dunn's post-hoc test. n.s. = not significant ** $p<0.01$ **** $p<0.0001$.

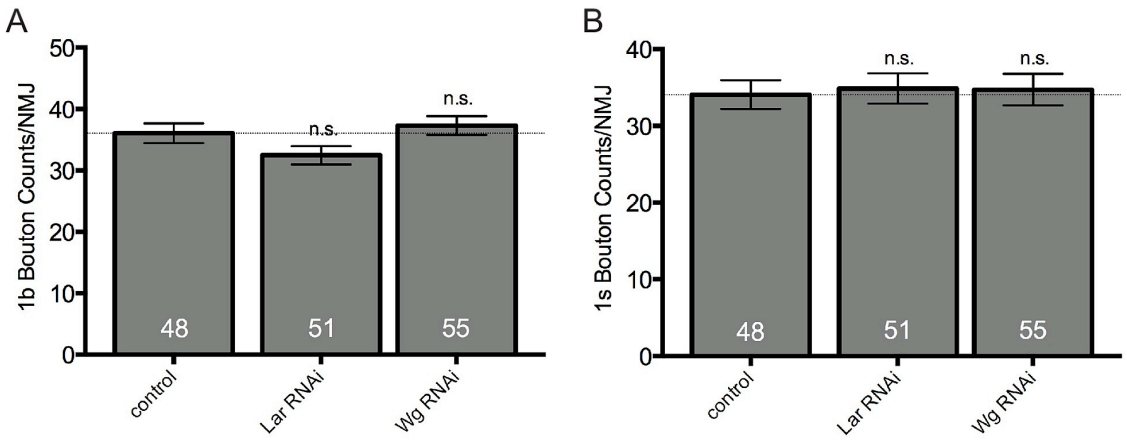

Figure 15 *lar* and *wg* RNAi has no effect on synaptic growth during development.
This figure is reproduced as published in Nesler et al., 2013.
(A-B) At the same NMJs analyzed Figure 14D, type 1b (big) and 1s (small) boutons were quantified. Note that disruption of *lar* and *wg* expression using transgenic hairpin RNAi constructs had no specific effect on either type 1b or 1s boutons. The degree of Lar and Wg reduction was not confirmed. Error bars indicate the mean ± SEM. (A-B) STATISTICS: One-way ANOVA with a Dunnett's post-hoc test. n.s. = not significant.

CHAPTER FOUR: *DROSOPHILA* CALCIUM/CALMODULIN-DEPENDENT PROTEIN KINASE II AND microRNA-289

While for our initial screen of putative target mRNAs we limited the scope to mRNAs predicted as targets of two or more activity-regulated miRNAs operating under the assumption that if an mRNA was a predicted target of more than one activity-regulated miRNA it was more likely to be involved in activity-dependent synaptic growth, we made one notable exception to this criterion. The *CamKII* 3'UTR has one predicted binding site for miR-289 identified both by Ashraf et al. 2006 and in our list of putative targets for miR-289 generated using our *in silico* target prediction approach. Because the *CamKII* 3'UTR does not have binding sites for any other activity-regulated miRNAs, it does not appear in Tables 1 or 2 as a mRNA targeted for co-regulation by multiple activity-regulated miRNAs. Nevertheless, because CamKII is such an important and well-defined modulator of synaptic plasticity in other systems, we saw this as an exciting opportunity to see if it plays a role in the control of activity-dependent axon terminal growth at the *Drosophila* larval NMJ.

4.1 CamKII displays presynaptic localization at the NMJ and is enriched in active zones

Our hypothesis that neuronal *Drosophila* CamKII is required for activity-dependent synaptic growth at the NMJ following spaced depolarization hinges on

CamKII being present in presynaptic axon terminals. In the *Drosophila* olfactory system the miRNA pathway modulates local translation of *CamKII* mRNA following induction of LTM using a classical conditioning paradigm (Ashraf et al., 2006). Based on this, we believe that the activity of miR-289 could likewise regulate the local translation of *CamKII* in axon terminals. To examine this possibility we first sought to determine if CamKII was expressed in larval motor neurons and if it displayed enrichment in axon terminals. Two antibodies have been used to visualize CamKII at the *Drosophila* larval NMJ. The first is a mouse monoclonal antibody generated against the bacterially expressed 490-amino acid form of *Drosophila* CamKII shows immunoreactivity at the larval NMJ, although specific localization with this antibody has not been fully characterized (Takamatsu et al., 2003). Second, a rabbit polyclonal antibody appeared to show strong co-localization with postsynaptic density 95 (PSD95) homolog discs-large (DLG) with limited immunoreactivity in presynaptic terminals in published work (Koh et al., 1999). We obtained both antibodies for our studies; the former (mouse) antibody is commercially available (CosmoBio Co.) and a limited quantity of the second (rabbit) anti-CamKII was on hand (a gift from S. Kunes). To examine CamKII localization at the larval NMJ we stained wild-type (*Canton S*) NMJs with mouse anti-CamKII antibody and axon terminal marker HRP (Figure 16A). In these images we observed strong staining for CamKII in axon terminals demarcated by positive staining for presynaptic marker HRP. Initial published characterization of this specific antibody noted immunofluorescence signal localized at the peripheral border for each synaptic bouton, but reporting less staining within the core of each bouton (Takamatsu et al., 2003). Our own image analysis revealed a staining pattern that we believe to be largely presynaptic

and in a punctate staining pattern reminiscent of active zones (Shakiryanova et al., 2011). To investigate the possibility that CamKII may be localized to presynaptic active zones at the larval NMJ, we stained NMJs with synaptic vesicle marker DVGLUT (rabbit anti-DVGLUT) and the mouse monoclonal CamKII antibody (Figure 16B lower panels; Daniels et al., 2008). These images revealed a large fraction of presynaptic CamKII appears to co-localize with DVGLUT, suggesting enrichment in active zones. To further characterize CamKII localization at the NMJ, we co-labeled wild-type *Canton S* larvae with primary antibodies against CamKII (rabbit), DLG (mouse), and HRP. We observe some (albeit limited) postsynaptic CamKII staining indicated by co-localization with our mouse anti-DLG antibody which is consistent with previous works (Figure 16B). However, contrary to published studies reporting that co-localization between this CamKII antibody and DLG occurs postsynaptically and primarily at bouton borders, we strongly believe the mouse monoclonal antibody displays presynaptic localization indicated by presence within axon terminals demarcated by HRP and only limited co-localization between DLG and CamKII, even at bouton borders (Figure 16B upper panels; Koh et al., 1999).

To examine if our mouse antibody staining was specific, we specifically disrupted CamKII expression on the presynaptic side of the synapse using a motor neuron specific Gal4 driver and a transgenic long hairpin RNAi construct (*C380-Gal4>UAS-CamKII*^{v38930}). We observed a complete depletion of CamKII staining in presynaptic terminals of larvae expressing the RNAi construct against CamKII in motoneurons (Figure 16C). In these images we observed a faint halo of CamKII staining directly around the border of the presynaptic terminals marked by HRP. We believe this staining

pattern represents postsynaptic CamKII and is consistent with numerous published reports that CamKII has a postsynaptic function and localization pattern in this and other systems (Koh et al., 1999; Takamatsu et al., 2003). Our observations on staining patterns in larvae expressing an RNAi construct against CamKII demonstrate two things: first, that our mouse anti-CamKII is specific; and second, by expressing a transgenic RNAi construct we are able to specifically disrupt CamKII expression in *Drosophila* motoneurons.

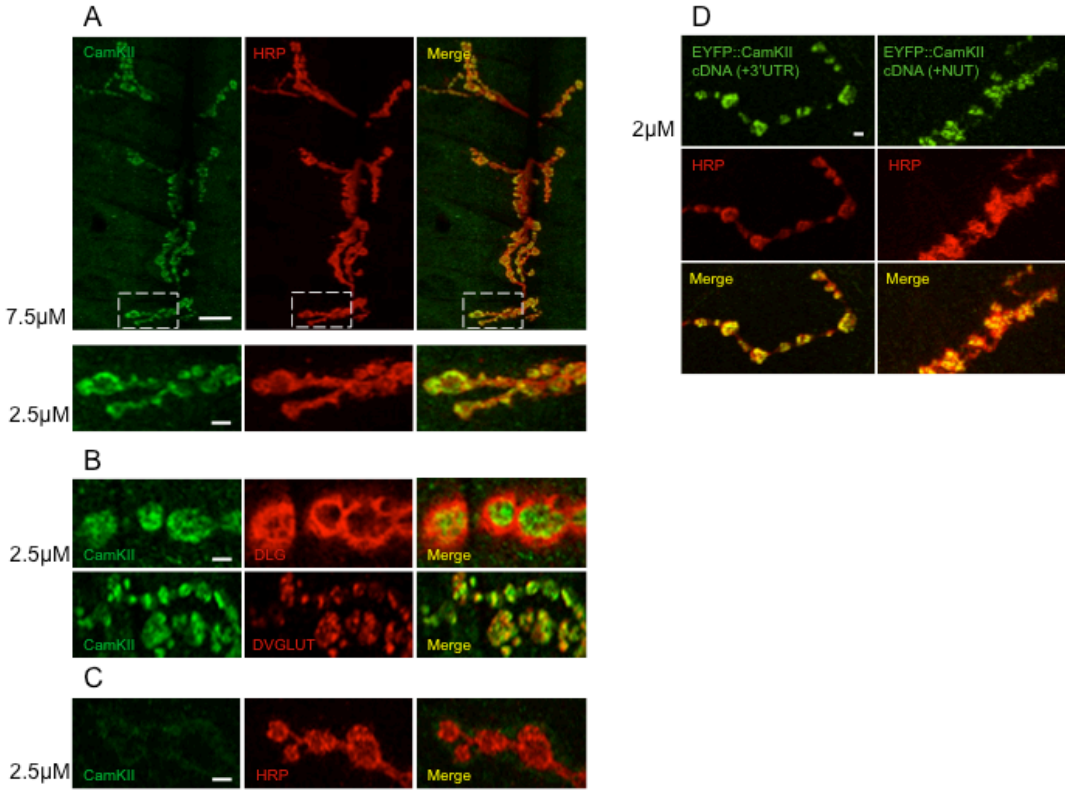

Figure 16. CamKII displays presynaptic localization in motor neuron axon terminals and specific enrichment in active zones.
All NMJ images in this figure were taken at M6/7, A3 in third instar larvae of the indicated genotypes. Scale bars are equivalent to the measurements indicated to the left of each figure panel. Images in A, C, and D represent a Z-series merged into a single image using the Olympus Fluoview Confocal microscope software. Images in B are representative of a single focal plane 0.2μM in thickness. (**A**) Wild-type *Canton S* larvae stained with mouse anti-CamKII and presynaptic marker HRP. Strong colocalization between CamKII presynaptic HRP is observed (Takamatsu et al., 2003; Koh et al., 1999). Images were taken at 100X magnification on a scanning confocal microscope. Lower panel images are magnified from the indicated region. (**B**) *Canton S* larvae are colabeled with rabbit anti-CamKII and mouse anti-DLG antibodies (DLG). A distinct halo of postsynaptic halo DLG staining can be observed around presynaptic CamKII staining. In the lower panels *Canton S* larvae are labeled with mouse anti-CamKII and rabbit anti-DVGLUT antibodies. CamKII displays enrichment in active zones as demarcated by colocalization with DVGLUT (the *Drosophila* vesicular glutamate transporter). (**C**) Larvae driving the expression of a transgenic RNAi construct against CamKII in motoneurons (C380-Gal4>*UAS-CamKII*^{V38930}) are stained with mouse anti-CamKII and presynaptic marker HRP. A faint halo of postsynaptic CamKII staining can be seen around the presynaptic terminals that are devoid of CamKII staining. (**D**) Two transgenic constructs expressing a translation fusion of EYFP to CamKII with the endogenous 3'UTR present (C380-Gal4>*EYFP::CamKII cDNA(+3'UTR)*; left-hand panels) or absent (C380-Gal4>*EYFP::CamKII cDNA (+NUT)*; right-hand panels) were labeled with HRP and imaged to examine the localization pattern of each CamKII construct at the NMJ.

4.2 CamKII is upregulated in presynaptic terminals following spaced depolarization.

Numerous previous studies have examined the function and expression of postsynaptic CamKII indicating that *CamKII* mRNA is present in distal postsynaptic sites and undergoes local translation. In cultured hippocampal neurons *CamKII* mRNA has been observed to localize to distal dendrites in granules, and following neuronal depolarization an increased number of such granules is present in dendrites (Rook et al., 2000). At the postsynaptic density in hippocampal neurons, synaptic activation induces polyadenylation of cytoplasmic polyadenylation element (CPE)-containing *αCamKII* mRNA (Wu et al., 1998). Additionally, following NMDA receptor activation, a GFP reporter fused to the *αCamKII* 3'UTR is activated in transfected hippocampal neurons and is polyadenylated in isolated synaptoneurosomes (Wells et al., 2001; Richter and Lorenz, 2002). In *Drosophila*, investigators have demonstrated that neural activity directs the *CamKII* mRNA to postsynaptic sites where it is rapidly translated; this result is likewise observed upon the induction of LTM (Ashraf et al., 2006). These data provide strong support for the idea that *CamKII* mRNA is present and locally translated at postsynaptic sites in neurons. Bearing these studies in mind, we hypothesized that a similar mechanism may be operating in *Drosophila* larval motoneurons following spaced depolarizations. To this end, we sought to determine if there is an activity-dependent increase in CamKII at the NMJ as assayed by CamKII fluorescence intensity following spaced depolarization. Wild-type *Canton S* larvae were subjected to the five times high K^+ spaced depolarization paradigm. Following treatment, unstimulated control larvae

were added to the dish and all larvae were labeled and imaged under identical conditions. To determine if CamKII levels increased specifically in boutons we quantified CamKII intensity relative to baseline measurements of presynaptic marker HRP in individual boutons. For these analyses we calculated an average for each NMJ as to not inherently bias our results toward larger NMJs with more numerous synaptic boutons. A similar method of quantification has been used in published work comparing intensity of Spectrin labeling ratiometrically to baseline HRP intensity at the larval NMJ (Loya et al., 2014). Following spaced depolarization, we observed a modest but statistically significant increase in CamKII in boutons in stimulated larvae as compared to the pseudostimulated control group (Figure 17A; $p<0.05$). This result indicates that there is an activity-dependent increase in CamKII following neuronal activity in axon terminals similar to the results seen in olfactory dendrites (Ashraf et al., 2006).

To further characterize this increase, and because we observed significant co-localization between CamKII and active zone marker DVGLUT (Figure 16B), we wanted to determine if the presynaptic increase in CamKII would be likewise observed specifically in active zones. Previous studies have shown that in neuronal cultures following prolonged depolarization, presynaptic CamKII redistributes from the cytoplasm to accumulate near active zones similar to the translocation of CamKII observed postsynaptically (Shakiyanova et al., 2011). To investigate the possibility that CamKII may be specifically increased in active zones at the NMJ following neuronal activity, we used the active zone marker DVGLUT to define active zones within presynaptic terminals and determine if CamKII increased specifically in these areas following the spaced-depolarization paradigm. To quantify CamKII brightness we

labeled and imaged high K^+-stimulated and pseudostimulated larvae under identical conditions as described above and quantified a ratio between CamKII and DVGLUT brightness, again calculating an average per NMJ so to not bias results. Following spaced depolarization, we did not observe an activity-dependent increase in CamKII specifically in active zones as we did overall in boutons (Figure 17A). Three possibilities can likely account for these results: 1) it is possible that the time course of this experiment is not long enough to see a significant increase in CamKII at active zones; 2) it is possible that DVGLUT is increasing proportionally following activity and 3) previous studies show that CamKII enrichment is limited to a subset of active zones, by quantifying all active zones as labeled by DVGLUT an increase in specific active zones may be obscured (Shakiyanova et al., 2011).

Numerous previous studies have demonstrated that CamKII increases in postsynaptic sites following rapid local translation (Ashraf et al., 2006; Wu et al., 1998; Wells et al., 2001). Furthermore, the rapid changes in synaptic structure observed at the *Drosophila* NMJ following spaced depolarization are dependent on transcription and translation. Blocking acute translation by including 100mM cycloheximide in the HL3 solutions during a high K^+ stimulation paradigm, new synaptic growth as assayed by ghost bouton formation is inhibited (Ataman et al., 2008). Based on these observations, we hypothesized that if local translation was inhibited following stimulation, we would not observe an activity-dependent increase of CamKII following spaced depolarization. To this end, we added the translational inhibitor cycloheximide to the resting HL3 dissection buffer following the final stimulation period to block the local translation that may occur following spaced depolarization. Larvae were again processed as above,

labeling and imaging under identical conditions. As predicted, when local translation was acutely blocked following spaced depolarization, we did not observe an activity-dependent increase in CamKII levels in boutons (Figure 17A) indicating that the presynaptic increase in CamKII we see following neuronal activity depends on local translation.

Studies of postsynaptic CamKII protein levels in adult *Drosophila* brains revealed an activity-dependent increase in CamKII protein level following induction of neural activity by nicotine (Ashraf et al., 2006). Because the spaced depolarization paradigm we utilize is a system that globally depolarizes neurons, we wanted to determine if the increase in CamKII following neural activity in our system occurs throughout the nervous system or if it is a phenomenon spatially restricted to axon terminals at the NMJ. To assess the possibility that an increase in CamKII protein levels may occur in the *Drosophila* CNS following spaced depolarization, we analyzed CamKII protein levels from explanted CNS of high K^+ stimulated and pseudostimulated control *Canton S* larvae by Western blot. This analysis revealed that following spaced stimulation with high K^+ there is no activity-dependent increase in CamKII protein levels in the larval CNS (Figure 17B). Taken together, these findings indicate that the increase in CamKII we see at the NMJ is a local, translation-dependent increase in axon terminals (but not specifically in active zones), and is not occurring on a detectable scale in the CNS (Figure 17).

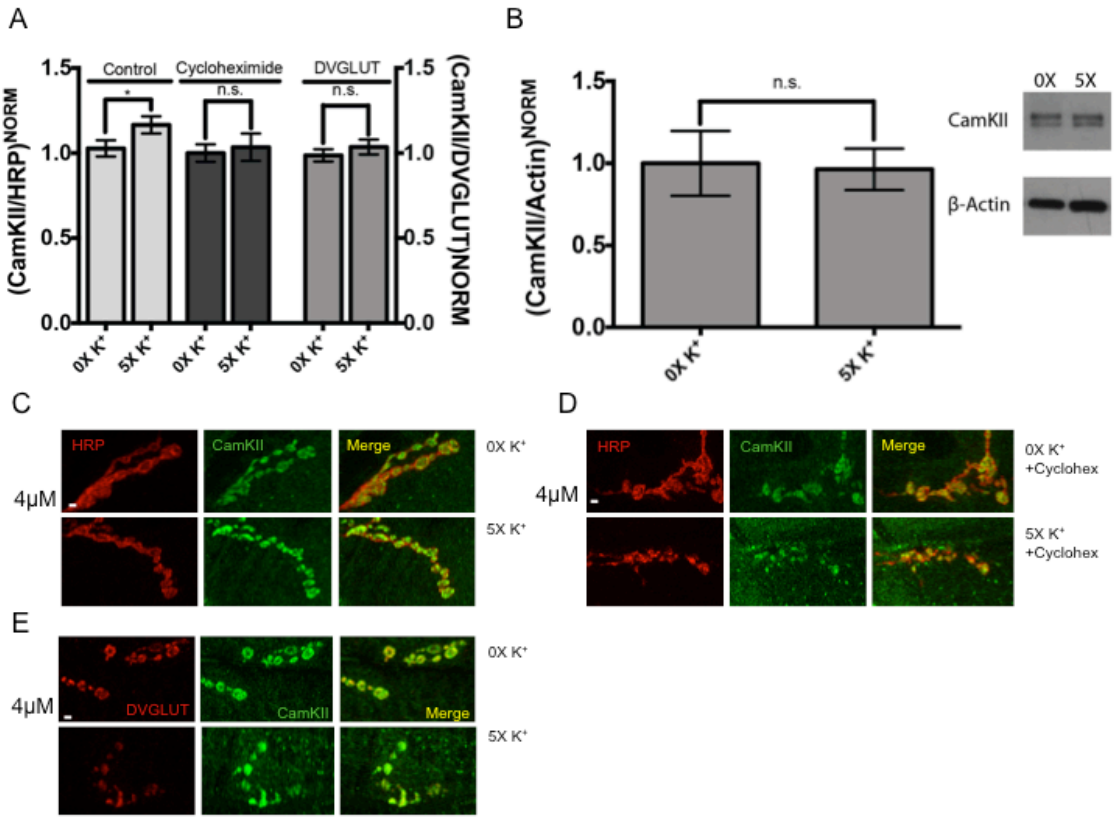

Figure 17 Spaced depolarization results in a presynaptic increase in CamKII at the *Drosophila* larval NMJ.

(**A, C D and E**) Wild-type *Canton S* larvae were subjected to high K^+ spaced-depolarization (5X K^+) or pseudostimulated control (0X K^+) paradigms. Control larvae (left; **C**) were labeled and imaged under identical conditions with CamKII and HRP antibodies. Boutons were individually circled in ImageJ and defined as an ROI for analysis where a ratio between HRP and CamKII fluorescence was calculated for each NMJ. All data is normalized to pseudostimulated controls. Cycloheximide larvae (middle; **D**) were treated exactly as the control larvae except in their final rest period following stimulation they were incubated in a bath of HL3 containing the translational inhibitor cycloheximide. DVGLUT larvae (right, **E**) were treated identically as control larvae except they were labeled with an antibody against active zone marker DVGLUT in addition to CamKII. Quantification for these defined ROIs as DVGLUT positive areas; ratios were calculated between CamKII and DVGLUT. Representative images for each treatment group are displayed in C, D, and E as magnified regions of boutons from Z-series images taken at 100X magnification. (**B**) *Canton S* larvae were pseudostimulated or stimulated using high K^+. Following each paradigm, an equal number of larval CNS were explanted for protein extraction and subsequent Western blot analysis. Densitometry analysis revealed no significant difference in CamKII protein levels between groups. Data is normalized to pseudostimulated controls. Images from the Western blot are presented at right. Blots were probed with mouse anti-CamKII (1:4000) and rabbit anti-β-actin (1:1000) as a loading control. Corresponding HRP conjugated secondary antibodies were used at a 1:3000 dilution.

4.3 Expression of a *CamKII* 3'UTR reporter is regulated by miR-289 *in vitro*

Our overarching hypothesis is that activity-regulated miRNAs regulate mRNA targets present in presynaptic terminals at the *Drosophila* NMJ and certain subsets of those mRNA targets play a role in activity-dependent synaptic growth. Specifically, we believe that in this case an activity-regulated decrease in miR-289 (Figure 9) results in an increase in local translation of *CamKII* mRNA in axon terminals. Subsequently, CamKII would then go on to phosphorylate and activate proteins requisite for new synaptic growth following spaced depolarization. As discussed previously, the miRNA pathway in *Drosophila* olfactory dendrites regulates CamKII expression and translation of *CamKII* mRNA occurs following stimulation in numerous other systems (Ashraf et al., 2006; Wu et al., 1998; Wells et al., 2001). The *CamKII* mRNA 3'UTR contains putative binding sites for miR-280 and activity-regulated miR-289, although in contrast to miR-289, our data indicate that miR-280 is not expressed in the larval CNS (Figure 8; Ashraf et al., 2006; Nesler et al., 2013). To test if *CamKII* is a bonafide target of activity-regulated miRNA miR-289 we again turned to the *in-vitro* luciferase-based validation system utilized to validate miRNA interactions with the *lar* and *wg* 3'UTRs (Figure 14). To test if miR-289 regulates the *CamKII* 3'UTR *in vitro* we began by co-transfecting *Drosophila* S2 cells with a reporter expressing FLuc under the control of the CamKII 3'UTR and a miR-289 expressing plasmid. In confirmation of our *in silico* analysis and the interaction predicted by Ashraf et al., we observed a significant reduction in *FLuc-CamKII* 3'UTR reporter expression as compared to empty vector controls (Figure 18A; ~47% reduction; $p<0.0001$). In contrast, when we co-transfect the same reporter with miR-276a, a miRNA not predicted to regulate the CamKII 3'UTR, we do not observe a significant

reduction in *FLuc-CamKII* 3'UTR reporter expression (Figure 18A). To further investigate the specificity of the interaction between the *CamKII* 3'UTR and activity-regulated miR-289, we mutagenized the binding site for miR-289 that bind to positions 3-5 of the miR-289 seed region (Figure 18B). Given that miRNA/mRNA interaction is largely determined by complementarity between a miRNA within the seed region (positions 2-8 at the 5' end; Lucas and Raikhel, 2013), a mutation within this critical binding region in an mRNA target should result in a disruption of miRNA/mRNA interaction thereby relieving the repressive effect. We found that the 3'UTR of *CamKII* is mutagenized within the seed region to disrupt the interaction between miR-289 and the mRNA, the effect of miR-289 on *CamKII* FLuc expression is completely abrogated (Figure 18A and B). These data suggest that activity-regulated miRNA-289 is capable of specifically regulating the *CamKII* 3'UTR mRNA translation *in vitro* in a manner dependent on perfect basepairing between miR-289 and the *CamKII* 3'UTR within the seed region.

In an effort to design a method to effectively knock down miR-289 for reduction in function analyses, we sought to generate a sequence from which we could ultimately use to create miR-289 sponge constructs similar to those we used in our miR-8 ROF experiments (Figure 11; Nesler et al., 2013). To begin, we generated a sequence designed to be a competitive inhibitor sponge of miR-289 following the specifications outlined in the original publication that introduced the method of miRNA sponge design (Ebert et al., 2007). When we co-transfected the FLuc coding sequence under control of our putative sponge sequence as an initial sensor with a vector expressing miR-289 in S2 cells, we observed no significant decrease in FLuc expression relative to empty vector

controls (data not shown). This negative result caused us to reevaluate our approach to sponge design in this case. In contrast to most miRNAs that range from 21-24 nucleotides in length, miR-289 is somewhat atypical in its 26-nucleotide length; therefore we believe it may not fit the standard criteria used for sponge sequence design (Okamura et al., 2008; Lai et al., 2003). To circumvent this issue we developed a new approach. We reasoned that if miR-289 is binding to the 3'UTR of *CamKII* thereby causing repression, it is likely that the miR-289 binding sequence within the *CamKII* 3'UTR would be an excellent candidate for a potential sponge sequence. To test this possibility, we designed oligonucleotides to replicate the miR-289 binding sequence within the *CamKII* 3'UTR that we could clone directly into our FLuc reporter vector. We found that upon co-transfection of S2 cells with this miRNA sensor and the miR-289 expression vector, a significant decrease in FLuc expression is observed relative to empty vector transfected controls (Figure 18A; ** $p<0.01$). These data indicate that using the miR-289 binding site within a bonafide target mRNA (in this case *CamKII*) could indeed provide a useful sequence for knocking down miR-289 using the miRNA sponge technique despite its atypical length, although further testing and construct is required before this approach could be utilized *in vivo*.

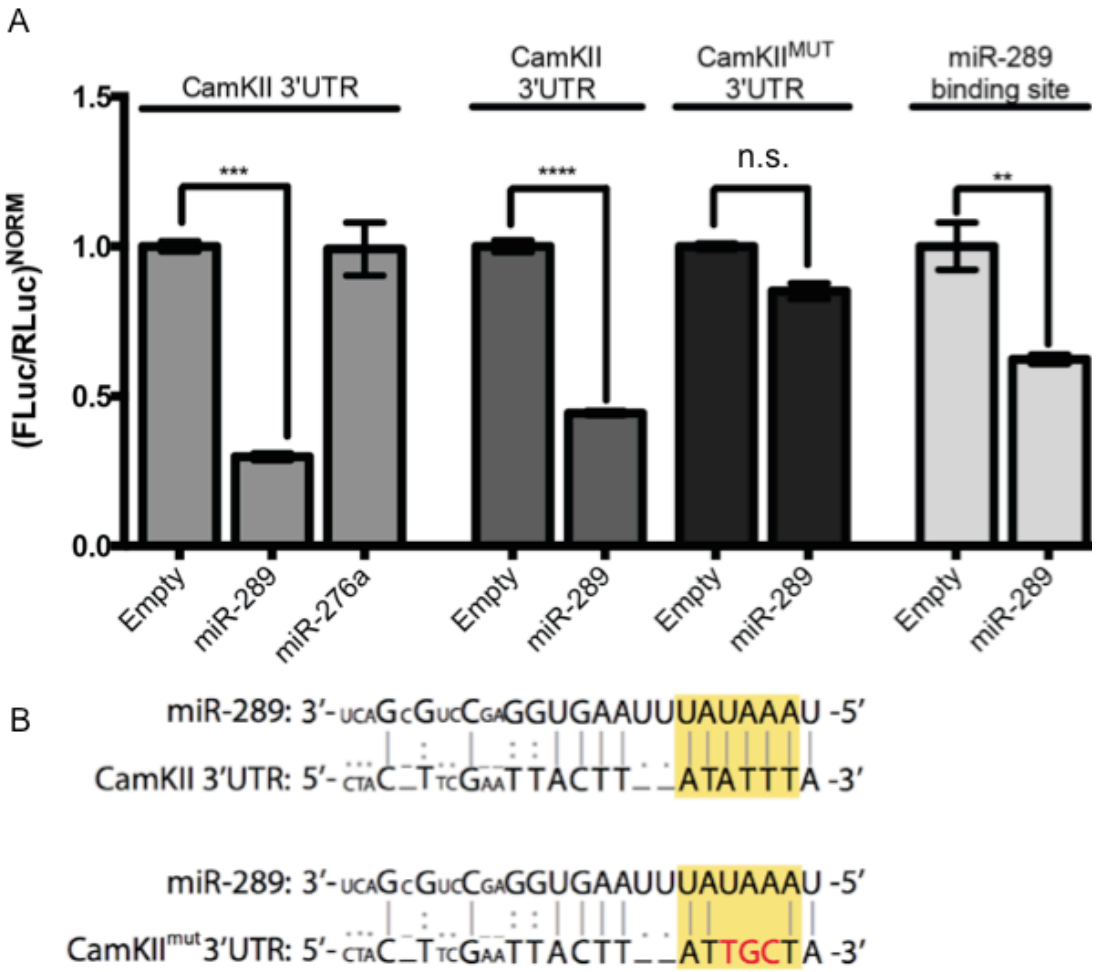

Figure 18. *CamKII* 3'UTR reporter is specifically regulated by miR-289.
Former undergraduate Nathan Boin generated constructs for the CamKII and CamKII^{MUT} 3'UTR experiments and conducted the S2 cell experiments using those constructs.
(A) Reporter plasmids constitutively expressing FLuc flaked by the 3'UTR of *CamKII*, a mutagenized version thereof, or a sensor expressing FLuc under the control of the miR-289 binding site were co-transfected into S2 cells with plasmids expressing miR-289, miR-276a or an empty vector (as controls). RLuc was included as a transfection control. FLuc activity was normalized to RLuc activity in three independent experiments. Normalized FLuc activities in the absence of miRNA-expressing vectors (empty vector controls) were set to 1. miR-289 significantly represses expression of endogenous *CamKII* 3'UTR but not of the *CamKII^{mut}* 3'UTR where site-directed mutagenesis has been conducted to mutagenize three nucleotides within the seed region of the *CamKII* mRNA. Error bars = mean ± SEM. n.s. = not significant. ** $p<0.01$, *** $p<0.001$, **** $p<0.0001$. (B) The upper sequence illustrates the endogenous *CamKII* 3'UTR and predicted binding site for miR-289. The seed region is highlighted in yellow. The lower sequence is the *CamKII^{MUT}* sequence generated through site directed mutagenesis, the seed region is again highlighted in yellow with mutated nucleotides depicted in red.

4.4 Presynaptic misexpression of miR-289 prevents activity-dependent increases in CamKII following spaced depolarization.

After validating CamKII as a target of miR-289 *in vitro* our next experimental goal centered around determining if miR-289 regulates CamKII in axon terminals in a manner relevant to activity-dependent new synaptic growth following spaced depolarization. In our model, activity-regulated miR-289 is significantly downregulated following spaced depolarization (Figure 11) allowing a subset of relevant presynaptic mRNA targets to be translated the net effect of which is ghost bouton formation. We reasoned that if CamKII is indeed a target of miR-289 relevant in activity-dependent synaptic growth, then presynaptic misexpression of miR-289 would inhibit activity-regulated *CamKII* local translation and subsequent function much like it inhibits ghost bouton formation (Figure 11). Our results indicate that upon spaced depolarization there is a modest but significant increase in CamKII fluorescence at the NMJ in wild-type *Canton S* larvae (Figure 17). To test the above hypothesis, we misexpressed miR-289 presynaptically predicting that upon stimulation we would not observe an increase in CamKII fluorescence following stimulation, similar to the result observed when local translation was acutely blocked with cycloheximide (Figure 17). Our prediction was accurate, in contrast to control larvae, when miR-289 was misexpressed presynaptically (C380-Gal4>*UAS-pri-miR-289*) there is no observable increase in CamKII fluorescence following spaced depolarization (Figure 19A-C).

We have demonstrated that it appears the molecular mechanisms underlying activity-dependent new synaptic growth and those responsible for axon growth during development can be uncoupled (Figure 11; Nesler et al., 2013). To determine if miR-289

likewise has an effect on CamKII levels during development we assayed CamKII/HRP fluorescence ratios at the NMJ in larvae misexpressing miR-289 presynaptically compared to genetic background controls. Interestingly, we observed no significant difference between miR-289 misexpressing and control larvae indicating that the regulatory effect miR-289 has on CamKII could be restricted to activity-regulated processes (Figure 19A and D).

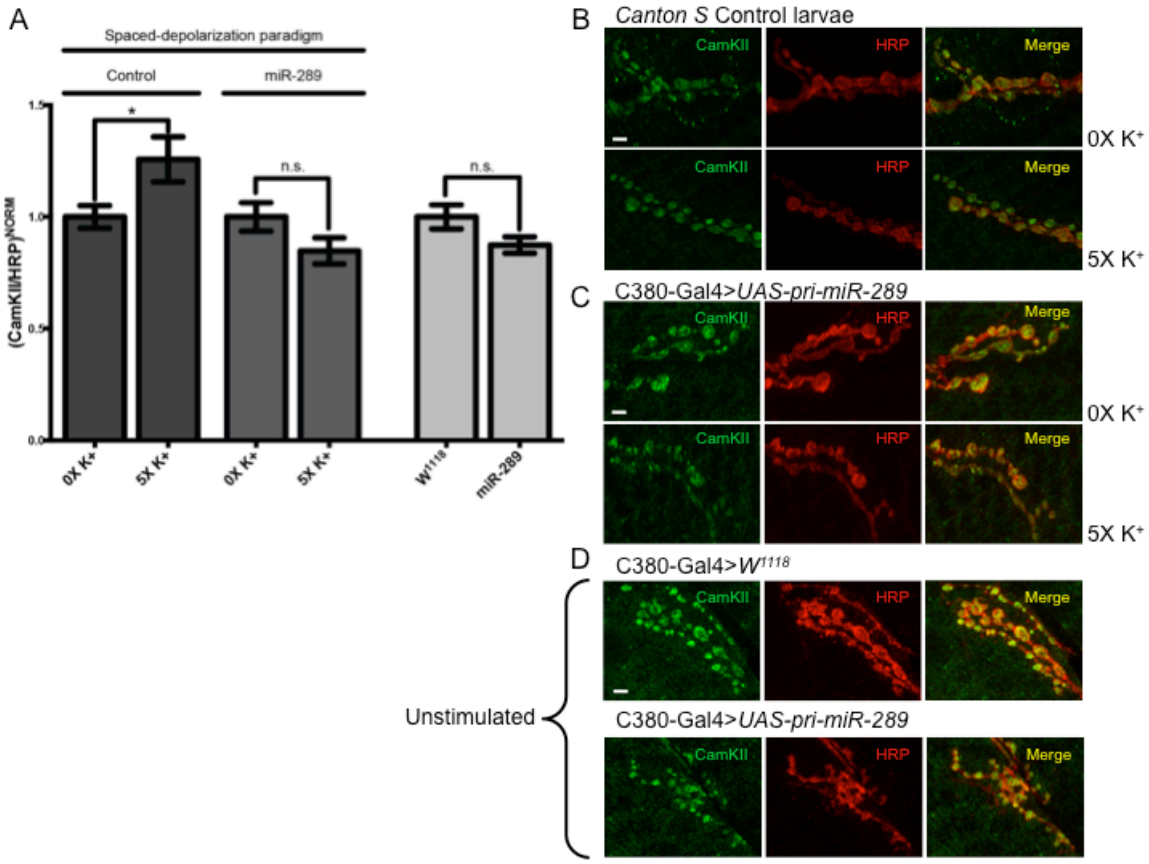

Figure 19 miR-289 misexpression prevents CamKII increase following stimulation *in vivo* but does not decrease CamKII expression during development.
(**A**) The four columns on the left hand side of the graph were subjected to the spaced depolarization or pseudostimulation paradigm as indicated below each column. 'Control' columns are wild-type *Canton S* larvae, 'miR-289' columns misexpress a *UAS-pri-miR-289* construct in motoneurons (C380-Gal4>*UAS-pri-miR-289*). The two rightmost columns represent C380-Gal4>W^{1118} genetic background control or C380-Gal4>*UAS-pri-miR-289* larvae. In each paired set of columns, larvae were labeled with mouse anti-CamKII and HRP primary antibodies in the same dish and imaged under identical conditions. As in Figure 17, ROIs were defined around each individual bouton demarcated by HRP, an average CamKII/HRP ratio was calculated per NMJ and data was normalized to the pseudostimulated (columns 1-4) or genetic background (columns 5 and 6) controls. A minimum of 20 paired NMJs were quantified in each column. Error bars = mean ± SEM. * $p<0.05$, n.s.= not significant. (**B-D**) Depict representative images from each of the genotypes indicated above each set of panels. Larvae subjected to the spaced depolarization paradigm (**B** and **C**) have their pseudostimulated or high K^+ treatment indicated to the right of each set of panels (0X K^+ and 5X K^+, respectively). Images display a magnified region of boutons from larger images of complete NMJs taken at 100X magnification and display a Z-series compiled on the Olympus FV1000 scanning confocal microscope. Scale bars = 10μM.

4.5 Presynaptic disruption of CamKII inhibits ghost bouton formation at the NMJ following spaced depolarization.

After validating the *CamKII* 3'UTR as a bonafide target of miR-289 *in vitro* (Figure 18) and identifying an activity-dependent increase in CamKII levels following stimulation (Figure 17) preventable by presynaptic misexpression of miR-289 (Figure 19) we set out to characterize the presynaptic effects of misexpression three distinct CamKII constructs and the effect of knocking down/inhibiting presynaptic CamKII on activity-dependent synaptic growth. First, we reasoned that if CamKII is required for activity-dependent synaptic growth and if we inhibited *CamKII* expression and/or function presynaptically, we would be able to phenocopy the results seen following misexpression of miR-289 following stimulation (Figure 11; Nesler et al., 2013). To test this hypothesis we obtained two distinct RNAi lines designed to express long hairpin constructs to knock down CamKII in a tissue-specific manner (*UAS-CamKII*^{v38930} and *UAS-CamKII*^{v47280}). We validated the effect of one such line by staining larval preparations from third instar larvae with this RNAi construct driven in motoneurons (C380-Gal4>*UAS-CamKII*^{v38930}) and observe a near total elimination of CamKII staining at the NMJ. This result validated both effectiveness of RNAi-mediated interruption of presynaptic CamKII and the specificity of our antibody (Figure 16C). We found that upon knockdown of presynaptic CamKII using either RNAi construct that ghost bouton formation following spaced depolarization is completely blocked, recapitulating the effect seen in miR-289 misexpressing larvae (Figure 20; Figure 11). The RNAi knockdown of CamKII allowed us to examine the effects of near complete loss of presynaptic CamKII expression. To assess the effect of inhibiting endogenous CamKII function presynaptically, we obtained

a line that expresses a specific inhibitor peptide of CamKII (ala) in a tissue-specific manner (*UAS-Ala*; Jin et al., 1998). This peptide inhibitor was developed such that it corresponds to the alanine (ala) inhibitory peptide in *Drosophila* mimicking the autoinhibitory domain of CamKII. Essentially, this inhibitory peptide binds within the catalytic domain of CamKII thereby inhibiting kinase function by preventing it from phosphorylating relevant targets (Griffith et al., 1993). By expressing this peptide in an inducible manner we were able to selectively inhibit CamKII function in motoneurons. We hypothesized that if presynaptic CamKII was forcibly locked in an inactive state and thus prevented from phosphorylating target proteins crucial for new synaptic growth, we would see an inhibition of ghost bouton formation following stimulation. As predicted, upon presynaptic inhibition of endogenous CamKII we observed a complete suppression of activity-dependent ghost bouton formation following high K^+ spaced-depolarization (Figure 20). Taken together, these data strongly indicate a requirement for active presynaptic CamKII function in rapid activity-dependent synaptic growth at the larval NMJ.

CamKII has the unique functional ability to autophosphorylate following activation with Ca^{2+}/CaM rendering the kinase autonomous for a period of time, the exact time course of autonomous activity following activation is still a matter of debate. Because CamKII is required for memory formation and is capable of autonomous activity, it is critical that kinase activity be switched off adequately (Lucchesi et al., 2011). Researchers have identified the threonine at position 287 in *Drosophila* (T287, T286 in mammals) as a critical site of autophosphorylation resulting in autonomous kinase activity (Jin et al., 1998; Coultrap et al., 2014). In its Ca^{2+}-activated state, CamKII

autophosphorylates this threonine residue located within the autoinhibitory domain (T287 in *Drosophila*, T286 in mammals). Once activated by Ca^{2+} influx and calmodulin (CaM) binding, the kinase retains autonomous activity that persists because after some subunits of the holoenzyme become dephosphorylated, neighboring subunits can rephosphorylate them, preventing reversion to the inactive state even after CaM dissociates from the kinase and Ca^{2+} returns to basal levels (Irvine et al., 2006). A threonine-to-aspartate (T287D) substitution at T287 in *Drosophila* CamKII results in a Ca^{2}+ independent form of CamKII, in contrast replacement of the same threonine with an alanine residue (T287A) results in a mutant form of CamKII incapable of autophosphorylation (Jin et al., 1998). In *Drosophila*, adults expressing a presynaptic CamKII construct that is Ca^{2+}-independent (T287D) eliminates habituation observed following repetitive stimulation in wild-type adults. In the same study, animals expressing a mutant Ca^{2+} dependent CamKII transgene (incapable of autophosphorylation, T287A) display a decreased basal CamKII activity level resulting in a decrease in initial response. This initial response decrease was followed by a rapid increase in sensitization mirroring the response of the animals expressing the Ca^{2+}-independent form of the kinase (Jin et al., 1998). We hypothesized that if expressed Ca^{2+}-independent (T287D) CamKII in presynaptic motoneuron terminals we would detect a faster response to spaced depolarization than is observed in genetic background control or Ca^{2+}-dependent (T287A) animals. To examine this possibility we drove expression of wild-type CamKII ($CamKII^{WT}$), Ca^{2+}-dependent CamKII ($CamKII^{T287A}$), and Ca^{2+}-independent CamKII ($CamKII^{T287D}$) presynaptically and subjected third instar larvae to 0X, 3X, and 5X spaced depolarization with high K^{+} HL3 (Figure 20). Contrary to our initial hypothesis, we did not observe a

significant increase in new synaptic growth following 3X stimulation in animals expressing Ca^{2+}-independent CamKII presynaptically, all treatment groups displayed results that paralleled genetic background controls (Figure 20B and D). While these data counter our original prediction, they are not inconsistent with published results. Studies on reflex habituation expressing these two mutant CamKII constructs presynaptically in sensory neurons indicate significantly different results in responses at the onset of stimulation with the T287A construct decreasing initial response time. While in animals expressing the T287D form they do notice an increase in dynamics that result in the inhibition of habituation, this is dynamic shift is not necessarily indicative of an increased response time in Ca^{2+}-independent animals (Jin et al., 1998).

Collectively these data indicate that presynaptic CamKII is required for activity-dependent new synaptic growth at the *Drosophila* NMJ (Figure 20A and C) but overexpression of three distinct CamKII constructs do not alter the time course of new synaptic growth following spaced depolarization (Figure 20B and D). We believe that CamKII likely acts to phosphorylate and thereby activate key presynaptic effector proteins required for ghost bouton formation at the NMJ. In this model, reduction of presynaptic CamKII by RNAi or inhibition of its function using an inhibitory peptide, these proteins are not activated and therefore the characteristic synaptic response of an increase in ghost bouton number following spaced depolarization is prevented.

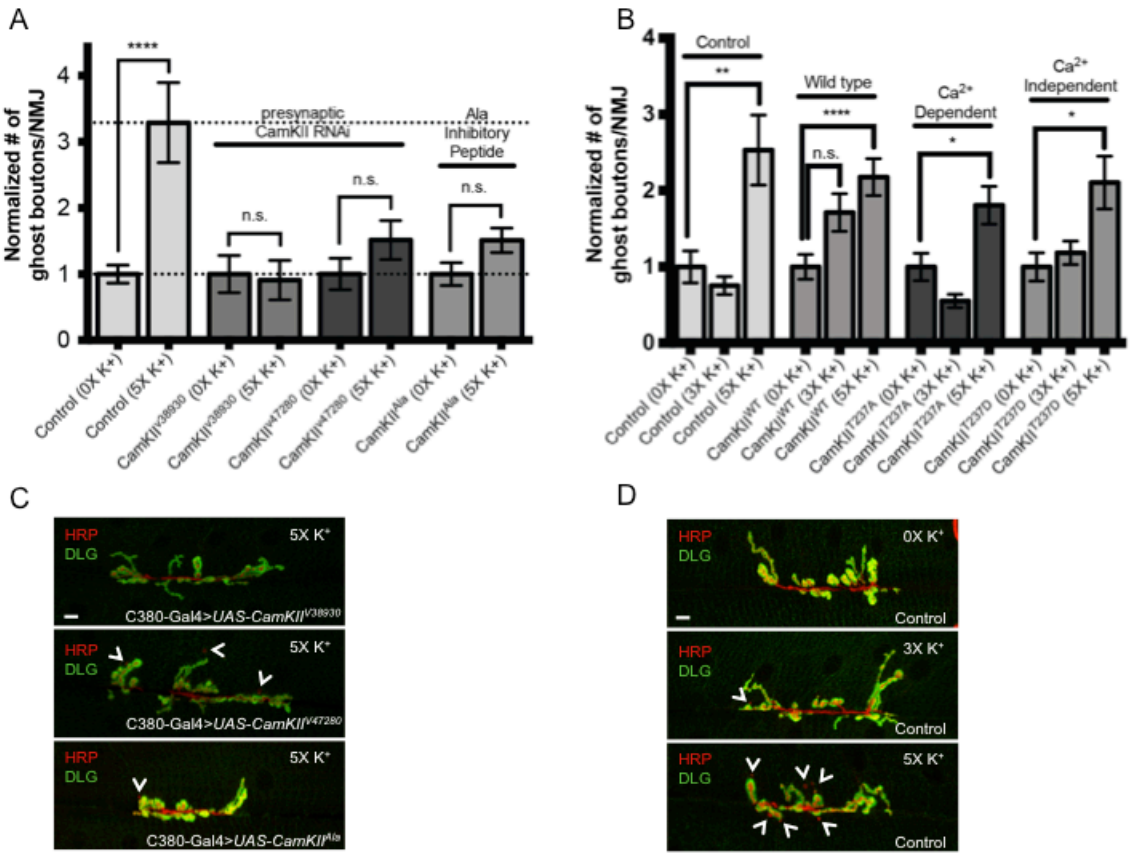

Figure 20. Active, presynaptic CamKII is required for activity-dependent new synaptic growth following neural stimulation.

(**A** and **B**) Larvae of the indicated genotypes were subjected to 0X, 3X, or 5X high K^+ stimulation as indicated. Error bars represent mean ± SEM. Ghost bouton numbers are presented as a fold increase normalized to controls. * $p<0.05$; ** $p<0.01$; **** $p<0.0001$; n.s. = not significant. (**A**) Reduction of function experiments were conducted using presynaptic motoneuron specific driver C380-Gal4 was used to drive the expression of RNAi constructs to knock down CamKII (*CamKII*^{V38930} and *CamKII*^{V47280}) and to inhibit CamKII function by expressing a peptide that mimics the autoinhibitory domain of CamKII preventing autophosophorylatoin (*CamKII*^{Ala}) genotypes are indicated below each column. (**B**)Three distinct CamKII gain of function constructs were driven presynaptically using motoneuron specific driver C380-Gal4. These expression constructs include wild-type CamKII (*CamKII*^{WT}), a mutant form of CamKII incapable of achieving $Ca2^+$ independence (*CamKII*^{T287A}), and lastly a $Ca2^+$ independent CamKII construct (*CamKII*^{T287D}). The three CamKII lines in **B** and the *CamKII*^{Ala} line in **A** are the same lines presented in Jin et al., 1998. (**C**) Representative images from C380-Gal4>*UAS-CamKII*^{V38930}, C380-Gal4>*UAS- CamKII*^{V47280}, and C380-Gal4>*UAS-CamKII*^{Ala} genotypes following 5X high K^+ stimulation. (**D**) Representitive images of genetic background control larvae (C380-Gal4>*W*^{1118}) following 0X, 3X and 5X K^+ stimulation respectively. No significant differences observed between genetic

background controls and CamKII misexpressing genotypes. In all images white arrowheads point to ghost boutons.

CHAPTER FIVE: DISCUSSION

This body of work demonstrates that following spaced depolarization, five neuronal miRNAs present in the *Drosophila* larval CNS are specifically downregulated. Additionally, three of these miRNAs play a critical role in the control of activity-regulated presynaptic growth at the NMJ. Evidence for these conclusions are provided by the following experimental findings. First, following a high K^+ spaced depolarization paradigm we observed a statistically and biologically significant downregulation of five neuronally expressed miRNAs-1, -8, -289, -314, and -958 (Figure 9; $\geq$ 2-fold decrease; $p<0.05$). Next, upon presynaptic misexpression of three of these miRNAs (miRs-8, -289, and -958), we see a complete suppression of new synaptic growth following spaced depolarization, indicating that each of these miRNAs alone is sufficient to inhibit ghost bouton formation following neuronal activity in this paradigm (Figure 11). In contrast, upon reduction or loss of presynaptic miR-8 function we observe a faster response to spaced depolarization lending additional support to the initial misexpression data (Figure 11). Additionally, using an *in silico*-based approach we observed we observed a significant enrichment in neuronal-related clusters in predicted mRNA targets of miRs-8 and -289 (Figure 13). Finally, we provide experimental evidence that miRs-8, -289, and -958 regulate the expression of 3'UTR reporters of important mRNA targets encoding for Wg, Lar, and CamKII proteins (Figure 14).

We demonstrate that miR-8 can regulate the expression of a *wg* 3'UTR *in vitro* (Figure 14). Previous studies and our own work show that upon inhibition of Wg expression by RNAi or in *wg* mutants activity-dependent ghost bouton formation is suppressed (Figure 14; Ataman et al., 2008). In *Drosophila*, Lar appears to interact negatively with tyrosine kinase Abl in control of motoneuron axon guidance and upon loss of *lar* function a significant decrease in synaptic boutons is observed at the NMJ, strongly suggesting a presynaptic role for *lar* function in the control of NMJ morphology during development (Pawson et al., 2008; Wills et al., 1999). Using our luciferase-based target validation approach, we confirmed that miRs-289 and -958 regulate the *lar* 3'UTR *in vitro* (Figure 14A-B). Furthermore, we are able to phenocopy the ghost bouton reduction following miR-289 and -958 presynaptic misexpression by expressing a presynaptic RNAi construct to disrupt Lar protein expression. This result strongly suggests a requirement for presynaptic *lar* in activity-regulated processes similar to the requirement for presynaptic *lar* in forming a normal number of synaptic boutons at the NMJ (Wills et al., 1999). Finally, we demonstrate that miR-289 regulates the expression of a *CamKII* 3'UTR reporter *in vitro* in a manner that is dependent on miRNA/mRNA seed region complementarity (Figure 18).

In mammals *CamKII* mRNA has been shown to be locally translated at postsynaptic sites in neurons during LTP, while in *Drosophila* LTM induction in the olfactory system results in transport to distal dendritic sites and subsequent local translation of *CamKII* mRNA in a process regulated by the miRNA pathway (Kindler and Kreienkamp, 2012; Ashraf et al., 2006). Our data supports a model where presynaptic CamKII expression is required for new synaptic growth following spaced depolarization.

This is supported by the evidence that disruption of presynaptic CamKII by RNAi recapitulates the suppression of ghost bouton formation observed in miR-289 misexpressing animals following high K^+ spaced depolarization (Figure 11). Collectively, these data indicate that activity-regulated miRNAs-8, -289, and -958 play a role in modulating the expression of specific neuronal mRNAs during the process of activity-dependent synaptic growth at the *Drosophila* larval NMJ.

5.1 A role for the miRNA pathway in modulation of developmental synaptic plasticity in *Drosophila*.

microRNAs have emerged as key non-coding RNAs involved in post-transcriptional gene regulation by complementary binding within the 3'UTRs of target mRNAs in neurons both pre- and postsynaptically (Kaplan et al., 2013; Bredy et al, 2011). Their transient and localized expression pattern and activity-dependent responses in neural compartments make them excellent candidates for the fine-tuning of neuronal gene expression in response to synaptic stimulation (Bredy et al., 2011; McNeill and Van Vactor, 2012). Importantly, several lines of evidence support a role for miRNA-mediated control of structure and/or function presynaptically in our system, the *Drosophila* larval NMJ. First, an interaction between key miRNA pathway protein Ago1 and fragile X mental retardation protein (FMRP) during larval development regulates NMJ growth during development (Jin, et al.; 2004a and b). In further support, proper function of synaptic transmission at the *Drosophila* NMJ hinges on presynaptic regulation of Kinesin-73 (Khc-73) by the miR-310 cluster (Tsurudome et al., 2010). Finally, upon loss of miR-124 function an increase in synaptic release is observed at the NMJ. This effect is attributed at least in part to miR-124 negatively regulating the expression of mRNAs

encoding components of the presynaptic BMP signaling pathway, including two BMP receptors Wit and Saxaphone (Sax) as well as Mothers against dpp (Mad), a downstream transcription factor in the BMP pathway (Sun et al., 2012). In addition to a presynaptic function for miRNAs in synaptic plasticity at the *Drosophila* NMJ, further studies indicate a role for miRNAs in the postsynaptic compartment during this process. Dicer-1 (Dcr-1) is one of two Dicer proteins found in *Drosophila* (Dcr-1 and Dcr-2) with distinct functions. During miRNA production, Dcr-1, an RNase III enzyme, is responsible for miRNA production by cleaving the terminal loop structure of the pre-miRNA structure thereby generating miRNA/miRNA* duplexes (Liu et al., 2007; Lucas and Raikhel, 2013). Upon postsynaptic knockdown of Dcr-1 thereby hindering miRNA biogenesis, a significant upregulation of glutamate receptor (GluR) mRNA and protein levels is observed hinting at the possibility that a miRNA (or miRNAs) may be modulating expression of this mRNA. More specifically, postsynaptic miR-284 is involved in regulation of GluR subunit availability at the NMJ (Karr et al., 2009). One miRNA involved postsynaptically in plasticity is a miRNA we have shown to be activity-regulated (miR-8; Figure 10). Upon postsynaptic downregulation of miR-8 using a sponge construct, a significant decrease in synapse size during development is seen (Loya et al., 2009). This control of NMJ morphogenesis during development is conferred by miR-8s regulation of Ena, a conserved member of the Ena/Vasodilator Activated Protein (Ena/VASP) protein family and that this regulation is dependent on a conserved miR-8 target site within the *ena* 3'UTR (Loya et al., 2014). Additionally, global disruption of miR-8 in null animals results in a decrease in spontaneous neurotransmitter release frequency and in quantal content, both indicators of a disruption of presynaptic

physiological responses while postsynaptic responses in miR-8-null animals remained relatively normal. Disruption of postsynaptic miR-8 target, *ena*, failed to recapitulate the presynaptic defects in physiological responses strongly indicating that postsynaptic modulation of *ena* by miR-8 is not sufficient to account for the physiological phenotype observed in miR-8-nulls and that there may additionally be a presynaptic functional requirement for miR-8 in this system (Loya et al., 2014). Collectively, these studies provide strong evidence in support of a role for miRNAs in modulation of gene expression during developmental plasticity at the *Drosophila* NMJ both pre- and postsynaptically. Our studies demonstrate that the processes of activity-regulated synaptic growth and control of neuronal growth during development appear to have molecular mechanisms that can be uncoupled. While our primary focus is the role of miRNAs in activity-regulated processes, miRNA-mediated gene regulation at this particular synapse during developmental processes is nonetheless pertinent, demonstrating that miRNAs are indeed active in controlling a form of synaptic plasticity at the *Drosophila* larval NMJ.

5.2 Control of synaptic plasticity in activity-regulated processes in *Drosophila* and mammals.

In *Drosophila* a role for the miRNA pathway in mRNA translational regulation has been demonstrated following induction of olfactory memory using a classical conditioning paradigm. Upon induction of LTM in this system, CamKII mRNA is localized to dendrites and key miRNA pathway component Armitage is degraded in a protesome-mediated manner resulting in local translation of *CamKII* mRNA (Ashraf et al., 2006). While the interaction between *CamKII* mRNA and activity-regulated miRNA-289 was not investigated in the previous study, a predicted binding site for miR-289

within the *CamKII* 3'UTR was identified by Ashraf et al. and additionally in our *in-silico* based target prediction approach. Additionally, as discussed in the previous section, miR-8 has a well-characterized role modulating synapse size during development of the larval NMJ and furthermore appears to have a role in presynaptic physiology in this system although this possibility has been less extensively examined (Loya et al., 2009 and 2014).

Our initial screen for activity-regulated miRNAs revealed a subdivision into two groups: first, mature miRNA levels of miRs-958 and -314 are very strongly decreased following spaced depolarization (7.5- and 5.2-fold, respectively; Figure 9C); second, we observe a less robust reduction in mature miRNA levels of miRs-1, -8, and -289 (2.4-, 1.8-, and 2.5-fold, respectively). Two miRNAs, miRs-1 and -8, show a high level of conservation from flies to humans, whereas miRs-289, -314, and -958 appear to be conserved exclusively in species of Drosophilids (Kozomara and Griffiths-Jones, 2011). This last observation raises the question of the applicability of study of activity-regulated miRNAs-289 and -958 to processes in higher order organisms.

Another curious artifact of our screen is that we only identified miRNAs that were significantly downregulated in response to neuronal activity. In mammals, a large body of work has demonstrated that synaptic activity results in an upregulation in miRNAs which thereby repress mRNA targets involved in modulation of synaptic structure and function in these systems (Siegel et al., 2011). One possible explanation for this phenomenon is that our screen was not comprehensive. At the time of our experiment, we were only able to assay miRNAs that had been identified at that time excluding those whose RT-qPCR primers did not pass quality control (Figure 9A-B). This subset of

miRNAs analyzed now represents ~35% of all *Drosophila* miRNAs currently annotated. It is possible that if another screen were conducted to additionally cover the currently annotated miRNAs that we would identify more miRNAs that are not only upregulated in response to synaptic activity but also translationally regulate mRNAs involved in activity-dependent neuron growth in *Drosophila*. This discrepancy may additionally be explained by a fundamental difference between neuronal miRNA function in mammals and Drosophilids, although it seems more likely that we have yet to identify miRNAs that are upregulated in response to neuronal activity in *Drosophila* that do indeed exist. Another possibility to explain why we only saw a downregulation in our trials is that these results could be an indirect consequence of our use of the high K^+ stimulation paradigm to induce activity for our RT-qPCR analysis. We do believe this is unlikely because we observe a significant correlation between our high K^+ RT-qPRC data and the results of our ChR2 light-stimulated microarray analysis using the completely different optogentic stimulation approach (Figure 10). Furthermore, while it is more common for miRNAs to be upregulated in mammalian neurons during learning and memory tasks, it is important to note that there are miRNAs that have been identified in mammalian systems that undergo an activity-dependent decrease. Examples of such miRNAs include miRs-124, -181 and Let-7d reduction in which leads to an alteration in Cocaine-CPP learning (Chandrasekar and Dreyer, 2009 and 2011). Further support of a role for reduced miRNA levels in learning and memory in mammalian systems is provided by evidence using a cell specific knockout of Dicer. When Dicer was knocked out thereby inhibiting miRNA biogenesis, an enhanced effect on synaptic plasticity and memory was observed following learning tasks including the Morris water maze (Konopka et al.,

2010; Bredy et al., 2011). These aforementioned results resulted in the decreased expression of numerous miRNAs among which are miRs-124 and -132, two miRNAs expressed locally and required for dendritic spine regulation (Edbauer et al., 2010; Rajasethupathy et al., 2009; Bredy et al., 2011).

5.3 Mechanisms of activity-regulated miRNA downregulation.

While our data strongly suggest a role for miRNAs and their target mRNAs in new synaptic growth following spaced depolarization, the mechanism by which miRNAs are being downregulated within these neurons has yet to be elucidated. In general, a decrease in miRNA levels could logically be accomplished during key steps during miRNA biogenesis including transcription and/or processing, through destabilization/decay of the existing mature miRNA population in the cell, or by some combination of the above.

First, two lines of evidence suggest that the activity-dependent decrease in miRNAs we observe is due to rapid transcriptional downregulation. Two activity-regulated miRNAs, miRs-12 and -304, display identical downregulation (Figure 9B-C) and belong to a cluster of co-regulated miRNAs (Ryazansky et al., 2011). Additionally, upon misexpression of pri-miRNA constructs for miRs-8, -289, and -958 we observe a significant suppression of activity-dependent synaptic growth as compared to genetic background controls (Figure 11B). This observation points to transcriptional regulation as a likely explanation for the decrease in mature miRNA levels we observe because by nature these pri-miRNA misexpression constructs circumvent the requirement for endogenous transcription mechanisms, needing only to be processed into mature miRNAs within the cell to be functional. While this evidence strongly suggests

transcriptional regulation is at play, an inhibition of new transcription would prohibit an increase in miRNA levels but alone does not necessarily explain the marked decrease we observe because it does not address the existing mature miRNA population. Therefore, we believe that transcriptional downregulation may work in conjunction with other mechanisms.

The second mechanism by which miRNA levels may be decreased in response to activity is at the level of processing. It is possible that a critical component of miRNA processing, such as Dicer, is inhibited following stimulation rendering the cell incapable of processing the pre-miRNA hairpin into a mature miRNA. One such example of miRNA processing being inhibited *in vivo* is during let-7 miRNA biogenesis. Evidence suggests that RNA binding protein Lin28 inhibits let-7 biogenesis at the level of processing by binding to let-7 pre-miRNA (Thornton et al., 2012). While possible, this mechanism still does not address the issue that there would be existing mature miRNA populations within neurons still capable of repressing their target genes.

The final prospect is that miRNA stability may be affected, resulting in decay. While a decrease in miRNA stability and subsequent decay would account for depletion in mature miRNA levels, we would expect that such a mechanism would affect all miRNAs equally. Nonetheless, several lines of evidence suggest that destabilizing specific miRNAs can occur in some systems. Following synaptic activity induced by dark adaptation can result in a rapid downregulation of specific miRNAs via miRNA decay and transcriptional inhibition in mouse optic lobes (Krol et al., 2010). Additionally, the degradation or inhibition of a critical component of the miRNA could result in release of bound miRNAs followed by destabilization and decay. Northern blot and micro-Array

analysis of miRNAs in primary culture human neural cells has revealed limited stability and a short half-life (~1.5-3.5h) of brain-enriched miRNAs indicating that unless specifically stabilized, certain brain-enriched miRNAs appear to represent a rapidly executed signaling system that employs highly transient effectors of CNS gene expression (Sethi and Lukiw, 2009). Collectively, our observations and these lines of evidence lead us to believe that the activity-dependent miRNA downregulation we observe depends on rapid transcriptional downregulation in conjunction with either (or both) of the above mechanisms. A model of the potential regulatory stages is presented in Figure 21. It would be of great interest to determine precisely which mechanisms are involved in this process in the future.

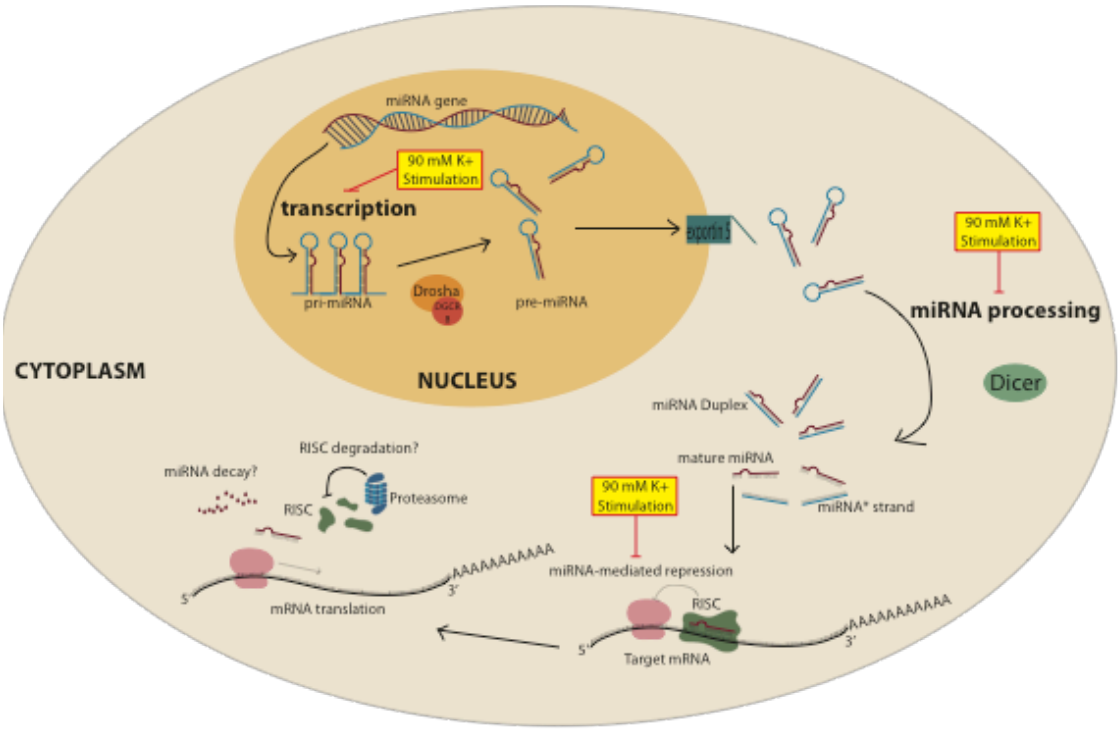

Figure 21. Model depicting potential stages for activity-dependent miRNA downregulation.
The above version highlights key stages during which a downregulation of activity-regulated miRNAs could be accomplished. The three stages include transcription, processing, and inhibition of miRNA/RISC function followed by subsequent destabilization and decay of formerly bound mature miRNAs. We believe that inhibition of transcription is likely working in conjunction with a mechanism inhibiting miRNA processing and/or leading to destabilization and decay of miRNAs as discussed above.

5.4 A role for *Drosophila* CamKII in activity-dependent synaptic growth.

Following identification and initial characterization of activity-regulated miRNAs-1, -8, -289, -314, and -958 and their roles in mediating activity dependent synaptic growth at the larval NMJ, including some preliminary experimental analysis of target mRNAs *wg* and *lar* (Figure 14), we focused our efforts on miR-289 and its putative target, CamKII. As indicated, CamKII has been studied extensively postsynaptically and its functions in LTM and more recently LTD are well characterized (Lucchesi et al., 2011; Coultrap et al., 2014). CamKII appears to phosphorylate a distinct set of substrates in opposing forms of plasticity (LTP vs LTD; Coultrap et al., 2014). Most presynaptic studies of CamKII center on synaptic transmission and to our knowledge, no evidence has been published defining a role for CamKII in activity-regulated synaptic growth. One study of synaptic transmission demonstrates that CamKII phosphorylates threonine 787 on the ether a go-go (eag) potassium channel. Inhibition of CamKII and mutation of *eag* both result in hyperexcitability at the larval NMJ and memory formation defects in the adult fly (Wang et al.. 2002). Additionally, CamKII levels in *Drosophila* sensory neurons appear to set response level and dynamics in response to habituation (Jin et al., 1998). More relevant to our application are studies implicating presynaptic CamKII in the control of the structural processes of synaptogenesis and growth cone guidance. In *Drosophila*, presynaptic CamKII is active in motoneurons modulating their response to the chemorepellent Sema-2a during synaptic refinement during both embryonic and larval stages (Carrillo et al., 2010). In growth cones of developing hippocampal neurons CamKII activity is required for a rapid increase in β-catenin (Kundel et al., 2009). The action of CamKII in this system functions downstream of neurotrophin-3 (NT3) and is

part of an exquisitely complex and coordinated process dependent on proper translational silencing and expression of mRNAs in response to external cues and signaling cascades (Jung et al., 2012). Another example of CamKII function modulating presynaptic structural processes is during growth cone guidance in cultured *Xenopus* neurons where CamKII is activated in response to Ca^{2+} elevation inducing growth cone attraction (Wen et al., 2004). Due to the limited study of presynaptic CamKII in the control axon structure and the complete lack of literature on presynaptic function for CamKII during activity-dependent axon terminal growth, we believe our studies represent a novel role for this kinase in neural plasticity.

5.4.1 CamKII displays a presynaptic localization pattern at the *Drosophila* NMJ intensified following spaced depolarization.

In order for CamKII to be a relevant target consistent with our overarching hypothesis, it must be present and active in presynaptic terminals at the *Drosophila* NMJ. To confirm first that CamKII is present at the NMJ and then to further characterize that localization we turned to immunoflourescent labeling using two distinct CamKII antibodies. Initial characterization studies of these antibodies in published works report a predominantly postsynaptic staining pattern using both the rabbit polyclonal anti-CamKII and mouse monoclonal anti-CamKII antibodies (Koh et al., 1999; Takamatsu et al., 2003). Our analysis strongly supports presynaptic localization of CamKII at the *Drosophila* NMJ in wild-type *Canton S* larvae (Figure 16). Notably, we noted strong co-localization with active zone marker DVGLUT in agreement with previous findings (Shakiyanova et al., 2011). In further support, in mammalian systems αCamKII has been observed at presynaptic terminals of inhibitory symmetric synapses in rodent cerebral

cortex and thalamus, a localization pattern unique to excitatory glutamatergic synapses whose cell bodies are known to express αCamKII mRNA (Liu et al., 1996 and 2013). Additionally, in the CA1 region of the rat hippocampus αCamKII is observed localizing to excitatory synapses (Liu and Jones, 1997).

Our data show that following spaced-depolarization, a significant increase in CamKII fluorescence is observed at the NMJ relative to presynaptic marker HRP (Figure 17 A and C). While we have not seen widespread use of this quantification approach, Loya et al. (2014) employ a similar ratiometric quantification approach in their analysis of synaptic Spectrin level increases seen at the larval NMJ in miR-8 null backgrounds Using this same approach, we demonstrate that this activity-regulated increase in CamKII is dependent on local translation by acutely inhibiting translation with cycloheximide (Figure 17). Western blot analysis following spaced depolarization did not reveal an increase in CamKII protein levels in the larval CNS over pseudostimulated controls (Figure 17B) indicating that the CamKII intensity increase we observe is likely due to local translation of *CamKII* mRNA specifically in synaptic boutons at the NMJ rather than a global upregulation. This observation is consistent with the activity-induced increase in local translation of *CamKII* mRNA observed in the *Drosophila* olfactory system (Ashraf et al., 2006). Several mammalian studies indicate an increase in *CamkII* translation following synaptic activation. First, polyadenylation of *αCamKII* mRNA occurs in the postsynaptic density of hippocampal neurons following, and when NMDA receptors are activated in that same synapse an increase in GFP reporter under the control of the *αCamKII* 3'UTR is observed (Wells et al., 2001; Richter and Lorenz, 2002).

5.4.2 The activity-regulated miRNA-289 modulates *CamKII* expression *in vitro* and following spaced depolarization at the *Drosophila* NMJ.

Studies show that *Drosophila CamKII* mRNA translation increases upon the induction of LTM formation in olfactory dendrites in a miRNA-mediated manner (Ashraf et al., 2006). Additionally, evidence shows *CamKII* mRNA is found in RNP particles containing widely conserved translational repressor Me31B in *Drosophila* olfactory synapses and upon loss of Me31B function results in a substantial elevation in CamKII translational reporter expression (Hillebrand et al., 2010). While the Ashraf et al. study does not specifically investigate the following interactions, it does identify putative binding sites for miR-280 and activity regulated miR-289 consistent with our *in-silico* target prediction. We find that *in vitro* the *CamKII* 3'UTR is regulated by miR-289 in a manner dependent on perfect baseparing between miR-289 and the *CamKII* 3'UTR within the seed region (Figure 18). Additionally, upon presynaptic misexpression of miR-289 we are able to recapitulate the result observed when local translation is acutely inhibited by cycloheximide (Figures 17 and 19). This result demonstrates that expressing a pri-miR-289 construct that cannot be transcriptionally downregulated upon synaptic stimulation results in an inability to induce the local increase in CamKII that is observed in wild-type animals (Figure 19). This set of experiments also demonstrated that upon misexpression of miR-289 during development, there is no significant decrease in CamKII fluorescence levels at the NMJ. This finding provides an additional piece of evidence to support the idea that developmental and activity-dependent processes can be

uncoupled and is not unsurprising given that presynaptic misexpression of miR-289 dos not result in an alteration in synapse size as assayed by total bouton count during development (Figures 11 and 12).

5.4.3 Presynaptic CamKII is required for activity-dependent ghost bouton formation at the *Drosophila* NMJ.

To determine if CamKII is required for activity-dependent ghost bouton formation at the NMJ we used RNAi-mediated interruption of CamKII in motoneuron terminals. As expected, upon reduction of CamKII function presynaptically we observed a complete suppression of activity-dependent ghost bouton formation (Figure 20). A similar result was also observed when we expressed a presynaptic inhibitory peptide to render presynaptic CamKII inactive (*UAS-Ala*; Figure 20A and C). Interestingly, when we expressed three distinct forms of CamKII one wild-type, one Ca^{2+}-dependent, and one Ca^{2+}-independent we did not observe any difference in activity-dependent response between any of these lines and controls nor among the CamKII misexpressing lines (Figure 20). This was not the result we anticipated; however there are several lines of evidence that may help explain this result. First, upon synaptic stimulation there is only a transient increase in Ca^{2+}-independent CamKII activity implicating a role for autophosphorylation in initial LTM formation but mutant mice expressing Ca^{2+}-dependent CamKII incapable of autophosphorylation are still capable of storing LTM following a massed training protocol (Irvine et al., 2006). Importantly, "autonomous" CamKII is not fully active by default, upon stimulation with Ca^{2+}/CaM an ~5-fold increase in stimulation can be induced (Coultrap et al., 2010 and 2014). Habituation studies in *Drosophila* using the same CamKII misexpression constructs we used

demonstrate a reduction in initial response time in mutant animals expressing Ca^{2+}-dependent CamKII. This initial response deficiency was rapidly overcome and additional kinase activity in Ca^{2+}-dependent and –independent CamKII expressing animals slowed the rate of presynaptic depression normally responsible for habituation (Jin et al., 1998). Based on these data it seems likely that while CamKII function is required for activity-dependent ghost bouton formation, autonomous/Ca^{2+}-independent CamKII function is not required nor does Ca^{2+}-independance confer an ability to respond to this kind of spaced training paradigm more rapidly.

5.5 Conclusions and future directions.

Altogether, the data presented in this body of work identify a specific set of miRNAs that are downregulated in response to neuronal stimulation and modulate gene expression of mRNAs responsible for activity-dependent synaptic growth at the *Drosophila* NMJ. We identified a significant number of mRNA predicted targets of these miRNAs that encode for guidance molecules in axon pathfinding pathways. A growing body of evidence implicates guidance molecules in synapse plasticity (Shen and Cowan, 2010). Based on this, it would be of great interest to explore whether some of these putative targets that encode guidance molecules are: a) *bona fide* targets of activity-regulated miRNAs and following validation if b) these molecules have a function in miRNA-mediated activity-dependent axon terminal growth. Targets of particular interest are highlighted in Table 1 and include ableson interacting protein (Abi), bazooka (Baz), longitudinals lacking (Lola), Plexin A (PlexA), the receptor tyrosine phosphatase PTP99A, roundabout (Robo), semaphorin-1A (Sema-1A) and wishful thinking (Wit). All of these genes have an annotated function in synaptic morphogenesis at the NMJ and/or

in controlling axon guidance. During our initial analysis, we limited the scope of our target screen to mRNAs that appeared as putative targets of two or more activity-regulated miRNAs in order to narrow the scope of the massive list of predicted targets we generated. Moving forward, it would be beneficial to explore the lists of putative targets of each activity-regulated miRNA in more detail to determine if there are any especially interesting and applicable target genes that escaped our notice originally.

One notable exception to our original criteria of evaluating mRNA targets that are predicted co-regulated of two or more activity-regulated miRNAs was CamKII. CamKII was a putative target of just one activity regulated miRNA, miR-289. We decided to make an exception and investigate CamKII as a target because of its well characterized function in synaptic plasticity; the knowledge that the *CamKII* mRNA is controlled by the miRNA pathway in some synapses, and undergoes activity-dependent local translation. Through our more extensive analysis of CamKII in activity-dependent synaptic growth we have demonstrated that functional CamKII is required for ghost bouton formation however autonomous CamKII is not necessary. Preliminary results using CamKII::EYFP fusion constructs indicate that CamKII is still transported to the NMJ in the absence of the endogenous *CamKII* 3'UTR (Figure 16D). It would be interesting to examine this localization in more detail and determine if there is an activity-regulated increase in expression of the construct containing the *CamKII* 3'UTR over the level of induction observed in the construct lacking the *CamKII* 3'UTR. Additionally, it would be of interest to generate deletion or sponge lines for miR-289 to determine if complete loss or a reduction of miR-289 function increases response time to spaced depolarization as we observe in larvae deficient in miR-8. Lastly, given our

hypothesis that CamKII will phosphorylate and thereby activate key effector proteins required for activity-dependent new synaptic growth, it would be interesting to explore what some of these phosphorylation targets are and characterize a role for them in this system.

REFERENCES

Aberle, H., et al. 2002. "Wishful thinking encodes a BMP type II recptor that regulates synaptic growth in *Drosophila*.". *Neuron* 33, no. 4: 545-545-558.

Ashraf, S., et al. 2006. "Synaptic Protein Synthesis Associated with memory is Regulated by the RISC Pathway in *Drosophila*.". *Cell* 124, no. 1: 191-191-205.

Ataman, B., et al. 2006. "Nuclear trafficking of *Drosophila* Frizzled-2 during the synapse development requires the PDZ protein dGRIP.". *Proc. Natl. Acad. Sci.* 103: 7841-7841-7846.

Ataman, B., et al. 2008. "Rapid activity-dependent modifications in synaptic structure and function require bidirectional Wnt signaling.". *Neuron* 57, no. 5: 705-705-718.

Baudent, M., A. Bellon, and C. Holt. 2013. "Role of microRNAs in Semaphorin function and neural circuit formation.". *Seminars in Cell and Developmental Biology* 24, no. 3: 146-146-155.

Berke, B., et al. 2013. "Retrograde BMP signaling at the synapse: a permissive signal for synapse maturation and activity-dependent plasticity.". *The Journal of Neuroscience* 33, no. 45: 17937-17937-17950.

Blockus, H. and A. Chedotal. 2014. "The multifaceted roles of Slits and Robos in cortical circuits: from proliferation to axon guidance and neurological disease.". *Current Opinion in Neurobiology* 27: 82-82-88.

Boeckers, T., et al. 2002. "ProSAP/Shank proteins- a family of higher order organizing molecules of the postsynaptic density with an emerging role in human neurological disease.". *Journal of Neurochemistry* 81, no. 5: 903-903-910.

Bredy, T., et al. 2011. "MicroRNA regulation of neural plasticity and memory..". *Neurobiology of Learning and Memory* 96, no. 1: 89-89-94.

Carroll, D. and A. Schaefer. 2013. "General Principals of miRNA Biogenesis and Regulation in the Brain.". *Neuropsychopharmacology Reviews* 38: 39-39-54.

Chandrasekar, V. and J. Dreyer. 2011. "Regulation of MiR-124, Let-7d, and MiR-181a in the accumbens affects the expression, extinction, and reinstatement of cocaine-induced conditioned place preference.". *Neuropsychopharmocology* 36, no. 6: 1149-1149-1164.

Chandrasekar, V. and J. Dreyer.. 2009. "microRNAs miR-124, let-7d and miR-181a regulate cocaine-induced plasticity.". *Molecular and cellular neurosciences* 42, no. 4: 350-350-362.

Chung, W. and B. Barres. 2009. "Selective remodeling: refining neural connectivity at the neuromuscular junction.". *PLOS Biology* 7, no. 8.

Costa-Mattioli, M., M. Bidinosti, and T. Dever. 2008. "Getting the message in protein synthesis. Keystone Symposium on Translational Regulatory Mechanisms.". *EMBO Reports* 9, no. 10: 954-959.

Costa-Mattioli, M., et al. 2009. "Translational control of long-lasting synaptic plasticity and memory.". *Neuron* 61, no. 1: 10-10-26.

Cougot, N., et al. 2008. "Dendrites of mammalian neurons contain specialized P-body-like structures that respond to neuronal activation.". *The Journal of neuroscience* 28, no. 51: 13793-13793-13804.

Coultrap, S., et al. 2010. "CaMKII autonomy is substrate-dependent and further stimulated by Ca2+/calmodulin.". *Journal of Biological Chemistry* 285, no. 23: 17930-17930-17937.

Coultrap, S., et al. 2014. "Autonomous CamKII mediates both LTP and LTD using a mechanism for differential substrate site selection.". *Cell Reports* 6: 431-431-437.

Crowner, D., et al. 2002. "Lola regulates midline crossing of CNS axons in Drosophila.". *Development* 129, no. 6: 1317-1317-1325.

Daniels, R., et al. 2008. "Visualizing glutamatergic cell bodies and synapses in *Drosophila* larval and adult CNS.". *Journal of Comparative Neurology* 508, no. 1: 131-131-152.

Denli, A., et al. 2004. "Processing of primary microRNAs by the Microprocessor complex.". *Nature* 432, no. 7014: 231-231-231.

Ebert, M., J. Neilson, and P. Sharp. 2007. "Competitive inhibitors of small RNAs in mammalian cells.". *Nature Methods* 4: 721-721-726.

Edbauer, D., et al. 2010. "Regulation of synaptic structure and function by FMRP-associated microRNAs miR-125b and miR-132.". *Neuron* 65, no. 3: 373-373-384.

Erondu, N. and M. Kennedy. 1985. "Regional distribution of type II Ca2+/calmodulin-dependent protein kinase in rat brain..". *The Journal of neuroscience* 5, no. 12: 3270-3270-3277.

Feig, S. and P. Lipton. 1993. "Paring the cholinergic agonist carbachol with patterned Schaffer collatral stimulation initates protein synthesis in hippocampal CA1 pyramidal cell dendrites via a muscarinic, NMDA-dependent mechanism.". *The Journal of neuroscience* 13, no. 3: 1010-1010-1021.

Freeman, A., et al. 2011. "NFAT regulates pre-synaptic development and activity-dependent plasticity in Drosophila.". *Molecular and cellular neurosciences* 46: 353-353-347.

Friedman, R., et al. 2009. "Most mammalian mRNAs are conserved targets of microRNAs.". *Genome Research* 19, no. 1: 92-92-105.

Fuentes-Mendel, Y., et al. 2009. "Glia and muscle scult neuromuscular arbors by engulfing destabilized synaptic boutons and shed presynaptic debris.". *PLOS Biology* 7, no. 8.

Garner, C., R. Tucker, and A. Matus. 1988. "Selective localization of messenger RNA for cytoskeletal protein MAP2 in dendrites.". *Nature* 336: 674-674-677.

Gkogkas, C., N. Sonenberg, and M. Costa-Mattioli. 2010. "Translational control mechanisms in long-lasting synaptic plasticity and memory.". *The Journal of biological chemistry* 285, no. 42: 31913-31913-31917.

Godenschwege, T., et al. 2002. "Bi-directional signaling by Semaphorin 1a during central synapse formation in Drosophila.". *Nature Neuroscience* 5, no. 12: 1294-1294-1301.

Gorelick, F., et al. 1988. "Autophosphorylation and activation of Ca^2+/calmodulin-dependent protein kinase II in intact nerve terminals.". *The Journal of biological chemistry* 263: 17209-17209-17212.

Griffith, L., et al. 1993. "Inhibition of Calcium/Calmodulin-Dependent Protein Kinase in *Drosophila* Disrupts Behavioral Plasticity.". *Neuron* 10: 501-501-509.

Griffiths-Jones, S., et al. 2006. "miRBase: microRNA sequences, targets and gene nomenclature.". *Nucleic Acids Research* 24: 140-140-144.

Griffiths-Jones, S., et al. 2008. "miRBase: tools for microRNA genomics.". *Nucleic Acids Research* 36: 154-154-158.

Grimson, A., et al. 2007. "MicroRNA targeting specificity in mammals: determinants beyond seed pairing.". *Molecular and Cellular Biology* 27, no. 1: 91-91-105.

Grun, D., et al. 2005. "microRNA target predictions across seven Drosophila species and comparison to mammalian targets.". *PLoS Computational Biology* 1, no. 1.

Han, J., et al. 2006. "Molecular basis for the recognition of primary microRNAs by the Drosha-DGCR8 complex..". *Cell* 125, no. 5: 887-887-901.

Hillebrand, J., S. Barbee, and M. Ramaswami. 2007. "P-body components, microRNA regulation, and synaptic plasticity.". *The Scientific World Journal* 7, no. 2: 178-178-190.

Hillebrand, J., et al. 2010. "The Me31B DEAD-Box Helicase Localizes to Postsynaptic Foci and Regulates Expression of a CaMKII Reporter mRNA in Dendrites of Drosophila Olfactory Projection Neurons.". *Front Neural Circuits* 4, no. 121.

Hinnebusch, A. and J. Lorsch. 2012. "The mechanism of eukaryotic translation initiation: new insights and challenges..". *Cold Spring Harbor Perspectives* 4, no. 10.

Holt, C. and E. Schuman. 2013. "The central dogma decentralized: new perspectives on RNA function and local translation in neurons.". *Neuron* 80, no. 3: 648-648-657.

Hornberg, H. and C. Holt. 2013. "RNA-binding proteins and translation regulation in axons and growth cones.". *Frontiers in Neuroscience* 7, no. 81: 81.

Huang, D., B. Sherman, and R. Lempicki. 2009. "Bioinformatics enrichment tools: paths toward the comprehensive functional analysis of large gene lists.". *Nucleic Acids Re* 37: 1-1-13.

Huang, D., B. Sherman, and R. Lempicki. 2009. "Systematic and integrative analysis of large gene lists using DAVID bioinformatics resources.". *Nature Protocols* 4: 44-44-57.

Irvine, E., et al. 2006. "alpha-CamKII autophosphorylation: a fast track to memory.". *Trends in neuroscience* 29, no. 8.

Jackson, R., C. Hellen, and T. Pestova. 2010. "The mechanism of eukaryotic translation initiation and principle of its regulation.". *Nature Reviews Molecular Cell Biology* 10: 113-127.

Jin, P., R. Alisch, and S. Warren. 2004. "RNA and microRNAs in fragile X mental retardation..". *Nature Cell Biology* 6, no. 11: 1048-1048-1053.

Jin, P., L. Griffith, and R. Murphey. 1998. "Presynaptic calcium/calmodulin-dependent protein kinase II regulates habituation of a simple reflex in adult *Drosophila*.". *The Journal of neuroscience* 18, no. 21: 8955-8955-8964.

Jin, P., L. Griffith, and R. Murphey.. 1998. "Presynaptic calcium/calmodulin-dependent protein kinase II regulates habituation of a simple reflex in adult *Drosophila*.". *The Journal of neuroscience* 18, no. 21: 8955-8955-8964.

Jin, P., et al. 2004. "Biochemical and genetic interaction between the fragile X mental retardation protein and the microRNA pathway..". *Nature Neuroscience* 7, no. 2: 113-113-117.

Jung, H., B. Yoon, and C. Holt. 2012. "Axonal mRNA localization and local protein synthesis in nervous system assembly, maintenance and repair.". *Nature reviews. Neuroscience* 13, no. 5: 308-308-324.

Kanai, Y., N. Dohmae, and N. Hirokawa. 2004. "Kinesin transports RNA: isolation and characterization of an RNA-transporting granule.". *Neuron* 43: 513-513-525.

Kaplan, B., et al. 2013. "MicroRNAs in the axon and presynaptic nerve terminal.". *Frontiers in cellular neuroscience*.

Karr, J., et al. 2009. "Regulation of glutamate receptor subunit availability by microRNAs.". *The Journal of Cell Biology* 185, no. 4: 685-685-697.

Karres, J., et al. 2007. "The conserved microRNA miR-8 tunes atrophin levels to prevent neurodegeneration in Drosophila..". *Cell* 131, no. 1: 136-136-45.

Kawamata, T. and Y. Tomari. 2010. "Making RISC..". *Trends in Biochemical Sciences* 35, no. 7: 368-368-376.

Kazama, H., A. Nose, and T. Morimoto. 2007. "Synaptic components necessary for retrograde signaling triggered by calcium/calmodulin-dependent protein kinase II during synaptogenesis..". *Neuroscience* 145, no. 3: 1007-1007-1015.

Kennedy, M. 1997. "The postsynaptic density at glutamatergic synapses.". *Trends in neurosciences* 20, no. 6: 264-264-268.

Kennell, J., et al. 2012. "The microRNA miR-8 is a Positive Regulator of Pigmentation and Eclosion in *Drosophila*.". *Developmental Dynamics* 241: 161-161-168.

Khvorova, A., A. Reynolds, and S. Jayasena. 2003. "Functional siRNAs and miRNAs exhibit strand bias..". *Cell* 115, no. 2: 209-209-216.

Kim, V., J. Han, and M. Siomi. 2009. "Biogenesis of small RNAs in animals..". *Nature Reviews Molecular Cell Biology* 10, no. 2: 126-126-139.

Kindler, S. and H. Kreienkamp. 2012. "Dendritic mRNA targeting and translation.". *Advances in Experimental Medicine and Biology* 970: 285-285-305.

Koh, Y., et al. 1999. "Regulation of DLG localization at synapses by CaMKII-dependent phosphorylation.". *Cell* 98, no. 3: 353-353-363.

Koles, K. and V. Budnik. 2012. "Exosomes go with the Wnt.". *Cellular Logistics* 2, no. 3: 169-169-173.

Kolodziej, S., et al. 2000. "Three-dimensional reconstructions of calcium/calmodulin-dependent (CaM) kinase IIalpha and truncated CaM kinase II alpha reveal a unique organization for its structural core and functional domains..". *The Journal of biological chemistry* 275, no. 19: 14354-14354-14359.

Konopka, W., et al. 2010. "MicroRNA loss enhances learning and memory in mice.". *The Journal of neuroscience* 30, no. 44: 14835-14835-14842.

Kozomara, A. and S. Griffiths-Jones. 2014. "miRBase: annotating high confidence microRNAs using deep sequencing data..". *Nucleic Acids Research* 24: 68-68-73.

Kozomara, A. and S. Griffiths-Jones. 2011. "miRBase: integrating microRNA annotation and deep-sequencing data.". *Nucleic Acids Research* 39: 152-152-157.

Krol, J., et al. 2010. "Characterizing light-regulated retinal microRNAs reveals rapid turnover as a common property of neuronalmicroRNAs.". *Cell* 141, no. 4: 618-618-631.

Krueger, N., et al. 1996. "The transmembrane tyrosine phosphatase DLAR controls motor axon guidance in Drosophila.". *Cell* 84, no. 4: 611-611-622.

Kundel, M., et al. 2009. "Cytoplasmic polyadenylation element-binding protein regulates neurotrophin-3-dependent beta-catenin mRNA translation in developing hippocampal neurons.". *The Journal of neuroscience* 29, no. 43: 13630-1369.

Kwon, C., et al. 2005. "MicroRNA1 influences cardiac differentiation in Drosophila and regulates Notch signaling.". *Proc. Natl. Acad. Sci.* 102, no. 52: 18986-18986-18991.

Lai, E. 2002. "MicroRNAs are complementary to 3'UTR sequence motifs that mediate negative post-transcriptional regulation.". *Nature Genetics* 30, no. 4: 363-363-364.

Lai, E., et al. 2003. "Computational identification of *Drosophila* microRNA genes.". *Genome Biology* 4, no. 7.

Lalima, L., K. Goutam, and B. Gopal. 2012. "Inter-domain interactions infulence the stability and catalytic activity of the bi-domain protein tyrosine phosphatase PTP99A.". *Biochimica et Biophysica Acta (BBA)-Proteins and Proteomics* 1824, no. 8: 983-983-990.

Lee, Y., et al. 2004. "MicroRNA genes are transcribed by RNA polymerase II.". *EMBO* 23, no. 20: 4051-4051-4060.

Lee, Y., et al.. 2004. "MicroRNA genes are transcribed by RNA polymerase II..". *EMBO* 23, no. 20: 4051-4051-4060.

Lewis, B., C. Burge, and D. Bartel. 2005. "Conserved seed pairing, often flanked by adenosines, indicates that thousands of human genes are microRNA targets..". *Cell* 120, no. 1: 15-15-20.

Lin, T., et al. 2009. "Abi plays an opposing role to Abl in Drosophila axonogenesis and synaptogenesis.". *Development* 136, no. 18: 3099-3099-30107.

Liu, S., Y. Ma, and E. Lee. 2013. "NMDA receptor signaling mediates the expression of protein inhibitor of activated STAT1 (PIAS1) in rat hippocampus.". *Neuropharmocology* 65: 101-101-113.

Liu, X. and E. Jones. 1997. "Alpha isoform of calcium-calmodulin dependent protein kinase II (CAM II kinase-alpha) restricted to excitatory synapses in the CA1 region of rat hippocampus.". *Neuroreport* 8, no. 6: 1475-1475-1479.

Liu, X., et al. 2007. "Dicer-1, but not Loquacious, is critical for assembly of miRNA-induced silencing complexes.". *RNA* 13, no. 12: 2324-2324-2329.

Livak, K. and T. Schmittgen. 2001. "Analysis of relative gene expression data using real-time quantitative PCR and the 2(-Delta Delta C(T)) Method..". *Methods* 25, no. 4: 402-402-408.

Llinas, R., et al. 1991. "Regulation by synapsin I and Ca^2+-calmodulin-dependent protein kinase II of the transmitter release in squid giant synapse.". *Journal of Physiology* 436: 257-257-282.

Llinas, R., et al. 1985. "Intraterminal injection of synapsin I or calcium/calmodulin-dependent protein kinase II alters neurotransmitter release at the squid giant synapse. .". *Proc. Natl. Acad. Sci.* 82, no. 9: 3035-3035-3039.

Loya, C., et al. 2009. "Transgenic microRNA inhibition with spatiotemporal specificity in intact organisms..". *Nature Methods* 6, no. 12: 897-897-903.

Loya, C., et al. 2014. "miR-8 controls synapse structure by repression of the actin regulator Enabled.". *Development* ahead of print.

Lucas, K. and A. Raikhel. 2013. "Insect microRNAs: biogenesis, expression profiling and biological functions.". *Insect biochemistry and molecular biology* 43, no. 1: 24-24-38.

Lucchesi, W., K. Mizuno, and K. Giese. 2011. "Novel insights into CamKII function and regulation during memory formation.". *Brain Research Bulletin* 85: 2-2-8.

Lund, E., et al. 2004. "Nuclear export of microRNA precursors..". *Science* 303, no. 5654: 95-95-98.

Magupalli, V., et al. 2013. "Ca2+-independent activation of Ca2+/calmodulin-dependent protein kinase II bound to the C-terminal domain of CaV2.1 calcium channels..". *The Journal of biological chemistry* 288, no. 7: 4637-4637-48.

Malinow, R., H. Schulman, and R. Tsien. 1989. "Inhibition of postsynaptic PKC or CaMKII blocks induction but not expression of LTP..". *Science* 245: 862-862-866.

Martin, K. and R. Zukin. 2006. "RNA trafficking and local protein synthesis in dendrites: an overview.". *The Journal of neuroscience* 26, no. 27: 7131-7131-7134.

McCabe, B., et al. 2003. "The BMP homolog Gbb provides a retrograde signal that regulates synaptic growth at the *Drosophila* neuromuscular junction.". *Neuron* 39: 241-241-254.

McGaugh, J. 2000. "Memory--a century of consolidation.". *Science* 14, no. 287: 248.

McNeill, E. and D. Van Vactor. 2012. "MicroRNAs shape the neuronal landscape.". *Neuron* 75, no. 3: 363-363-379.

Merianda, T., et al. 2009. "A functional equivalent of endoplasmic reticulum and Golgi in axons for secretion of locally synthesized proteins.". *Molecular and cellular neurosciences* 40, no. 2: 128-128-142.

Miech, C., H. Pauer, and T. Schwarz. 2008. "Presynaptic local signaling by a canonical wingless pathway regulates development of the Drosophila neuromuscular junction.". *The Journal of neuroscience* 28, no. 43: 10875-10875-10884.

Miller, S., L. Patton, and B. Kennedy. 1988. "Sequences of of autophosphorylation sites in neuronal type II CaM Kinase that control Ca2+-independent activity.". *Neuron* 1: 593-593-604.

Miller, S., et al. 2002. "Disruption of dendritic translation of CaMKIIalpha impairs stabilization of synaptic plasticity and memory consolidation.". *Neuron* 36, no. 3: 507-507-519.

Mockett, B., et al. 2011. "Calcium/calmodulin-dependent protein kinase II mediates group I metabotropic glutamate receptor-dependent protein synthesis and long-term depression in rat hippocampus..". *The Journal of neuroscience*31, no. 20: 7380-7380-7391.

Morimoto, T., et al. 2010. "Subunit-specific and homeostatic regulation of glutamate receptor localization by CaMKII in *Drosophila* neuromuscular junctions.". *Neuroscience* 165, no. 4: 1284-1284-1292.

Motulsky, H. and R. Brown. 2006. "Detecting outliers when fitting data with nonlinear regression - a new method based on robust nonlinear regression and the false discovery rate.". *BMC Bioinformatics* 7: 123.

Nagel, G., et al. 2002. "Channelrhodopsin-1: a light-gated proton channel in green algae..". *Science* 296, no. 5577: 2395-2395-8.

Nesler, K., et al. 2013. "The miRNA pathway controls rapid changes in activity-dependent synaptic structure at the Drosophila melanogaster neuromuscular junction.". *PLoS One* 8, no. 7.

Nichols, R., et al. 1990. "Calcium/calmodulin-dependent protein kinase II increases glutamate and noradrenaline release from synaptosomes..". *Nature* 343, no. 6259: 647-647-651.

Okamura, K., W. Chung, and E. Lai. 2008. "The long and short of inverted repeat genes in animals: microRNAs, mirtrons and hairpin RNAs.". *Cell Cycle* 7, no. 18: 2840-2840-2845.

Ouimet, C., T. McGuinness, and P. Greengard. 1984. "Immunocytochemical localization of calcium/calmodulin-dependent protein kinase II in rat brain..". *Proc. Natl. Acad. Sci.* 81, no. 17: 5604-5604-5608.

Pawson, C., B. Eaton, and G. Davis. 2008. "Formin-dependent synaptic growth: evidence that Dlar signals via Diaphanous to modulate synaptic actin and dynamic pioneer microtubules..". *The Journal of neuroscience* 28, no. 44: 11111-11111-11123.

Perycz, M., et al. 2011. "Zipcode binding protein 1 regulates the development of dendritic arbors in hippocampal neurons.". *The Journal of neuroscience* 31, no. 14: 5271-5271-5285.

Pestova, T. and C. Hellen. 2000. "The structure and function of initiation factors in eukaryotic protein synthesis.". *CMLS, Cell. Mol. Life Sci.* 57: 651-651-674.

Pfaffl, M., et al. 2004. "Determination of stable housekeeping genes, differentially regulated target genes and sample integrity: BestKeeper–Excel-based tool using pair-wise correlations.". *Biotechnology Letters* 26: 509-509-515.

Rajasethupathy, P., et al. 2009. "Characterization of small RNAs in Aplysia reveals a role for miR-124 in constraining synaptic plasticity through CREB.". *Neuron* 63, no. 6: 803-803-817.

Rehmsmeier, M., et al. 2004. "Fast and effective prediction of microRNA/target duplexes.". *RNA* 10, no. 10: 1507-1507-1517.

Rehwinkel, J., et al. 2006. "Genome-wide analysis of mRNAs regulated by drosha and argonaute proteins in *Drosophila melanogaster*.". *Molecular and Cellular Biology* 26, no. 8: 2965-2965-2975.

Richter, J. and L. Lorenz. 2002. "Selective translation of mRNAs at synapses.". *Current Opinion in Neurobiology* 12, no. 3: 300-300-304.

Ritchie, M., et al. 2007. "A comparison of background correction methods for two-colour microarrays.". *Bioinformatics* 23: 2700-2700-2707.

Roche, J., et al. 2002. "Regulation of synaptic plasticity and synaptic vesicle dynamics by the PDZ protein Scribble.". *The Journal of neuroscience* 22: 6471-6471-6479.

Rodriguez, A., et al. 2004. "Identification of mammalian microRNA host genes and trasncription units.". *Genome Research* 14, no. 10a: 1902-1902-1910.

Rook, M., M. Lu, and K. Kosik. 2000. "CaMKIIalpha 3' untranslated region-directed mRNA translocation in living neurons: visualization by GFP linkage.". *The Journal of neuroscience* 20, no. 17: 6385-6385-6393.

Rosenberg, O., et al. 2005. "Structure of the autoinhibited kinase domain of CamKII and SAXS analysis of the holoenzyme.". *Cell* 123, no. 5: 849-849-860.

Rubio, M., et al. 2013. "Regulation of atrophin by both strands of the mir-8 precursor..". *Insect biochemistry and molecular biology* 43, no. 11: 1009-1009-1014.

Ruiz-Canada, C., et al. 2004. "New synaptic bouton formation is disrupted by misregulation of microtubule stability in aPKC mutants.". *Neuron* 42, no. 4: 567-567-580.

Ryazansky, S., V. Gvozdev, and E. Berezikov. 2011. "Evidence for post-transcriptional regulation of clustered microRNAs in Drosophila.". *BMC Genomics* 12, no. 371.

Schroll, C., et al. 2006. "Light-induced activation of distinct modulatory neurons triggers appetitive or aversive learning in Drosophila larvae..". *Curr Biol.* 16, no. 17: 1741-1741-7.

Sethi, P. and W. Lukiw. 2009. "Micro-RNA abundance and stability in human brain: specific alterations in Alzheimer's disease temporal lobe neocortex.". *Neuroscience Letters* 459, no. 2: 100-100-104.

Shakiryanova, D., et al. 2007. "Presynaptic ryanodine receptor-activated calmodulin kinase II increases vesicle mobility and potentiates neuropeptide release..". *The Journal of neuroscience* 27, no. 29: 7799-7799-806.

Shakiryanova, D., et al. 2011. "Differential control of presynaptic CamKII activation and translocation to active zones.". *The Journal of neuroscience* 31, no. 25: 9093-9093-9100.

Shen, K. and C. Cowan. 2010. "Guidance molecules in synapse formation and plasticity.". *Cold Spring Harbor Perspectives* 2, no. 4.

Siegel, G., R. Saba, and G. Schratt. 2011. "microRNAs in neurons: manifold regulatory roles at the synapse.". *Current Opinion in Genetic Development* 21, no. 4: 491-491-497.

Silva, A., et al. 1992. "Impaired spatial learning in alpha-calcium-calmodulin kinase II mutant mice.". *Science* 257, no. 5067: 206-206-211.

Sinnamon, J. and K. Czaplinski. 2011. "mRNA trafficking and local translation: the Yin and Yang of regulating mRNA localization in neurons.". *ABBS Acta Biochimica et Biophysica Sinca* 43, no. 9: 663-663-670.

Smirnova, L., et al. 2005. "Regulation of miRNA expression during neural cell specification.". *The Journal of neuroscience* 21: 1469.

Sonenberg, N. and A. Hinnebusch. 2009. "Regulation of translation in eukaryotes: mechanisms and biological targets.". *Cell* 136, no. 4: 731-731-745.

Sotelo-Silveira, J., et al. 2008. "Myelinated axons contain β-actin mRNA and ZBP-1 in periaxoplasmic ribosomal plaques and depend on cyclic AMP and F-actin integrity for in vitro translation.". *Journal of Neurochemistry* 104, no. 2: 545-545-557.

Steward, O. and W. Levy. 1982. "Preferential localization of polyribosomes under the base of dendritic spines in granule ells of the dentate gyrus.". *The Journal of neuroscience* 2, no. 3: 284-2840291.

Steward, O. and E. Schuman. "Protein synthesis at synaptic sites on dendrites.". *2001*: 299-299-325.

Sun, Q., et al. 2000. "Receptor tyrosine phosphatases regulate axon guidance across the midline of the Drosophila embryo.". *Development* 127, no. 4: 801-801-812.

Takamatsu, Y., Y. Kishimoto, and S. Osako. 2003. "Immunohistochemichal study of Ca^{2+}/calmodulin-dependent protein kinase II in the *Drosophila* brain using a specific monoclonal antibody.". *Brain Research* 974, no. 1-2: 99-99-116.

Tcherkezian, J., et al. 2010. "Transmembrane receptor DCC associates with protein synthesis machinery and regulates translation.". *Cell* 141, no. 4: 632-632-644.

Thiel, G., et al. 1988. "Ca2'/calmodulin-dependent protein kinase II: Identification of associated with the generation of Ca2-independent activity .". *Proc. Natl. Acad. Sci.* 85: 6337-6337-6341.

Thornton, J., et al. 2012. "Lin28-mediated control of let-7 microRNA expression by alternative TUTases Zcchc11 (TUT4) and Zcchc6 (TUT7).". *RNA* 18, no. 10: 1875-1875-1885.

Torre, E. and O. Steward. 1992. "Demonstration of local protein synthesis within dendrites using a new cell culture system that permits the isolation of living axons and dendrites from their cell bodies.". *The Journal of neuroscience* 12, no. 3: 762-762-772.

Tsurudome, K., et al. 2010. "The Drosophila miR-310 cluster negatively regulates synaptic strength at the neuromuscular junction.". *Neuron* 68, no. 5: 879-879-893.

Wang, D., K. Martin, and R. Zukin. 2010. "Spatially restricting gene expression by local translation at synapses.". *Trends in neurosciences* 33, no. 4: 173-173-182.

Wang, X., et al. 2002. "Mechanisms of the release of anterogradely transported neurotrophin-3 from axon terminals..". *The Journal of biological chemistry* 22, no. 3: 931-931-45.

Waxham, M., et al. 1993. "Calcium/calmodulin-dependent protein kinase II regulates hippocampal synaptic transmission..". *Brain Research* 609, no. 1-2: 1-1-8.

Weill, L., et al. 2012. "Translational control by changes in poly(A) tail length: recycling mRNAs.". *Nature Structural & Molelcular Biology* 19: 577-577-585.

Wells, D., et al. 2001. "A role for the cytoplasmic polyadenylation element in NMDA receptor-regulated mRNA translation in neurons.". *The Journal of neuroscience* 21: 9541-9541-9548.

Wen, Z., et al. 2004. "A CaMKII/calcineurin switch controls the direction of Ca(2+)-dependent growth cone guidance..". *Neuron* 43, no. 6: 835-835-846.

Wills, Z., et al. 1999. "The tyrosine kinase Abl and its substrate enabled collaborate with receptor phosphatase Dlar to control motor axon guidance.". *Neuron* 22, no. 2: 301-301-312.

Winberg, M., et al. 1998. "Plexin A is a neuronal semaphorin receptor that controls axon guidance.". *Cell* 95, no. 7: 903-903-916.

Winter, J. and S. Diederichs. 2013. "Argonaut-2 activates the let-7a passenger strand microRNA.". *RNA Biology* 10, no. 10.

Wu, L., et al. 1998. "CPEB-mediated cytoplasmic polyadenylation and the regulation of experience-dependent translation of alpha-CamKII mRNA at synapses.". *Neuron* 21: 1129-1129-1139.

Xiao, F., et al. 2009. "miRecords: an integrated resource for microRNA-target interactions..". *Nucleic Acids Research* 37: 105-105-110.

Yang, E. and H. Schulman. 1999. "Structural examination of autoregulation of multifunctional calcium/calmodulin-dependent protein kinase II..". *The Journal of biological chemistry* 274, no. 37: 26199-26199-26208.

Yang, X., et al. 2013. "Both mature miR-17-5p and passenger strand miR-17-3p target TIMP3 and induce prostate tumor growth and invasion..". *Nucleic Acids Research* 41, no. 21: 9688-9688-06704.

Yi, R., et al. 2003. "Exportin-5 mediates the nuclear export of pre-microRNAs and short hairpin RNAs..". *Genes Dev.* 17, no. 24: 3011-3011-3016.

Yu, L., et al. 2010. "Plexin a-semaphorin-1a signaling regulates photoreceptor axon guidance in Drosophila.". *The Journal of neuroscience* 30, no. 36: 12151-12151-12156.

Yuan, K., et al. 2013. "Decreased levels of miR-224 and the passenger strand of miR-221 increase MBD2, suppressing maspin and promoting colorectal tumor growth and metastasis in mice..". *Gastroenterology* 145, no. 4: 853-853-864.

Zlatic, M., et al. 2009. "Positional cues in the Drosophila nerve cord: semaphornis pattern the dorso-ventral axis.". *PLOS Biology* 7, no. 6.